Astbury Centre for Structural Molecular Biology

UNIVERSITY OF LEEDS

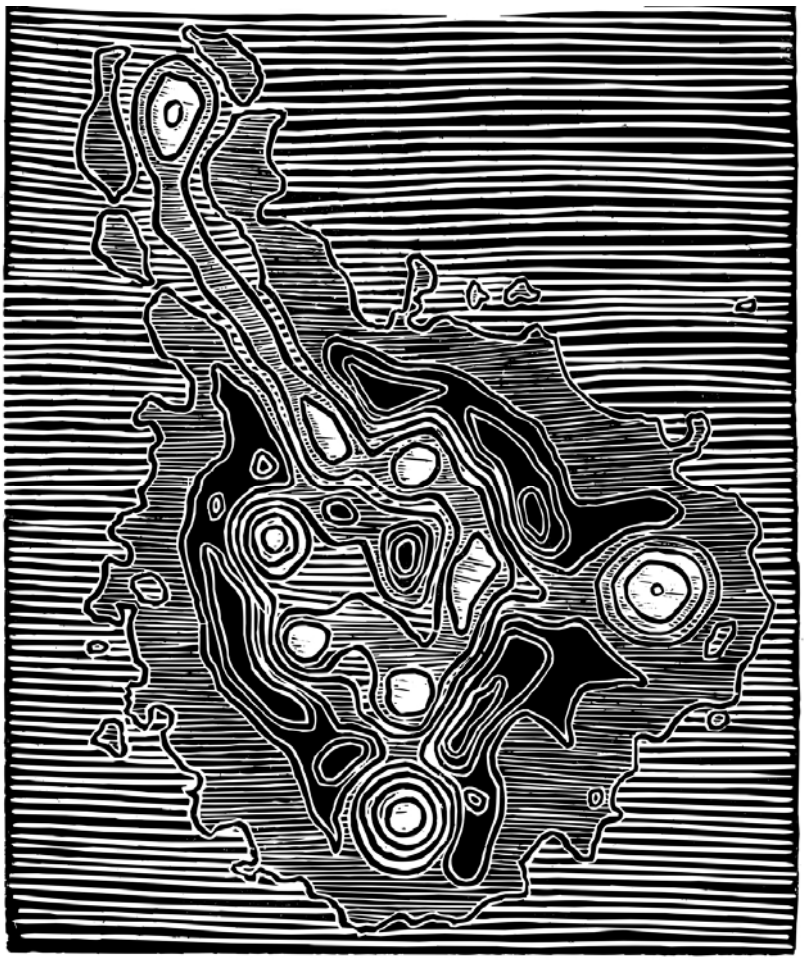

Annual Report 2009

Front cover illustration: dyneins are microtubule motor proteins that transport a wide variety of cargo within the cell. Stan Burgess' group used electron microscopy and image processing to locate GFP tags within engineered dyneins to define the main conformational change in the motor (Roberts *et al*. (2009) *Cell*, **136**:485-495). The cover shows a lino-cut of a contoured image of dynein's motor domain tagged with GFP and BFP. Artwork by Bara Malkova.

Acknowledgement

The Astbury Centre for Structural Molecular Biology thanks its many sponsors for support of the work and its members for writing these reports. The report is edited by David Brockwell.

This report is also available electronically via http://www.astbury.leeds.ac.uk

Mission Statement

The Astbury Centre for Structural Molecular Biology will promote interdisciplinary research of the highest standard on the structure and function of biological molecules, biomolecular assemblies and complexes using physico-chemical, molecular biological and computational approaches.

Introduction

I am delighted to write the Introduction to the Annual Report on the activities of the Astbury Centre in for Structural Molecular Biology in 2009. The year marked the tenth anniversary of the establishment of the Astbury Centre as a formal University Centre, which was celebrated at the Astbury@10 meeting in June. In its first ten years, the Astbury Centre has thrived as an interdisciplinary research centre, bringing together scientists from diverse backgrounds from across the University of Leeds.

This annual report provides a snapshot of the Astbury Centre's research portfolio in 2009. The report describes many scientific advances within the Centre that have addressed major problems in modern biology. Many of the reports demonstrate that an interdisciplinary approach can have a tremendous impact on problems that are relevant to global society. The Biology Faculty of 1000 highlighted research from the Centre on prion protein lipid rafts (Hooper), the vacuolar ATPase motor (Trinick), the synthesis of diverse small molecules (Nelson), and the mechanism of the dynein motor (Burgess, Knight). Rongjun Chen was awarded two prizes recognising the potential of his research to impact on business and industry. Alison Ashcroft and Adam Nelson delivered major lectures associated with the Hites Award (for an outstanding publication in *Journal of the American Society of Mass Spectrometry*) and the Royal Society of Chemistry Corday-Morgan medal respectively.

A major highlight of 2009 was, undoubtedly, the residential research retreat held in Kendal in September. The retreat was attended by 120 members including many postdoctoral researchers and PhD students. Over 60 people presented their research in the form of a poster or a lecture, and the diversity of the science presented reflected the broad remit of the Centre. The standard of the research presented was remarkably high, and the quality of the meeting certainly surpassed the international conferences that I attended in 2009!

Astbury Centre members continue to be very successful in raising external grant income, including many of our newly appointed staff who have succeeded in getting their first major grants funded. In addition, Andrew Wilson secured one of the University's first two European Research Council Starter grants; and Sheena Radford and David Brockwell are investigators on the first BBSRC Lola (Longer and Larger) grant to be awarded to the University. At the end of 2009, Astbury Centre members were applicants on grants totaling around £46M. Developing strong and sustained links with relevant industries has been a major objective within the Centre this year, and we were delighted to host 17 delegates from 11 companies to our Industry Open Day in the autumn.

Postdoctoral researchers and postgraduate students continue to make major contributions to the activities of the Centre. Nicole Timms has done a superb job leading the Astbury Society which has organised many enjoyable social and scientific events this year including the Sports Day and barbecue associated with the Astbury@10 meeting. The Society organised the Murder Mystery networking event that formed part of the research retreat: this event was exceptionally ingenious, and will, I'm sure, be remembered by members for many years to come! Many researchers have been externally recognized for the excellence of their work including George Preston and Martin Fisher, who won prizes at RSC events; James Kendall, who won a poster prize at an EU-funded training course on membrane proteins; and Gareth

Morgan won a poster prize at the White Rose Protein Forum. In 2009, 32 postgraduate students were awarded a PhD degree, and 36 new PhD students initiated a research project with a supervisor from the Astbury Centre.

The Astbury Centre continues to host a vibrant and highly international seminar programme. The Astbury@10 meeting featured presentations from Peter Knight; Simon Phillips, our founding Director; and Ben Davis and Kim Nasmyth from the University of Oxford. The talks spanned many of the broad research interests of members of the Centre including structural biology, biophysics, chemical biology and molecular interactions in cells. In total, there were 18 seminars in 2009 which were presented by visitors from institutions in 9 different countries.

We have formally welcomed 5 new members to the Astbury Centre in 2009: Stefan Auer, Robin Bon, Lorna Dougan, Alex O'Neill and Sarah Staniland. Carola Hunt left the University to move to a Chair at the University of Freiburg. We were very sorry that Donna Fletcher left the University in 2009, having provided many years of unstinting administrative support to the Centre.

2010 promises to be an exciting year for the Centre. We are planning a research away day in the autumn that will be held at the Thackray museum in Leeds. In addition, the Centre is contributing to a major exhibition at the museum celebrating the career of William Astbury as part of the Royal Society's celebration of its 350th anniversary; the exhibition will describe Astbury's enduring contributions to structural biology, and will highlight his legacy in the context of research from the Centre that is relevant to society today.

The Centre produces a regular electronic Newsletter that describes our on-going activities. Details of how to receive an electronic copy of this Newsletter may be found on the Astbury Centre website. This annual report (as well as those from previous years) is also available as a PDF document that can be downloaded from our website.

Finally, I would like to thank our editors, Alan Berry and David Brockwell, for leading the preparation of this Report, ably assisted by Sue Wright.

Adam Nelson

Director, Astbury Centre for Structural Molecular Biology

Leeds, April 2010

Contents

Contributions indexed by Astbury Centre Principal Investigator

Biomolecular mass spectrometry

James Ault, Tom Knapman, Lynsey Jones, John Hodkinson, Aneika Leney, Bethny Morrissey, Victoria Morton, James Muldoon, Caroline Pritchard, Dale Shepherd, David Smith, Lucy Woods, Sheena Radford, Peter Stockley, Nicola Stonehouse, Andrew Wilson, Peter Henderson, Sarah Harris and Alison Ashcroft.

Introduction

The focus of our research is the development and application of mass spectrometric techniques to investigate the tertiary and quaternary structures of biomolecules. We use non-covalent electrospray ionisation mass spectrometry (ESI-MS) and tandem mass spectrometry (MS/MS) to determine the mass, conformational properties, stoichiometry, stability, and binding characteristics of proteins and protein complexes. We are also pioneers of ion mobility spectrometry-mass spectrometry (IMS-MS), which offers a unique opportunity to separate co-populated biomolecular entities on the basis of their physical shape and to measure the molecular mass and cross-sectional area (Ω) of each individual component in a single, rapid (≤ 2 mins) experiment. Thus, this technique can separate ions of the same mass (e.g., protein conformers), or the same m/z ratio (e.g., oligomers).

Results

We have used ESI-IMS-MS to identify and structurally characterise the oligomers formed during *in vitro* amyloid assembly from β_2-microglobulin (β_2m) (Figure 1). During the lag phase of fibril formation, β_2m oligomers have been found to have collision cross-sections consistent with monomeric units arranged in elongated assemblies. The separation and quantification of these transient species indicated that monomers to tetramers are populated throughout the lag phase with no evidence for larger oligomers under the conditions employed. However, the data have revealed a decrease in oligomer dynamics concomitant with increasing oligomer size and the co-population of dynamic dimeric and trimeric species with more stable trimeric and tetrameric species. The results give a clear insight into the structural characteristics and dynamic nature of the co-populated β_2m oligomers, demonstrating for the first time the existence of elongated assemblies arising from an intact amyloidogenic protein during fibril formation.

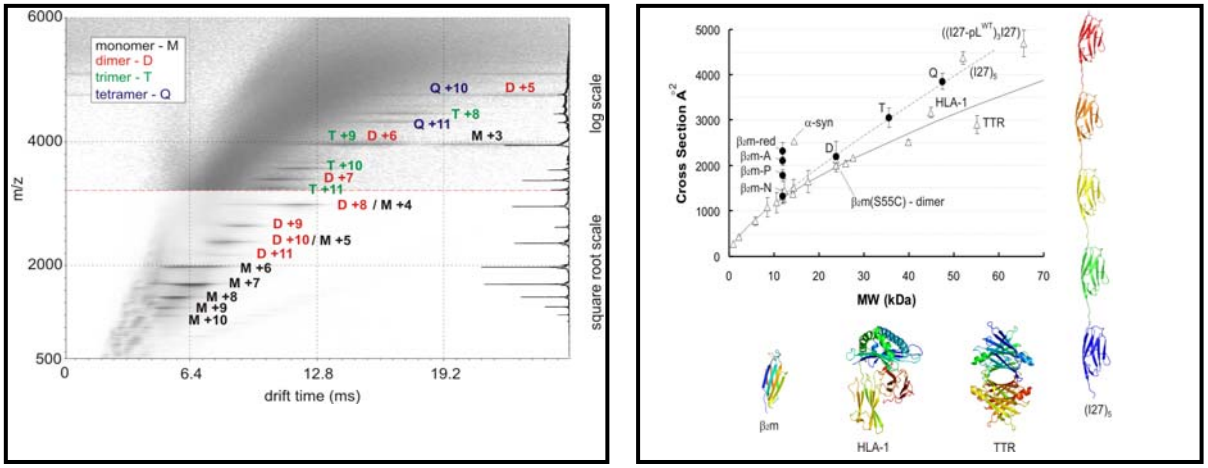

Figure 1: (left) ESI-IMS-MS driftscope plot showing the separation of β_2m monomer (M, black), dimer (D, red), trimer (T, green) and tetramer (Q, blue); **(right)** molecular weight *vs.* Ω measured by ESI-IMS-MS for β_2m (•) monomer (11.9 kDa, N=native, P=partially folded, A=acid unfolded, red=disulphide bond reduced), dimer (D), trimer (T) and tetramer (Q), together with a range of globular proteins (Δ) and the $(I27)_5$ concatamer. The elongated nature of the β_2m trimer and tetramer is apparent.

Our other projects include determining the conformational properties of viral capsid assembly intermediates, studying the protein-protein interactions involved in bacterial pilus assembly, and defining the specific regions of membrane proteins that govern their mode of function.

Publications

Hodkinson, J., Jahn, T., Radford, S. and Ashcroft, A. (2009) HDX-ESI-MS reveals enhanced conformational dynamics of the amyloidogenic protein beta2-microglobulin upon release from the MHC-1. *J Am Soc Mass Spectrom,* **20**:278-286.

Smith, D., Knapman, T., Campuzano, I., Malham, R., Berryman, J., Radford, S. and Ashcroft, A. (2009) Deciphering drift time measurements from travelling wave ion mobility spectrometry-mass spectrometry studies. *Eur J Mass Spectrom (Chichester, Eng)*, **15**: 113-130.

Fadouloglou, V., Bastaki, M., Ashcroft, A., Phillips, S., Panopoulos, N., Glykos, N. and Kokkinidis, M. (2009) On the quaternary association of the type III secretion system HrcQB-C protein: experimental evidence differentiates among the various oligomerization models, V. E. *J Struct Biol* **166**:14-25.

Taylor, D., Parkin, E., Cocklin, S., Ault, J., Ashcroft, A. Turner, A. and Hooper, N. (2009) Role of ADAMs in the ectodomain shedding and conformational conversion of the prion protein. *J Biol Chem*, **284**:22590-22600.

Knapman, T., Berryman, J., Campuzano, I., Harris, S. and Ashcroft, A. (2009) Considerations in experimental and theoretical collision cross-section measurements of small molecules using travelling wave ion mobility spectrometry – mass spectrometry, *Int. J. Mass Spectrom.,* in press.

Muldoon, J., Ashcroft, A. and Wilson, A. (2010) Selective protein-surface sensing using ruthenium (II) tris-(bipyridine) complexes, *Chem Eur J,* **16**:100-103.

Basnak, G., Morton, V., Rolfsson, O., Stonehouse, N., Ashcroft, A. and Stockley, P. (2010) Viral genomic ssRNA directs the pathway towards a *T*=3 capsid, *J Mol Biol*, **395**:924-936.

Jones, L., Baldwin, S., Henderson, P., Ashcroft, A. (2010) Defining topological features of membrane proteins by electrospray ionisation-mass spectrometry, *Rapid Commun Mass Spectrom,* **24**:276-284.

Smith, D., Radford, S., Ashcroft, A. (2010) Elongated oligomers in β_2-microglobulin amyloid assembly revealed by ion mobility spectrometry-mass spectrometry, *Proc Natl Acad Sci USA,* **107**:6794-6798.

Funding

This work was funded by the BBSRC, the EPSRC, the Wellcome Trust, Waters UK Ltd., and the Laboratory of the Government Chemist. We thank the BMSS for student travel grants.

Collaborators

Dr Gavin O'Connor (Laboratory of the Government Chemist, Middx., UK), Prof. Gabriel Waksman (Birkbeck College, London, UK), Prof. Christian Cambillau (University of Marseilles, France), Dr Steve Arscott (CNRS, Lille, France), Dr John Hoyes (Waters UK Ltd., Manchester, UK).

Simulating the self assembly and nucleation of peptides into amyloid fibrils

Stefan Auer

Introduction

The main goal of our research is to reveal the physical aspects of the self-assembly and nucleation of polypeptide chains into amyloid-like structures. In order to achieve our goals we use computational/theoretical methods developed to investigate phase transitions in atomic and colloidal systems and apply them to investigate the transitions in the more complex biomolecular systems. In the last year we have been able to calculate the nucleation barrier associated with the homogeneous nucleation of peptides into a β-sheet, and we simulated peptide aggregation on a nanoparticle surface.

Self-templated nucleation in peptide and protein aggregation

Peptides and proteins exhibit a common tendency to assemble into highly ordered fibrillar aggregates, whose formation proceeds in a nucleation-dependent manner that is often preceded by the formation of disordered oligomeric assemblies. This process has received much attention because disordered oligomeric aggregates have been associated with neurodegenerative disorders such as Alzheimer's and Parkinson's diseases. Here we describe a self-templated nucleation mechanism that determines the transition between the initial condensation of polypeptide chains into disordered assemblies and their reordering into fibrillar structures. The results that we present show that at the molecular level this transition is due to the ability of polypeptide chains to reorder within oligomers into fibrillar assemblies whose surfaces act as templates that stabilize the disordered assemblies.

A condensation-ordering mechanism in naoparticle-catalyzed peptide aggregation.

Nanoparticles introduced in living cells are capable of strongly promoting the aggregation of peptides and proteins. We use here molecular dynamics simulations to characterise in detail the process by which nanoparticle surfaces catalyze the self assembly of peptides into fibrillar structures. The simulation of a system of hundreds of peptides over the millisecond timescale enables us to show that the mechanism of aggregation involves a first phase in which small structurally disordered oligomers assemble onto the nanoparticle and a second phase in which they evolve into highly ordered β-sheets as their size increases.

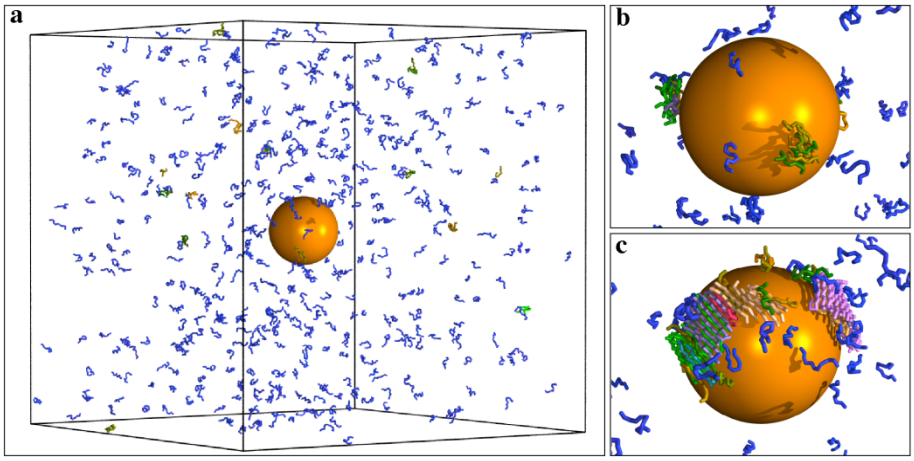

Figure 1: illustration of the condensation-ordering transition in nanoparticle-catalized peptide aggregation obtained from Molecular Dynamics simulations as a function of the time; **(a)** t=3.9 microseconds, **(b)** t=0.1 milliseconds, **(c)** t=0.3 milliseconds.

Publications

Auer, S., Dobson, C., Vendruscolo, M. and Maritan, A. (2008) Self-templated nucleation in peptide and protein aggregation. *Phys Rev Lett.* **101**:258101.

Auer, S., Trovato, A. and Vendruscolo, M. (2009) A condensation-ordering mechanism in naoparticle-catalyzed peptide aggregation. *PLoS Comput Biol* **5**, e1000458.

Funding

This work was supported by the RCUK.

Collaborators

Michele Vendruscolo (Cambridge), Antonio Trovato and Amos Maritan (both Padova)

Insights into membrane protein function from molecular modelling

Jocelyn Baldwin, Alison Baker, Helen Bradley, Li Dong, Lin-Hua Jiang, Carine De Marcos Lousa, Zhu-Zhong Mei and Stephen Baldwin

Introduction

In most organisms, up to 30% of the genome encodes membrane proteins, which perform diverse tasks ranging from the uptake of nutrients to communication between cells via chemical or electrical signals. These proteins represent more than half of current therapeutic drug targets in humans, and are involved in many serious diseases. Despite this importance, high resolution structures are available for fewer than 250 membrane proteins, reflecting the experimental difficulty of working with them. Our laboratory is currently engaged in research aimed at speeding up the rate at which novel membrane protein structures can be obtained, by developing improved, high-throughput technologies. However, in parallel we are exploiting the limited number of existing structures known, to gain insights into the molecular mechanisms of membrane proteins and the ways in which mutations can lead to disease. This typically requires specialised approaches to enable the modelling of the membrane protein targets of interest, because of their evolutionary distance from known structural templates. Three examples of the success of such modelling during the past year are described below.

Results

Recent genome-wide studies have shown that a mutation in the human zinc transporter Znt8 gene, resulting in the replacement of a tryptophan residue with arginine, increases the risk of type 2 diabetes. This transporter is found in the insulin-containing secretory granules of pancreatic β-cells, consistent with a possible role of the mutation in decreasing insulin secretion and/or proinsulin processing. Working in collaboration with Prof. Guy Rutter's group at Imperial College, we sought to explore the underlying mechanism by modelling the human protein on the distantly-related bacterial zinc transporter YiiP. This revealed that the mutation is located at the interface between protomers in the dimeric transporter, where it may disturb structurally-important zinc-binding sites (Figure 1).

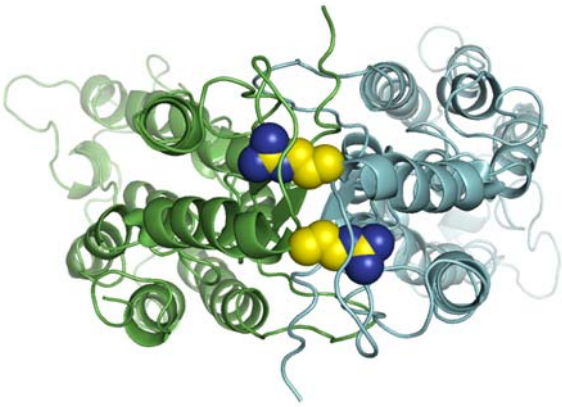

Figure 1: location of diabetes-associated mutations in the human zinc transporter Znt8. Subunits of the dimeric transporter, shown in blue and green cartoon form, are viewed from the cytoplasmic side of the membrane, with the arginine residues associated with diabetes risk shown in solid molecular representation.

Continuing the theme of using models of human membrane proteins to understand disease, we have also modelled the structure of the human $P2X_7$ receptor. This receptor is an ATP-activated cation channel, which plays critical roles in immune responses, inflammation and perception of pain. Moreover, single non-synonymous nucleotide polymorphisms (SNPs) in the corresponding gene have been linked to affective mood disorders such as major depression. In a collaboration between the laboratories of Lin-Hua Jiang and Steve Baldwin at Leeds, we have attempted to identify the mechanisms underlying such linkage by modelling the human protein on the recently-determined structure of the zebrafish $P2X_4$ receptor (Figure 2). Examination of the model revealed that several of the mutations, which were shown to affect channel function, were located close to the proposed ATP-binding site,

consistent with effects on ATP-binding and channel gating.

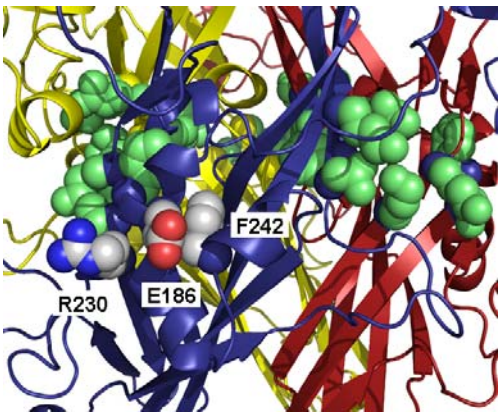

Figure 2: location of glutamate 186 in a model of the human $P2X_7$ receptor. Mutation of this residue to lysine causes complete loss of function, probably via altered interactions with adjacent residues R230 and F242. The three subunits of the trimeric receptor are shown in red, blue and yellow cartoon form, while residues predicted to comprise the ATP binding sites are shown, in solid molecular representation, in green.

In addition to our work on human proteins, we have also successfully applied our modelling strategies to gain an understanding of the link between mutation and phenotype in the peroxisomal ABC transporter "comatose" from the plant *Arabidopsis thaliana*. This protein is required for import of substrates for peroxisomal β-oxidation, and is a homologue of an ABC transporter, ALDP, involved in the human genetic disease adrenoleukodystrophy. In a collaboration between the laboratories of Alison Baker and Steve Baldwin at Leeds, we have built a model of comatose based on the structure of a bacterial multidrug transporter. This has allowed us to investigate the role of interactions between the transmembrane and nucleotide-binding domains of the protein in its transport function, and to predict likely substrate-binding residues for future mutagenesis studies.

Taken together, the results of the investigations described above indicate the utility of molecular modelling of membrane proteins, even in the majority of cases where structural templates are only distantly related to the proteins being modelled.

Publications

Dietrich, D., Schmuths, H., De Marcos, L., Baldwin, J., Baldwin, S., Baker, A., Theodoulou, F. and Holdsworth, M. (2009) Mutations in the *Arabidopsis* peroxisomal ABC transporter COMATOSE allow differentiation between multiple functions in planta: insights from an allelic series. *Mol Biol Cell* **20:**530-543.

Nicolson, T., Bellomo1, E., Wijesekara, N., Loder, M., Baldwin, J., Gyulkhandanyan, A., Koshkin, V., Tarasov, A., Carzaniga, R., Kronenberger, K., Taneja, T., da Silva Xavier, G., Libert, S., Froguel, P., Scharfmann R., Stetsyuk, V., Ravassard, P., Parker, H., Gribble, F., Reimann, F., Sladek, R., Hughes, S.J., Johnson, P., Masseboeuf, M., Burcelin, R., Baldwin, S., Liu, M., Lara-Lemus, R., Arvan, P., Schuit, F., Wheeler, M., Chimienti, F. and Rutter, G. (2009) Insulin storage and glucose homeostasis in mice null for the granule zinc transporter ZnT8 and studies of the type 2 diabetes-associated variants. *Diabetes* **58**:2070-2083.

Roger, S., Mei, Z., Baldwin, J., Dong, L., Bradley, H., Baldwin, S., Surprenant, A. and Jiang, L. (2010) Single nucleotide polymorphisms that were identified in affective mood disorders affect ATP-activated $P2X_7$ receptor functions. *J Psychiatr Res* **44**:347-355.

Funding

This work was funded by the BBSRC, the MRC and The Wellcome Trust.

Collaborators

Prof. Michael J. Holdsworth, University of Nottingham, Loughborough, UK
Prof. Guy A. Rutter, Imperial College London, UK
Dr. Frederica L. Theodoulou, Rothamsted Research, Harpenden, UK

Repair of essential terminal sequences by a negative stranded RNA virus.

Cheryl Walter and John Barr

The genomic termini of RNA viruses contain essential *cis*-acting signals for such diverse functions as packaging, genome translation, mRNA transcription and RNA replication, and thus preservation of their sequence integrity is critical for virus viability. Sequence alteration can arise due to cellular mechanisms that add or remove nucleotides from terminal regions, or alternatively from introduction of sequence errors through nucleotide mis-incorporation by the error-prone viral RNA dependent RNA polymerase (RdRp). To preserve template function, many RNA viruses utilize repair mechanisms to prevent accumulation of terminal alterations. Here we show that *Bunyamwera virus* (BUNV), the prototype of the *Bunyaviridae* family of segmented negative-sense RNA viruses, also can repair its genomic termini. When an intact non-translated region (NTR) was added to the anti-genomic 3' end, it was precisely removed, to restore both length and RNA synthesis function of the wild-type template. Furthermore, when up to 15 nucleotides were removed from the anti-genome 3' end, and replaced with a duplicate and intact NTR, both the external NTR was removed, and the missing nucleotides were restored, thus indicating that the BUNV RdRp can both remove and add nucleotides to the template. We show that the mechanism for removal of terminal extensions is likely that of internal entry of the viral RdRp during genome synthesis. In contrast we propose that repair of missing terminal nucleotides occurs through a RdRp-mediated homologous recombination event.

This mechanism is particularly interesting in the context of a segmented RNA virus such as BUNV, as it is possible that sequences from one segment may be used to repair the damaged sequences of another.

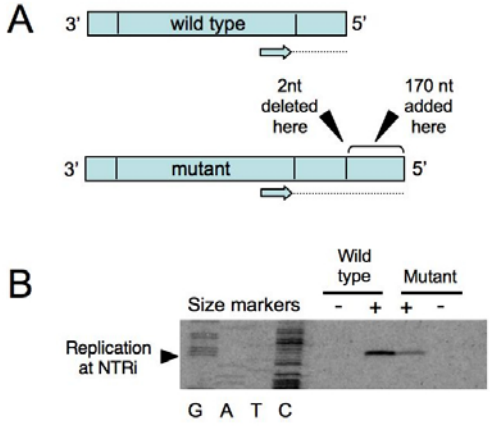

Figure 1: (a) schematic of wild-type and mutant Bunyamwera virus RNA templates. The mutant template has an additional 170 nucleotides at its 5' end, as well as 2 nucleotides deleted, as indicated. Primer extension analysis using a primer that anneals as indicated by the arrow can determine the length of the replicated RNA. **(b)** Primer extension analysis shows that following replication, the wild type and mutant templates are the same length, indicating both the removal additional nucleotides, and repair of the deleted nucleotides.

Publications

Walter, C. and Barr, J. (2010) Bunyamwera virus can repair both insertions and deletions during RNA replication. *RNA*, **16**:1138-1145.

Barr, J. and Fearns, R. (2010) How RNA viruses maintain their genome integrity. *J Gen Virol*, **91**:1373-1387.

Funding

Work in the Barr laboratory is funded by The Wellcome Trust, and the Health Protection agency, and is gratefully acknowledged.

Unravelling complexity in the energy landscape of proteins

Neal Crampton, Khalid Al-Zahrani Oliver Farrance, Simon Connell and David Brockwell

Introduction

Dynamic force spectroscopy is a powerful method able to probe the underlying features of the potential energy landscape of non-covalent interactions. This is achieved by applying a mechanical force in a defined direction to the particular interaction under study, whether this is a ligand-receptor interaction, or the ensemble of interactions in a natively folded protein polypeptide. Application of a force tilts the potential energy landscape exponentially increasing the unbinding or unfolding rate. When this force is applied at differing loading rates a dynamic force spectrum is obtained, from which the position and height of significant transition barriers along the unfolding (or rupture) pathway can be identified. These experiments can be conducted using optical tweezers, the biomembrane force probe, or the atomic force microscope (AFM). We use the latter instrument which is able to measure relatively high forces (above 25 pN) over short distances (nm), to investigate the effect of force on the non-covalent interactions that stabilise proteins and their complexes.

Extending the reach of AFM

The B1 domain of Protein L (herein referred to as protein L) is naturally expressed in *Peptostreptococcus magnus* as one of five homologous tandem domains which occur in the cell walls of 10% of isolates of this species. These domains bind to a range of immunogloblins with high affinity at a site distinct to the antigen binding site allowing the bacteria to evade the host's immune system. We have used the topologically simple protein L domain (Figure 1A) as a model protein with which to explore the determinants of mechanical strength and showed that this protein displays significant mechanical strength despite having no mechanical function. However, in order to fully explore the mechanical unfolding landscape it is necessary to characterise force induced unfolding of proteins over a wide range of pulling speeds. Conventional AFM apparatus is unable to achieve this because force is applied onto the biomolecular system via a compliant Hookean cantilever. This limits the dynamic range of the AFM, preventing the identification of unfolding barriers close to the native state. In addition, the recoil of the cantilever after unfolding may mask the presence of metastable intermediates.

To address these issues a new technique, constant deflection AFM (CD-AFM) has been developed in Leeds. This uses a secondary high powered feedback-controlled laser to lock the deflection of a commercially available AFM cantilever to a defined set-point. The laser drive voltage required to maintain the deflection set-point is then used to determine the force applied onto the protein. This allows constant velocity experiments, but without the need for a deflecting cantilever (Figure 1B). Measuring the dynamic force spectrum of a pemtameric construct of protein L using CD-AFM reveals two novel features:

(i) Two force regimes govern unfolding. The regime at low loading rates reports on the unfolding barrier we described previously using conventional AFM. At higher pulling velocities (greater than 400 nm/s) a previously hidden inner barrier becomes rate limiting in the unfolding pathway of protein L. This suggests that the energy landscape for protein unfolding is rougher than previously estimated and allows one protein to display very different mechanical behaviour under different levels of applied force.

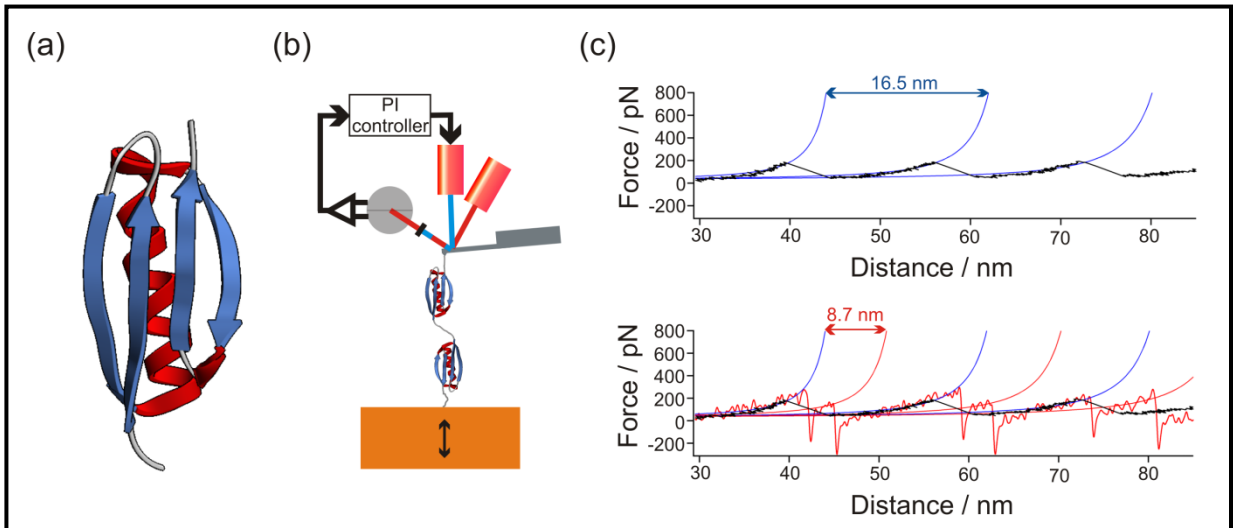

Figure 1: using CD- AFM to identify intermediates in the folding of protein L. **(a)** Three dimensional structure of the B1 domain from Protein L (pdb code: 1 Hz6). **(b)** Instrument design. In standard AFM, the deflection of a laser (red line) reflected of a cantilever of known spring constant is measured by the split photodiode (filled grey circle) and this is used to calculate the force applied onto the protein. In CD-AFM a secondary laser (blue line) deflects the cantilever to a set point. Feedback from the split photodiode varies the laser power to maintain to maintain the set-point deflection. **(c)** Identification of folding intermediates. Three unfolding events from a $(\text{protein L})_5$ polyprotein using standard AFM show 'saw-toothed' force-extension profiles (black line, top), reflecting a single unfolding step followed by entropic extension of the unfolded polypeptide chain (described by a worm-like chain, blue line). Overlaying these data with force-extension profiles for $(\text{protein L})_5$ obtained using CD-AFM (red line, bottom), shows an initial rising phase identical to that above, immediately followed by a second rising phase. This is due to partial folding of protein L under conditions of low levels of applied force immediately after unfolding.

(ii) protein L refolds via an intermediate. In standard AFM unfolding experiments, protein refolding is prevented by the recoil of the cantilever. Examination of the force-extension profile for $(\text{protein L})_5$ obtained using CD-AFM reveals the formation of a force-resistant intermediate (Figure 1C), approximately one third of the size of the natively folded protein. This highlights differences in vectorial folding where one or more ends of the protein are constrained (as occurs using CD-AFM and during translation on the ribosome) and classical *in vitro* folding studies that are triggered by dilution of dentaurant.

Publications

Sadler, D. Petrik, E., Taniguchi, Y. Pullen J., Kawakami, M., Radford, S. and Brockwell D. (2009) Identification of a mechanical rheostat in the hydrophobic core of protein L. *J Mol Biol* **393**:237-248.

Beddard, G. and Brockwell, D. (2009) A statistical approach to the estimation of mechanical unfolding parameters from the unfolding patterns of protein heteropolymers. *Phys Biol*, **7**:14001-14001.

Funding

We thank Keith Ainley for technical support and the BBSRC and EPSRC for funding. NC is an EPSRC Life Science Interface Research Fellow.

Collaborators

Godfrey Beddard, School of Chemistry, University of Leeds.
Emanuele Paci, Institute of Molecular and Cellular Biology, University of Leeds.
Masaru Kawakami, School of Materials Science, Japan Advanced Institute of Science and Technology, Japan.

Structural studies of the motor proteins dynein and myosin

Anthony Roberts, Bara Malkova, Yusuke Kato, Hiroshi Imai and Stan Burgess

Introduction/Background

Dynein is a family of minus-end directed microtubule motors that function in a wide diversity of cellular processes in eukaryotes including the trafficking of numerous cargoes (e.g. vesicles, mRNA, mitochondria), the positioning of the nucleus, Golgi apparatus and the mitotic spindle as well as driving the propagated-bending waves of cilia and flagella. Dynein is one of three different families of molecular motors, the others being kinesin and the actin-based motor myosin, and by far the least well understood. Dynein is large (~ 520 kDa), with a motor domain ~ten times larger than that of the other microtubule-based motor kinesin and has an evolutionary origin within the AAA+ superfamily of mechanoenzymes, unlike kinesin and myosin.

My lab is interested in discovering the mechanism of action of the motor domain of dynein. We have shown by electron microscopy (EM) that dynein has a stalk-head-tail structure. The head is ring-like and contains six AAA+ domains. ATP hydrolysis primarily in AAA1 drives the conformational changes associated with the power stroke and those governing its binding to and release from, the microtubule track via a small domain at the end of the ~12nm long anti-parallel coiled coil of the stalk.

In collaboration with Prof. Kazuo Sutoh's group (University of Tokyo) we mapped the locations of key sites within the motor domain using GFP-labeled fusion proteins and truncated motor domain constructs. We showed that the N-terminal sequence defines an elongated lever which undergoes a nucleotide-driven swinging action. We also showed that sliding of the two a-helices in the stalk governs microtubule-binding and ATP hydrolysis by dynein.

Main body

Studies in my lab are focused on understanding the structure and mechanisms of the molecular motor dynein alongside continuing studies of myosin motors in collaboration with Profs Peter Knight and John Trinick within the Astbury Centre.

My lab is pursuing the 3D structures of dynein by cryo-EM (in collaboration with Prof. Kazuhiro Oiwa's group, KARC, Kobe, Japan) and recombinant cytoplasmic dyneins (in collaboration with Prof. Sutoh and Dr. Kon, University of Tokyo), funded by BBSRC. In collaboration with Dr Andrerw Carter (LMB-MRC) we are examining by EM recombinant dynein's from fungi.

A new project funded by the Human Frontiers Science Program (HFSP) is to investigate the biochemical and biophysical properties of dimeric cytoplasmic dynein bound to microtubules as well as their structure(s) by cryo-EM. The collaborators in my team are Dr. Takahide Kon and Prof. Hideo Higuchi (University of Tokyo) and Dr. Andrej Vilfan (Ljubljana, Slovenia).

Finally, in collaboration with Dr. Tom Edwards (University of Leeds) and Dr. Dan Mulvihill (University of Kent), we are pursuing atomic resolution structures of subdomains of the motor. Expression trials of various subdomains are currently underway.

Publications

Kon, T., Imamula, K., Roberts, A., Ohkura, R., Knight, P., Gibbons, I., Burgess, S. and Sutoh, K. (2009) Helix sliding in the stalk of dynein modulates ATPase and microtubule binding. *Nat Struct Mol Biol* **16**:325-333.

Roberts, A., Numata, N., Walker, M., Malkova, B., Kon, T., Ohkura, R., Arisaka, F., Knight, P., Sutoh, K. and Burgess, S. (2009) AAA+ ring and linker swing mechanism in the dynein motor.*Cell* **136**: 485-495.

Oke, O., Burgess, S., Forgacs, E., Knight, P., Sakamoto, T., Sellers, J., White, H. and Trinick J. (2010) Influence of lever structure on myosin 5a walking. *Proc Natl Acad Sci USA* **107**:2509-2514.

Funding
This work is funded by BBSRC, HFSP and The Wellcome Trust.

Collaborators
Prof. Kazuhiro Oiwa and Dr Hitoshi Sakakibara, KARC, Kobe, Japan
Prof. Kazuo Sutoh and Dr. Kon, University of Tokyo, Japan
Dr. Andrew Carter, LMB-MRC, Cambridge, UK

Responsive biomaterials for medical applications

Rongjun Chen

Introduction

1. pH-responsive biomimetic polymers for drug delivery

Advances in genomics and proteomics have enabled the development of biomacromolecular drugs (e.g. nucleic acids and proteins) with potential for the treatment of a wide variety of diseases. Amongst other problems, their clinical applications may be impaired by degradation by lysosomal enzymes during uptake into cells. In order to achieve efficient intracellular delivery of such drugs, delivery systems are required that facilitate their release into the cytoplasm by destabilising endosomal membranes under mildly acidic conditions (pH 5.0–6.8). Amphiphilic polymers containing weakly ionizable carboxyl groups and hydrophobic alkyl side chains can mimic the cell-transduction function of viral peptides. Such polymers display a change of conformation from extended chains to collapsed, hydrophobically stabilized globular structures in response to acidification below their pKa ranges. This change leads to increased binding of polymers to eukaryotic cell membranes and subsequent membrane disruption. The pH-mediated conformational change depends principally on the balance between the hydrophobic interaction associated with hydrophobic moieties and the electrostatic repulsion resulting from charged carboxyl groups.

2. Biopolymer mediated trehalose uptake for enhanced erythrocyte cryosurvival

High viability storage of erythrocytes and nucleated mammalian cells is increasingly important in clinical medicine and biopharmaceutical development. Cryopreservation is currently the only technology that allows for reliable long term stabilization of most cells. As cryopreservation is traditionally accomplished using high concentrations of toxic vitrification agents, significant interest exists in the use of alternative protectants such as As disaccharides are normally impermeable to sugars, most notably trehalose. the phospholipid bilayer, the primary obstacle to the realization of viable cryopreservation of mammalian cells using trehalose is the requirement of high trehalose concentrations not only around but also within cells for optimum bioprotection. Delivery of trehalose into erythrocytes is notably challenging due to a lack of transduction pathways and safety concerns associated with the application of bacterial toxins to transfusion cells.

3. Parckaging cell lines for manufacturable viral vectors

Viruses dominate the types of vectors being tested in clinical gene therapy trials. Lentiviral vectors are attractive for gene therapy applications and their clinical promise for the treatment of HIV/AIDS has been demonstrated. Amongst other problems, the progress in lentiviral gene therapy has been hampered by the requirement for production of purified lentiviral vectors with high titre. Viruses are often purified using conventional downstream processing methods including density-gradient centrifugation, precipitation and filtration. These processes are time-consuming and some are scale limited and generally result in low recoveries of infectious viral particles. Ion-exchange chromotagraphy has been used in the multi-step purification of lentiviral vectors for at least one Phase 1 clinical trial. However such low specificity processes are now almost entirely superseded by affinity processes in order to exploit the resolution and simplicity of such chromatography.

Main body

1. pH-responsive biomimetic polymers for drug delivery

We have developed novel pH-responsive, endosomal-membrane-disruptive, metabolite-derived polymers by grafting hydrophobic amino acids — valine, leucine, and phenylalanine — onto the carboxylic acid moieties along the backbone of poly(L-lysine iso-phthalamide), which is a polyamide synthesized from tri-functional amino acids and diacyl chlorides. These biodegradable polymers were designed to mimic factors that enable efficient viral transfection, but they are safer and have more controllable structures. The effects of hydrophobicity and structure of grafted side chains and degree of grafting on the pH responsiveness of polymer conformation and aggregation, cell-membrane-disruptive activity, in-vitro cytotoxicity, and intracellular trafficking of the grafted polymers have been demonstrated. Of these derivatives, the polymer with the optimal properties for endosomal membrane disruption is the phenylalanine derivatized polymer PP-75 at a stoichiometric degree of substitution of 75 mol% (Mn = 24.9 kDa, degree of grafting = 63.2%). In sheep erythrocyte models of endosomes, PP-75 was 35-fold more membrane disruptive on a molar basis than the highly lytic bee-sting peptide melittin at pH 6.5, within the pH range characteristic of early endosomes. These polymers were not cytotoxic toward mammalian cells. It has been demonstrated in-vitro that, in cultured mammalian cells, the amphiphilic polymers displayed endosomolytic behaviour and facilitated targeted delivery of drugs, including doxorubicin, MBP-apoptin fusion protein and siRNA, very efficiently to the cytoplasm and nucleus, indicating promising applications for disease therapy (Figure 1).

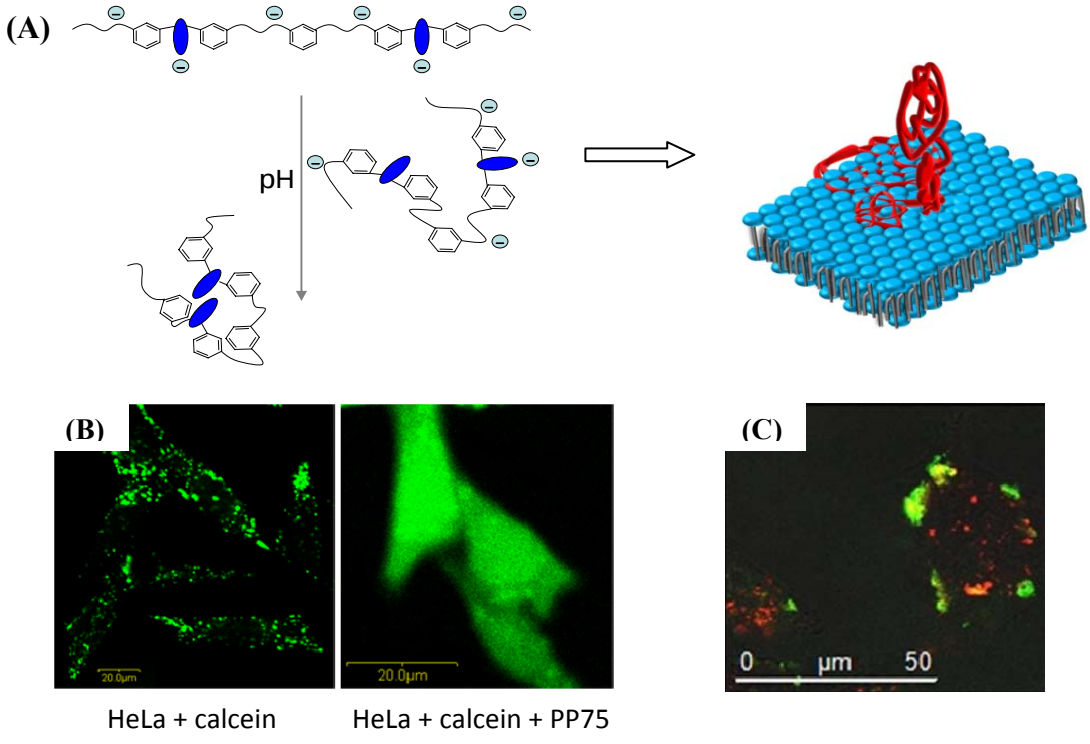

Figure 1: (A) schematic pH-responsive conformational change of polymers and resultant membrane disruption. **(B)** Endosomal release of endocytosed membrane-impermeable calcein in HeLa cells following pH-responsive polymer (PP-75) mediated membrane disruption. [calcein] = 2 mg mL^{-1}; [PP-75] = 0.1 mg mL^{-1}; cells were imaged at 3.5 h of further incubation after 30 min of treatment. **(C)** Nuclear translocation of therapeutic protein MBP-apoptin-AF647 (red) following PP-75-FITC (green) mediated endosomal release in Saos-2 cells. [PP-75-FITC] = 100 mg mL^{-1}; [MBP-apoptin-AF647] = 33 mg mL^{-1}; cells were imaged at 5 h further incubation after 1 h of treatment.

2. Biopolymer mediated trehalose uptake for enhanced erythrocyte cryosurvival

The abovementioned pH-responsive biopolymers designed for drug delivery have also been been shown to facilitate efficient delivery of trehalose, a bioprotectant normally impermeable to the phospholipid bilayer, into ovine erythrocytes. Cellular uptake of trehalose was found to be dependent on polymer pendant amino acid type and degree of grafting, polymer concentration, pH, external trehalose concentration, incubation temperature and time (Figure 2). Under optimized conditions, an intracellular trehalose concentration of 123 ± 16 mM was achieved; this loading resulted in 83 ± 3 % erythrocyte survival after freeze-thaw, an improvement of 20.4 ± 5.6 % in cryosurvival over unloaded erythrocytes. Intracellular trehalose was shown to impart cellular osmoprotection up to an external osmolarity of 230 mOsm and increased osmotic sensitivity above this threshold. Both effects were approximately proportional to intracellular trehalose concentration. Biopolymer mediated membrane permeability was shown to be rapidly and completely reversible via washing with phosphate buffered saline. These results provide a foundation for the cryopreservation of erythrocytes using non-toxic sugars and a step towards viable lyophilization of erythrocytes and other mammalian cells. An international patent application claiming the use of the amphiphilic biopolymers for biopreservation of live cells has just been filed in early 2010.

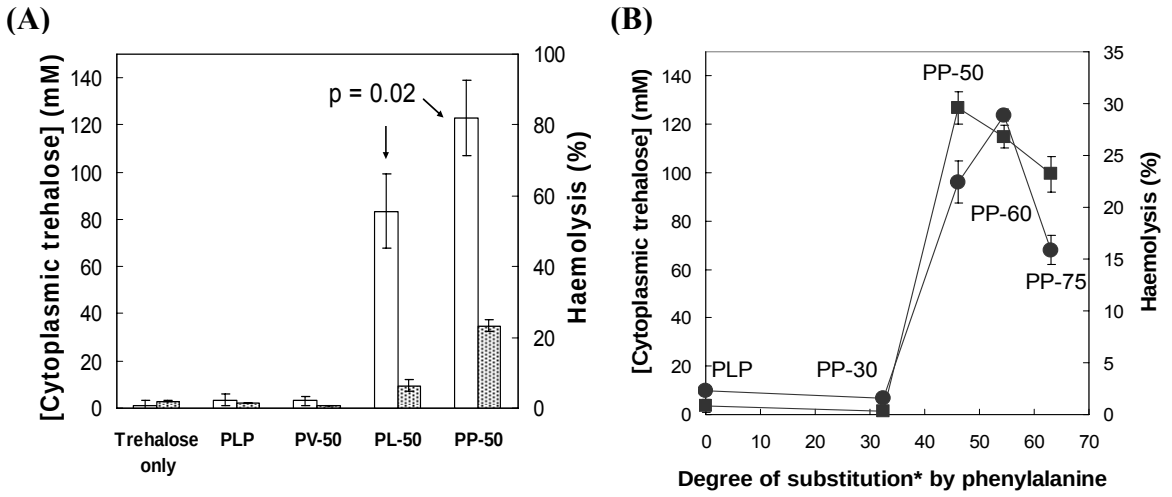

Figure 2: (A) Impact of polymer pendant group on trehalose loading (blank) and haemolysis (stippled). **(B)** Impact of polymer degree of substitution by phenylalanine on trehalose loading (■) and haemolysis (●). [Trehalose] = 0.36 M; [polymer] = 100 μg mL^{-1}; temperature = 37°C; pH = 7.05; incubation time = 9 hrs. *Degree of substitution is defined as the number of phenylalanine grafts per 100 carboxylic acid groups and determined by ^{1}H-NMR in d_6-DMSO at room temperature. Data were derived from four replicates. Error bars represent standard deviations.

3. Packaging cell lines for manufacturable viral vectors

We have developed technologies to label cell surfaces by both chemical and metabolic biotinylation. We have engineered a novel human 293T based packaging cell line BL15, which metabolically produces spontaneously biotin-tagged lentiviral vectors requiring only biotin in the culture medium. This metabolic biotinylation strategy in manufacturing is limited because: (i) the crude supernatants containing biotinylated viruses are contaminated with competing free-biotin; (ii) the high-affinity binding of biotin to streptavidin makes it unsuitable for processes requiring efficient elution of viruses from affinity supports under physiological conditions. To address these two limitations, We have chemically synthesized 7,8 diaminopelargonic acid (7-DAPA), which is a precursor to desthiobiotin in *Escherichia coli* and has no affinity for streptavidin. A new packaging cell line, DBL, has been developed

by cloning and expressing synthase bioD in BL15 cells such that 7-DAPA is then converted back into desthiobiotin inside the cell by the enzymatic action of bioD (Figure 3A). Thus we will be able to provide a feedstock of viruses for purification which are affinity tagged with desthiobiotin, but with no competition from free avidin-binding contaminants. Desthiobiotin has a lower affinity for streptavidin than biotin, and the labelled vectors are therefore more amenable to gentle elution strategies. This novel 7-DAPA mediated desthiobiotinylation technology enables affinity-mediated paramagnetic-particle and chromatographic capture and recovery of lentiviral particles with a very high purity in a highly efficient and fast way (overall recovery of infectious lentiviruses at 68% and the majority were eluted within 45 min) (Figure 3B). The technology can provide a generic simple affinity recovery process for scalable production of viral vectors for clinical gene therapy. An international patent application claiming this technology has just been filed in early 2010.

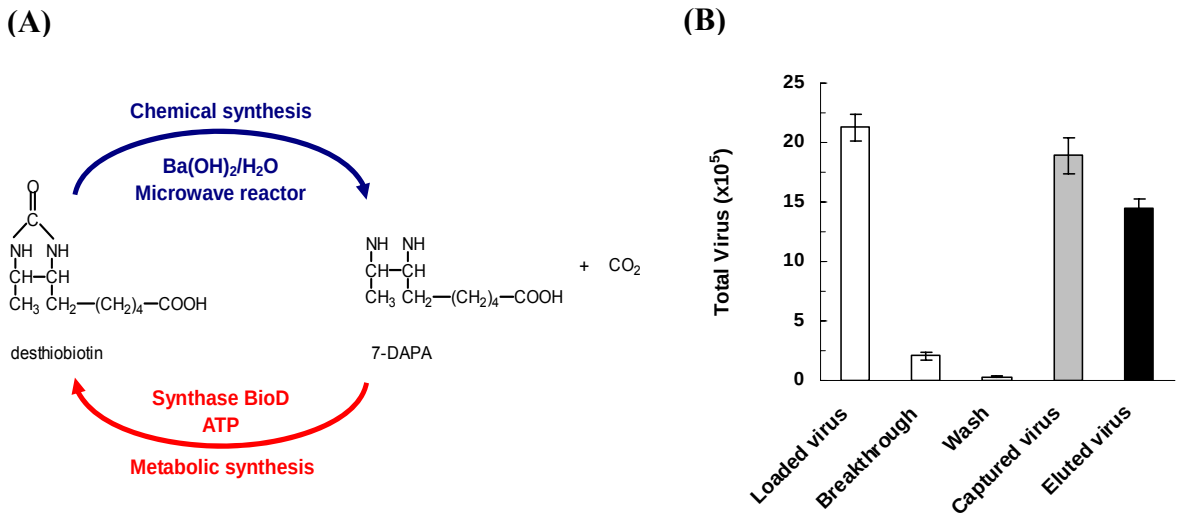

Figure 3: (A) Chemical synthesis of 7-DAPA from desthiobiotin, followed by metabolic synthesis back to desthiobiotin in engineered eukaryotic cells. **(B)** Column-based purification of lentiviral vectors produced from DBL cells in contact with 2 mM 7-DAPA. Monomeric avidin coated columns (Pierce, 2 mL) were loaded with 12 mL of crude, 7-DAPA containing lentiviral feedstocks by gravity flow, washed with 8 mL of PBS buffer, and eluted with 22 mL of 2 mM biotin. Column fractions of breakthrough, wash and elution were analyzed after infection by flow cytometric analysis of the percentage of GFP expressing cells.

Publications

Chen, R., Khormaee S., Eccleston, M., Slater, N. (2009). The role of hydrophobic amino acid grafts in the enhancement of membrane-disruptive activity of pH-responsive pseudo-peptides. *Biomaterials* **30**:1954-1961.

Chen, R., Eccleston, M., Yue, Z. and Slater, N. (2009). Synthesis and pH-responsive properties of pseudo-peptides containing hydrophobic amino acid grafts. *J Mater Chem* **19**:4217-4224.

Chen, R., Khormaee, S., Eccleston, M. and Slater, Nigel (2009). Effect of L-leucine graft content on aqueous solution behaviour and membrane-lytic activity of a pH-responsive pseudo-peptide. *Biomacromolecules* **10**:2601-2608.

Liechty, W., Chen, R., Farzaneh, F., Tavassoli, M. and Slater, N. (2009). Synthetic pH-responsive polymers for protein transduction. *Adv Mater* **21**:3910-3914.

Ho, V., Barcza, A., Chen, R., Müller, K., Darton, N. and Slater, N. (2009). The precise control of cell labelling with streptavidin paramagnetic particles. *Biomaterials* **30**:6548–6555.

Funding
This work was supported by BBSRC, Pfizer Inc and Gates Cambridge Trust.

Collaborators
Prof Nigel K.H. Slater, Department of Chemical Engineering and Biotechnology, University of Cambridge.
Profs Farzin Farzaneh and Mahvash Tavassoli, Department of Haematological and Molecular Medicine, King's College London.

Single molecule characterisation of protein folding and dynamics

Lorna Dougan

Introduction

Significant progress has been made in our understanding of the folding of small globular proteins under simple in vitro conditions. This work has set the stage for discovering new principles that govern the folding of larger proteins under conditions that more closely mimic the cellular environment. In order to produce a comprehensive understanding of protein folding and dynamics that brings us closer to biological conditions, our research will strive towards developing quantitative experimental tools to explore the folding dynamics of single proteins in interesting solvent environments. The outcome of this research will set the stage for providing an integrated picture of the folding and dynamics of single proteins in these environments and has strong potential to lead to other significant research projects.

The Research

In recent years single molecule force-clamp spectroscopy has emerged as a powerful tool to explore the mechanical stability and folding pathways of individual proteins (Figure 1).

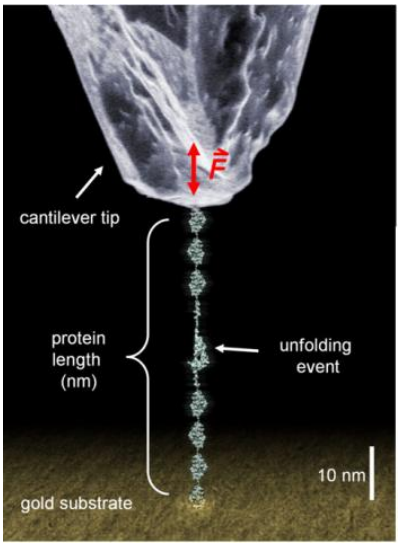

Figure 1: In a force-clamp experiment a single polyprotein is held between a cantilever tip and the substrate, at a constant stretching force. Unfolding of a single protein results in a staircase-like elongation of the protein as a function of time.

This technique is used to apply a constant stretching force along a well-defined reaction coordinate, the end-to-end length of the protein, driving proteins to a fully extended unfolded state. We have built a new force-clamp instrument, adding to the existing single molecule instrumentaion currently available at Leeds and the UK. By measuring the unfolding and folding trajectories of individual proteins as a function of force, insight can be gained into the physical mechanisms of protein folding. In particular, recent studies have demonstrated that this technique can be used to capture the role of solvent molecules, such as the cryoprotectant glycerol, in protein folding. These experiments of protein unfolding in aqueous glycerol solutions suggested that glycerol molecules are actively involved in the unfolding transition state structure of a protein. We have demonstrated that the collapse mechanism of a single extended protein can be probed. In particular, we have shown that specific solvent environments can be utilized to tune the strength of hydrophobic collapse in an individual protein (Figure 2). We have investigated the effect of solvent environment on the transition state geometry of a disulphide bond reduction in a protein by incorporating glycerol into the solution, providing a direct test of theoretical calculations of the role of solvent molecules in the reduction reaction. We have completed an array of force-clamp experiments to identify

the role of solvent hydrogen bonds in protein folding and chemical reactions. Furthermore we have recently developed a strategy to generate an experimental fingerprint to unambiguously

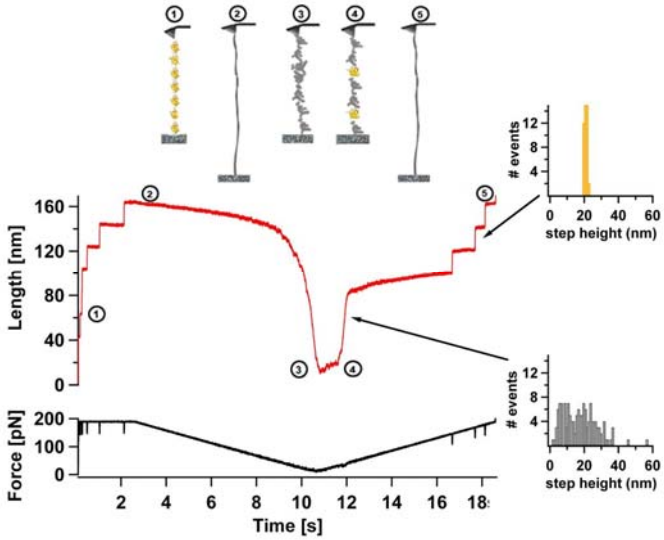

Figure 2: Force-clamp trajectories of polyproteins provide a characteristic staircase-like pattern that serves as a fingerprint of single molecules in experiments of mechanical unfolding and refolding. The ubiquitin polyprotein is first unfolded under a constant force of 190 pN during 2.5 s, resulting in a well-defined series of step increases in length of 20 nm that mark the unfolding and extension of the individual modules in the chain (1). The force is then relaxed linearly down to 10 pN, while monitoring the contraction of the end-to-end length of the highly extended ubiquitin polyprotein as it undergoes hydrophobic collapse (2-3). Upon reaching 10 pN, the force is linearly ramped back up again to 190 pN (4-5). When the force value reaches approximately 50–60 pN, the protein undergoes a heterogeneous stepwise extension marking the unraveling of the ensemble of collapsed conformations. At a much higher force of approximately 150 pN we observe the appearance of the 20 nm steps that mark the native ensemble.

identify and characterize single polyglutamine chains. Through a combination of force spectroscopy and polyprotein engineering this, and future work, has the ability to reveal critical information on the physics and function of biological machinery and self-assembly.

Publications

Dougan, L., Li, J., Badilla, C., Berne, B., and Fernandez, J. (2009) Single homopolypeptide chains collapse into mechanically rigid conformations, *Proc Natl Acad Sci USA*, **106**:12605-12610.

Garcia-Manyes, S., Dougan, L. and Fernandez, J. (2009) Osmolyte-induced separation of the mechanical folding phases of ubiquitin, *Proc Natl Acad Sci USA*, **106**: 10540-10545.

Garcia-Manyes, S., Dougan, L., Badilla, C., Brujic, J., and Fernandez, J. (2009) Direct observation of an ensemble of stable collapsed states in the mechanical folding of ubiquitin, *Proc Natl Acad Sci USA*, **106**: 10534-10539.

Funding

This work is being funded by EPSRC (2010-EP/H020616/1)

Collaborators

Prof. Hui Lu, University of Chicago, USA
Prof. Bruce Berne, Columbia Univeristy, USA

The molecular basis for cellular asymmetry

Huw Jenkins, Miriam Walden and Thomas Edwards

Introduction

Control of eukaryotic gene expression at the translation level is vital for many important physiological processes. This control is mediated by hundreds of cytoplasmic RNA binding proteins (RBPs) that regulate the processing, localisation, translation and decay of mRNA. One well characterised example of the importance of translational control by RBPs occurs in *Drosophila* where repression of translation of localised maternal mRNA is required for anterior/posterior patterning during early embryogenesis. Pumilio (Pum) binds to a pair of specific sequences termed the Nanos response elements (NREs) in the 3'-UTR of *hunchback* (hb) mRNAs and represses translation through recruitment of Nanos (Nos) and Brain Tumor (Brat) proteins.

Later in development, RNA and protein components of neuroblast stem cells are segregated during asymmetric cell division. One daughter cell remains a stem cell whereas the other terminally differentites into neuorns. Miranda is a scaffold protein for the recruitment of Prospero, Inscuteable and more which are localised by molecular motors during cell division such that the cargoes are delivered appropriately.

We are using structural biology especially X-ray crystallography to investigate the protein-protein and protein-RNA complexes controlling these processes.

Structure of mouse Pum2

Puf proteins control translation through the interaction of a C-terminal Puf-domain with specific sequences present in the 3' untranslated region of messenger RNAs. In *Drosophila*, binding of the protein Pumilio to mRNA leads to translational repression, which is required for anterior/posterior patterning during embryogenesis. The vertebrate Pumilio homologue 2 (Pum2) has been implicated in controlling germ cell development through interactions with the RNA-binding proteins Deleted in Azoospermia (DAZ), DAZ-like (DAZL) and Boule. We present the 1.6 Å resolution X-ray crystal structure of the Puf domain from murine Pum2 (Figure 1) and demonstrate that this domain is capable of binding with nanomolar affinity to RNA sequences (Figure 2) from the *hunchback* Nanos response element (NRE) and a previously identified Pum2 binding element (PBE).

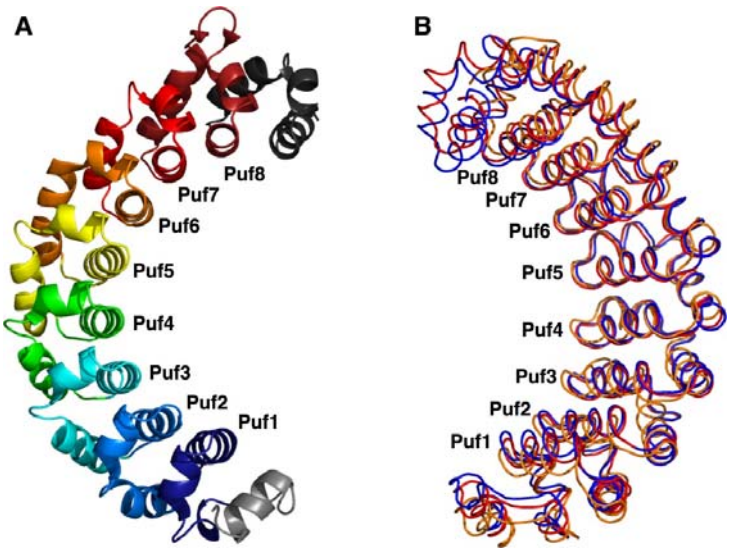

Figure 1: (A) the 1.6 Å X-ray crystal structure of the Puf domain of mouse Pumilio-2. **(B)** superposition of mPum2 (blue) with human Pum1 (red) and *Drosophila* Pumilio (orange). Puf repeats 1-8 are labeled. For clarity, the orientation in (B) is rotated about the y-axis by ~220° compared to (A).

Asymmetric Cell Division in Drosophila Neuroblasts

Asymmetric cell division plays a key role in the development of many organisms. This process allows a small group of multipotent stem cells to repeatedly divide and differentiate to generate a vast number of functionally diverse cells. In the developing *Drosophila* CNS, stem cell-like neuroblasts undergo asymmetric cell division to produce 2 daughter cells, a new neuroblast and a smaller ganglion mother cell (GMC). The GMC divides again to produce two terminally differentiated neurons and glia. During mitosis of these neuroblasts, several molecules have been shown to be asymmetrically localised and partitioned into the GMC, including *prospero* mRNA and Miranda, Brat and Prospero proteins. These proteins act in the GMC to determine neuronal cell fate. Asymmetric localisation is dependent on the interactions between these proteins but it is unknown exactly how they occur.

The aim of this project is to study the structural mechanisms behind asymmetric cell division using X-ray crystallographic and biochemical/physical techniques. We are trying to express fragments of these proteins that interact, to study complex formation in vitro and to elucidate the structures of these proteins both individually and in their complexes.

Publications

Jenkins H., Baker-Wilding R. and Edwards T. (2009) Structure and RNA binding of the mouse Pumilio-2 Puf Domain. *J Struct Biol* **167**:271-6.

Gupta Y., Lee T., Edwards T., Escalante C., Kadyrova L., Wharton R. and Aggarwal A. (2009). Co-occupancy of two Pumilio molecules on a single hunchback NRE. *RNA.* **15**:1029-35.

Funding

We gratefully acknowledge BBSRC, The Wellcome Trust, the Royal Society, Yorkshire Cancer Research and The European Research Council for financial support of this research.

Collaborators

We gratefully acknowledge Aneel Aggarwal (Mt. Sinai Med. School, New York), and Robin Wharton (Ohio State) for materials and discussion.

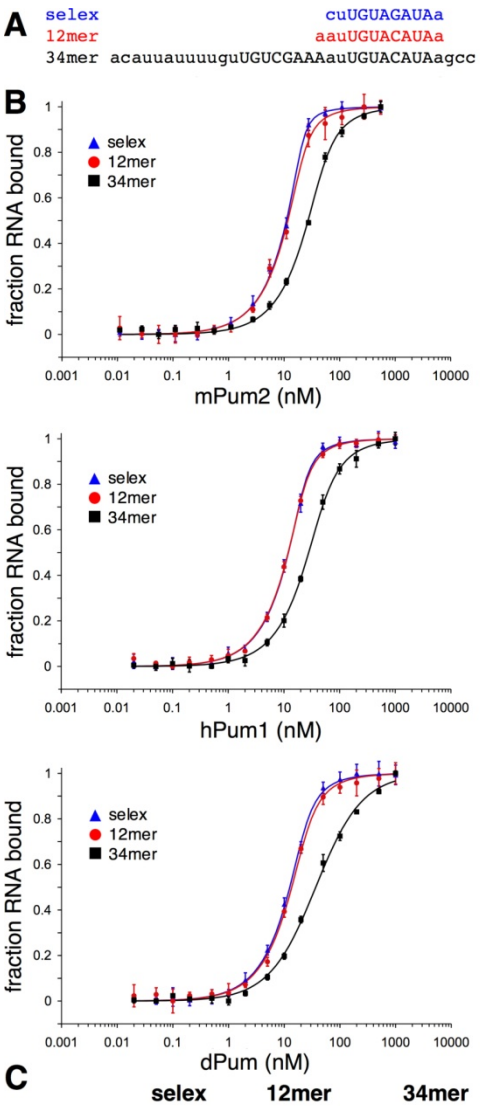

Figure 2: Binding of mouse Pum2, human PUM1 and *Drosophila* Pumilio to RNA. **(A)** RNA sequences used in the fluorescence polarisation binding experiments with the 8 bases that bind to the 8 Puf repeats shown in upper case. **(B)** Binding isotherms (mean and standard deviation from experiments performed in triplicate) for mouse Pum2 (mPum2), human PUM1 (hPum1) and *Drosophila* Pumilio (dPum) binding to the RNA sequences shown in (A). **(C)** Dissociation constants (nM) ± standard error from fits to data in (B).

Targeting viral ion channels for therapy

Toshana Foster, Mark Verow, Jamel Mankouri, Lynsey Corless, Elizabeth Atkins, Barnabas King, Carsten Zothner, Mark Harris and Stephen Griffin

Introduction/Background

In 2002/3 we demonstrated that the hepatitis C virus (HCV) p7 protein formed an oligomeric ion channel whose activity was blocked by the antiviral drug, amantadine. HCV represents a massive global health concern, infecting 170-200 million individuals and causing severe liver disease including cirrhosis and hepatocellular carcinoma. Current therapies for HCV are inadequate and the speed of new drug development may not be sufficient to avoid the onset of resistance, generating an urgent need to expand the repertoire of HCV drug targets.

p7 inhibitors are able to prevent the production of infectious virions in the HCV culture system, providing proof of concept for their efficacy. We are applying both rational and high throughput approaches to the development of novel p7 inhibitors as well as studying HCV assembly as a therapuetic target. In addition, we are applying techniques developed during the study of p7 to ion channels from other clinically important viruses including influenza, papillomavirus, respiratory syncitial virus and viral encephalitis/haemorrhagic fevers.

Current Projects:

1) Validating p7 inhibitors by identifying resistance determinants: The evolution of resistance is indicative of the specific effects of antiviral drugs. In collaboration with Prof. Colin Fishwick, we have identified that a mutation observed in amantadine clinical trials represents a genuine amantadine resistance mutation. Using this information, we have developed detailed molecular models for the hepatameric p7 ion channel complex and determined the binding site for drugs like amantadine (Figure 1). This is a key finding for the rational devlopment of novel inhibitors.

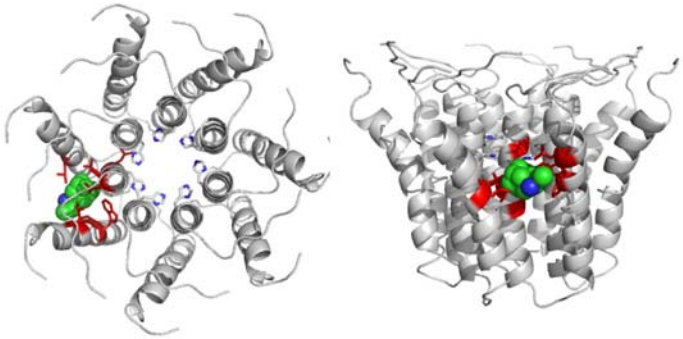

Figure 1: rimantadine bound to the heptameric p7 channel complex.

2) The structure of the p7 ion channel by NMR: With Prof. Steven Homans, we have solved the solution structure of monomeric p7 (Figure 2) and are making great progess on the complete channel complex. This information will enable both the refinement of rational drug design and the study of protein-drug dynamics in solution.

3) Rational and high throughput antiviral development: We previously developed a rapid throughput assay for channel activity that was amenable to 384+ well formats. In collaboration with Prof Fishwick and Dr Richard Foster we are optimising this system for the high throughput screening of compound libraries. In addition, our molecular models and structural data permit *in silico* high throughput screening, as well as fragment-based drug design using the in-house SPROUT programme developed by Prof. Fishwick. Combining these approaches is generating novel compounds for testing in HCV culture and will provide the platform for future drug discovery.

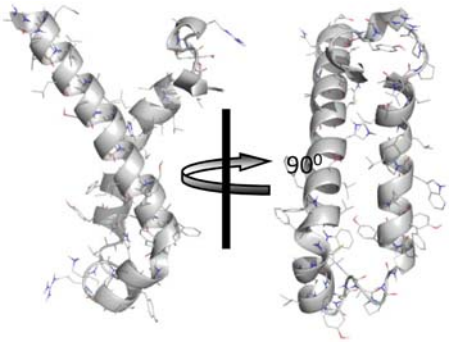

Figure 2: p7 solution NMR structure.

4) The role of p7 during the HCV life cycle: With Prof Steven Weinmann (University of Kansas, USA), we have recently demonstrated p7 proton channel activity in live cells infected by HCV. Furthermore, we have shown that this activity is specifically required for the formation of new virions and correlated the effects of antiviral drugs with its inhibition. We are mapping the effects this activity has on de novo virus particles and alternative points in the HCV life cycle where drugs may have an effect. In addition, we are investigating non-ion channel functions of p7, including its interaction with the viral NS2 protein.

5) Cellular pathways involved in HCV assembly: HCV must hijack cellular processes in order to form new virions, acquire a membrane envelope and traffic virions to the cell surface where they are released. In collaboration with Dr Colin Crump (University of Cambridge), we recently demonstrated that HCV requires the cellular Endosomal Sorting Complex Required for Transport, or "ESCRT" complex, in order to secrete infectious virions. We are going on to map the precise route that virions take as they leave the cell and critical cellular factors involved. Inhibiting these virus-host interactions could be a future target for antivirals.

6) Targeting other viroporins for therapy: The framework developed for the study of p7 can readily be applied to other viral ion channels. We have therefore extended our interests to include proteins from highly pathogenic influenza in collaboration with Dr Paul Targett-Adams (Pfizer, UK), papillomavirus with Dr Andrew Macdonald, respiratory syncitial virus (RSV) with Dr John Barr and flaviviruses that cause arthropod-bourne encephalitis and haemorrhagic fevers.

Publications

Adair, R., Patel, A., Corless, L., Griffin, S., Rowlands, D. and McCormick, C. (2009) Expression of hepatitis C virus (HCV) structural proteins in *trans* facilitates encapsidation and transmission of HCV subgenomic RNA. *J Gen Virol*, **90**:833-842.

Griffin, S. (2009) Plugging the holes in hepatitis C virus antiviral therapy. *Proc Natl Acad Sci USA*, **106**:12567-12568.

Hughes, M., Griffin, S. and Harris, M. (2009) Domain III of NS5A contributes to both RNA replication and assembly of hepatitis C virus particles. *J Gen Virol*, **90**:1329-1334.

Hughes, M., Gretton, S., Shelton, H., Brown, D., McCormick, C., Angus, A., Patel, A. Griffin, S. and Harris, M. (2009) A conserved proline between domains II and III of hepatitis C virus NS5A influences both RNA replication and virus assembly. *J Virol*, **83**:10788-10796.

StGelais, C., Foster, T., Verow, M., Atkins, E., Fishwick, C., Rowlands, D., Harris, M. and Griffin, S. (2009) Determinants of hepatitis C virus p7 ion channel function and drug sensitivity identified *in vitro*. *J Virol*, **83**:7970-7981.

Mankouri, J., Dallas, M., Hughes, M., Griffin, S., Macdonald, A., Peers, C. and Harris, M. (2009) Suppression of a pro-apoptotic K+ channel as a mechanism for hepatitis C virus persistence. *Proc Natl Acad Sci USA* **106**:15903-15908.

Corless, L., Crump, C., Griffin, S. and Harris, M. (2010) Vps4 and the ESCRT-III complex are required for the release of infectious hepatitis C virus particles. *J Gen Virol*, **91**:362-372.

Griffin, S. (2010) Inhibition of HCV p7 as a therapeutic target. *Curr Opin Investig Drugs*, **11**:175-181.

Funding

Work in the laboratory is funded by grants from the MRC, Wellcome Trust (JM), Pfizer and the Royal Society. EA received Pfizer-funded CASE studentship from the BBSRC, and MV also received a BBSRC studentship. TF is funded by the Wellcome Trust PhD programme. SG is UoL Biomedical Health Research Centre Senior Translational Research Fellow.

Collaborators

Prof Steven Homans (UoL), Dr Andrew Macdonald (UoL), Prof Colin Fishwick (UoL), Dr Richard Foster (UoL), Dr John Barr (UoL), Prof Steven Weinmann (University of Kansas), Dr Paul Targett-Adams (Pfizer, UK), Dr Nicola Rose (NIBSC), Dr Alain Kohl (University of Edinburgh), Prof Wendy Barclay (Imperial)

Studies on hepatitis C virus replication and pathogenesis

Jamel Mankouri, Mair Hughes, Toshana Foster, Lynsey Corless, Bjorn-Patrick Mohl, Barnabas King, Zsofia Igloi, Doug Ross, Elizabeth Atkins, Carsten Zothner, Arwen Pearson, Steve Griffin and Mark Harris

Hepatitis C virus (HCV) infects 170 million individuals and is a major cause of chronic liver disease, including fibrosis, cirrhosis and hepatocellular carcinoma. The virus has a single stranded positive sense RNA genome of 9.5kb that contains a long open reading frame encoding a single polyprotein of 3000 amino acids which is cleaved into 10 individual polypeptides by a combination of host cell and virus specific proteases. The molecular mechanisms of virus replication and pathogenesis remain to be elucidated, however, recently a clone of the virus that is able to replicate in cell culture has been identified and we are using this model extensively to understand how the virus replicates and causes pathology.

A major focus of work is the NS5A protein, particularly in terms of perturbation of cellular signalling pathways. We showed that NS5A disrupts oxidative stress induced p38 MAPK signalling and prevents the activation of a pro-apoptotic potassium channel, Kv2.1. This exciting observation is one of the first documented specific effect of virus infection on the activity of a host cell ion channel.

We are also investigating the role of NS5A in virus replication. We are generating a series of NS5A mutants – particularly in PxxP motifs that interact with cellular SH3 domains – to characterise the role of these interactions in viral replication. These data have revealed genotype specific differences with regard to the requirement for specific proline residues. We have also focussed on domain III of NS5A - mutagenesis has revealed a role for serine residues in this domain in virus assembly but not RNA replication.

Structural studies are ongoing - we are investigating the structure of domains II and III of NS5A by NMR, these experiments suggest that both domains are natively unfolded. Additionally we have analysed the ability of NS5A to bind to RNA and have shown that all three domains contribute to this activity.

Further studies are investigating the role of the cellular ESCRT pathway for release of infectious virus particles, and also the potential interplay between HCV and autophagy.

Publications:

Hughes, M., Gretton, S., Shelton, H., Brown, D., McCormick, C., Angus, A., Patel, A., Griffin, S. and Harris, M. (2009) A conserved proline between domains II and III of hepatitis C virus NS5A influences both RNA replication and virus assembly. *J Virol*, **83**:10788-10796.

Hughes, M., Griffin, S. and Harris, M. (2009) Domain III of NS5A contributes to both RNA replication and assembly of hepatitis C virus particles. *J Gen Virol* **90**:1329-1334.

Mankouri, J., Dallas, M., Hughes, M., Griffin, S., MacDonald, A., Peers, C. and Harris, M. (2009) Suppression of a pro-apoptotic K+ channel as a mechanism for hepatitis C virus persistence. *Proc Natl Acad Sci USA*, **106**:15903-15908.

Corless L., Crump C., Griffin S. and Harris M., (2010) Vps4 and the ESCRT-III complex are required for the release of infectious hepatitis C virus particles. *J Gen Virol* **91**:362-372.

Funding
This work is funded by the Wellcome Trust, MRC, Yorkshire Cancer Research and BBSRC.

Collaborators
Chris Peers, Faculty of Medicine and Health, University of Leeds.
Colin Crump, University of Cambridge
Kalle Saksela, University of Helsinki, Finland
John McLauchlan, MRC Virology Unit, Glasgow
Mair Hughes and Doug Ross hold Arrow Therapeutics CASE studentships, Bjorn Patrick Mohl holds a Glaxo-Smith Kline CASE studentship and Elizabeth Atkins holds a Pfizer CASE studentship.

Characterisation of the Mhp1 hydantoin transport protein

Scott Jackson, Ekaterina Ivanova, Katie Simmonds, David Sharples, Nicholas Rutherford, Jonathan Hadden, Jocelyn Baldwin, Lynsey Jones, Alison Ashcroft, Colin Fishwick, Peter Johnson, Stephen Baldwin and Peter Henderson

Introduction

Members of the Nuclobase-Cation-Symport (NCS-1) family of membrane transport proteins are widely distributed in eubacteria and fungi. Genes encoding family members have also been identified in green plants and archaea, although no functional characterisation of such proteins is yet reported. No NCS-1 family transporters have yet been found in metazoans. The mechanism by which transport is energised in these proteins was previously unclear, but the elucidation of the three outward-open, substrate-occluded, and inward-open structures of Mhp1 in a collaboration with Imperial College and Oxford have now clarified the 'alternating access' cycle of reciprocating conformational changes that effect transport. In Leeds we are continuing to characterise the biochemistry of the Mhp1 protein by a number of the following biophysical and genetical approaches.

Results

An SeMet-labelled His-tagged Mhp1 protein has been prepared in Leeds and supplied to So Iwata and his collaborators at Imperial College and the Membrane Protein Laboratory at the Diamond Light Source. Hexagonal crystals different from those previously obtained provided diffraction data sufficient to determine the structure of an inward-facing form at 3.8Å resolution in which the sodium-binding site was essentially abolished. With the assistance of Molecular Dynamics Simulations done by Oliver Beckstein and Mark Sansom at Oxford a plausible model for the transitions between the three known conformations was derived and visualized as a movie. This model provides a sound basis to design experiments for elucidating the roles of ligand binding and individual amino acid residues in effecting the conformational changes.

Binding of sodium and hydantoin to Mhp1 can be measured by spectrophoto-fluorimetry. The addition of BH elicits a modest quenching of the natural tryptophan fluorescence of the purified Mhp1 protein, which is readily interpreted in terms of two tryptophan molecules immediately adjacent to the hydantoin in its binding site. The rate of change of the fluorescence is not significantly changed in the presence of sodium when measured by stop-flow techniques, but the extent of the fluorescence change is markedly enhanced. At the steady state the binding of the hydantoin is characterized by an apparent affinity about 10-fold higher in the presence of 15mM sodium.

The extent of the fluorescence change is modified by the alteration of key amino acids in the structure of the protein. So far, twelve mutations have been made, and the ligand binding properties of about half examined. Some of the mutations apparently enhance the binding of sodium/BH, some depress the binding, and some have no effect.

There are three cysteine residues in Mhp1, and dynamic simulations performed in a collaboration with Oxford predict that their accessibility to the aqueous phase varies considerably between the individual residues, and that this is altered quite profoundly by a change of the conformation of Mhp1. These predictions are being tested by measuring the rates of reaction of the cysteine residues with N-ethylmaleimide, and also by altering each of the cysteines separately into an unreactive residue using mass spectrometry to detect and identify reactivity of each cysteine.

Starting from the coordinates of the outward-facing and inward-facing forms of Mhp1, chemists at Leeds have employed *in silico* design and screening to devise a prioritised list of compounds likely to bind to Mhp1. Some of these are commercially available and some have been synthesized. The

fluorimetric assay method is unsuitable for a number of these that absorb at the excitation and/or emission wavelengths for tryptophan. Nevertheless, at least two of these compounds are already shown to be ligands for Mhp1.

By combining these approaches together and with others such as ITC and partial proteolysis we are seeking to establish the exquisite details of the molecular mechanism of one membrane transport protein that will apply, at least in part, to a wide variety of proteins of similar structure found in all organisms including man. A number of these are targets for clinical intervention, including in the treatment of diabetes and depression.

Publications

Blake, K., O'Neill, A., Mengin-Lecreuix, D., Henderson, P., Bostock, J., Dunsmore, C., Simmons, K., Fishwick, C., Leeds, J. and Chopra, I. (2009) The nature of *Staphylococcus aureus* MurA and MurZ and approaches for detection of peptidoglycan biosynthesis inhibitors. *Mol Microbiol*, **72**:335-343.

Jeuken, L., Weiss, S., Henderson, P., Evans, S. and Bushby, R. (2009) Impedance spectroscopy of bacterial membranes: Co-enzyme Q diffusion in a finite diffusion layer. *Anal Chem* **80**:9084-9090.

Psakis, G., Saidijam, M., Shibayama, K., Polaczek, J., Bettaney, K., Baldwin, J., Baldwin, S., Hope, R., Essen, L.-O., Essenberg, R. and Henderson, P. (2009) The sodium-dependent D-glucose transport protein of *Helicobacter pylori*. *Mol Microbiol*, **71**:391-403.

Tanabe, M., Szakonyi, G., Brown, K., Henderson, P., Nield, J. and Byrne, B. (2009). The multidrug resistance efflux complex, EmrAB from *Escherichia coli* forms a dimer *in vitro*. *Biochem Biophys Res Commun* **380**:338-342.

Weiss, S., Bushby, R., Evans, S., Henderson, P. and Jeuken, L. (2009) Characterization of cytochrome bo3 activity in a native-like surface-tethered membrane. *Biochem J* **417**:555-560.

Jones, L., Baldwin, S., Henderson, P. and Ashcroft, A. (2010). Defining topological features of membrane proteins by nanoelectrospray ionization - mass spectrometry. *Rapid Commun Mass Spectr* **24**:1-9.

Shimamura, T., Weyand, S., Beckstein, O., Rutherford, N., Hadden, J., Sharples, D., Sansom, M., Iwata, S., Henderson, P. and Cameron, A. (2010) Molecular basis of alternating access membrane transport by the sodium-hydantoin transporter Mhp1. *Science* **328**:470-473.

Funding

This work is funded by the BBSRC and the EU EMeP and EDICT consortia

Collaborators

Iwata, S., Cameron, A.D., Shimamura, T., Weyand, S., in the Membrane Protein Laboratory at the Diamond Light Source in Oxfordshire and Byrne, B. in Imperial College London with funding from the Wellcome Trust, the BBSRC and the EU EDICT grant.
Sansom, , M.S.P. and Beckstein, O. in the Structural Bioinformatics and Computational Biochemistry Unit specializing in membrane proteins at the University of Oxford funded by the EU EDICT grant.

Conformational changes during β_2-microglobulin amyloid assembly

Timo Eichner, Arnout Kalverda, Gary Thompson,
Sheena Radford and Steve Homans

Introduction

Numerous studies of amyloid assembly using different protein systems under a variety of conditions have indicated that partially unfolded states are responsible for initiating aggregation *in vitro* and *in vivo*; however, little is known about the structure of key amyloid intermediates in atomic detail. Here we use ΔN6, a truncation variant of the naturally amyloidogenic protein β_2-microglobulin (β_2m), to determine, for the first time, the structure of a non-native amyloidogenic intermediate at high resolution in solution using nuclear magnetic resonance (NMR)

Real-time NMR refolding studies confirm the structural analogy of ΔN6 and I_T

In order to validate whether the non-native slow folding intermediate I_T shares a common structure with ΔN6, wild-type β_2m was denatured in 8 M urea and then refolded by ~10-fold dilution of the denaturant in 25 mM sodium phosphate pH 7.5 at 25°C. The re-equilibration back to the native state via the trapped amyloidogenic intermediate I_T state was monitored using SOFAST- ^{1}H-^{15}N HMQC spectra at 25°C acquired ~2 min after dilution. Figure 1A shows the superposition of the ^{1}H-^{15}N spectra of ΔN6 and the kinetic intermediate I_T. After ~2 min of refolding the spectrum (Figure 1) is predominantly (>75%) I_T (Eichner *et al.*, 2009) and the spectra reveals 76 cross peaks corresponding to the I_T state 68 of which overlay well with those measured for ΔN6 (N_{WT}) (^{1}H/^{15}N within ± 0.05/0.5 ppm)

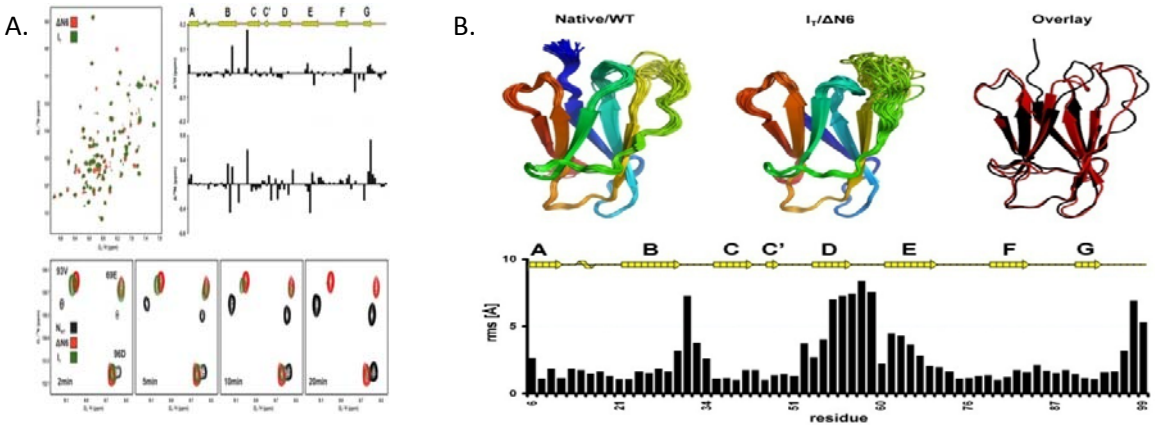

Figure 1: (A) ^{1}H-^{15}N-HSQC spectra of WT I_T state and ΔN6 β2M. **(B)** NMR solution structures of WT (left) and ΔN6 β2M (right).

The high-resolution solution structure of I_T reveals a native-like Ig fold

After having validated that ΔN6 mimics structurally the amyloidogenic intermediate I_T a full chemical shift assignment and structure calculation of the wild-type protein and ΔN6 was carried out at pH 7.5, and 25°C. The resulting structural ensembles (Figure 1B) revealed that ΔN6 has a native-like Ig β-sandwich fold, which is quite similar to the native fold with some loss of secondary structure elements and rearrangement of residues around Phe 30.

Publications

Eichner, T. and Radford, S. (2009) A Generic Mechanism of beta2-Microglobulin amyloid assembly at neutral pH involving a specific proline switch. *J Mol Biol*, **386**:1312-1326.

Funding

We are grateful to the University of Leeds for financial support.

NMR solution structure of the hepatitis C virus p7 ion channel

Toshana Foster, Arnout Kalverda, Gary Thompson, Arwen Pearson,
Mark Harris, Stephen Griffin and Steve Homans

Hepatitis C virus chronically infects 170 million individuals worldwide. Persistent infection is associated with variable degrees of liver damage which often progress into life-threatening cases of chronic hepatitis, liver cirrhosis and hepatocellular carcinoma. There is no vaccine and current therapies are of low efficacy and specificity. The virus encodes a 63-residue transmembrane protein, p7, which is essential for the production and release of infectious HCV particles and has been shown to homo-oligomerise to form heptameric cation specific ion channels. In cell culture, specific mutations and p7 inhibitors prevent the release of HCV particles, suggesting that the channel activity is essential at a late stage in the virus life cycle. p7 is therefore an ideal target for the development of specific anti-HCV drugs. We have sought to determine the structure of the monomeric and oligomeric forms of p7 using solution NMR studies for future structure-based drug design. The structure of monomeric p7 shows that it possesses two transmembrane helices connected by a short cytoplasmic loop (Figure 1 A-B).

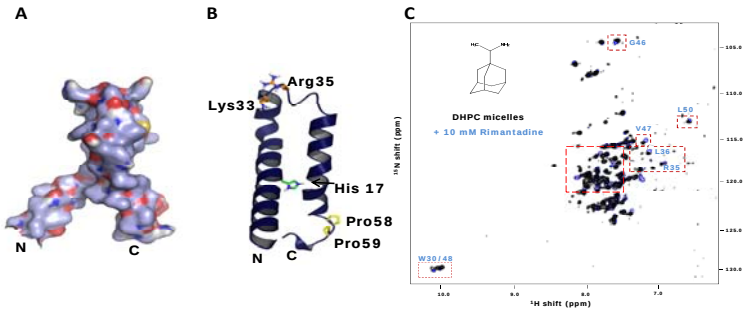

Figure 1: (A) the amphipathic nature of the p7 *trans*-membrane domains is illustrated by side views of the surface representation of the monomer. The N-terminal helix of p7 is predicted to line the pore of the ion channel complex whilst the C-terminal helix interacts with the membrane. **(B)** Residues Lys33 and Arg35 of the basic charged loop are shown and the putative proton sensor residue, His17, lies in a position where it would face the channel lumen upon oligomerisation. Pro58 and Pro 59 are shown to form kinks at the end of the C-terminal helix. **(C)** TROSY-HSQC spectrum of p7 oligomer in DHPC micelles with and without the drug rimantadine.

Drug interaction NMR experiments with the anti-viral drug rimantadine have shown that the drug binds to the C-terminal helix of the protein in its monomeric state. This drug interaction site is similar to that identified by NMR analysis of the oligomeric form of the protein. p7 oligomerises efficiently in the membrane-mimetic detergent diheptanoylphosphatidylcholine (DHPC) forming a heptameric complex in micelles of ~90 kDa. The introduction of TROSY (transverse relaxation-optimized spectroscopy) has permitted the study of large protein complexes by solution NMR. The spectra allow assignment of p7 protein resonances and drug binding data suggest that changes occur mainly in the C-terminus of the protein when binding rimantadine (Figure 1C). The resultant conformational changes may stabilise the closed form of the channel thereby affecting channel conductance. Investigations will be focussed on determining the structure of the oligomeric complex to understand the mechanism of p7 channel formation.

Publications

StGelais, C., Foster, T., Verow, M., Atkins, E., Fishwick, C., Rowlands, D., Harris, M. and Griffin, S. (2009) Determinants of hepatitis C virus p7 ion channel function and drug sensitivity identified *in vitro*. *J Virol*, **83**:7970-7981.

Funding

We would like to thank the Wellcome Trust for financial support.

Proteolysis and protein:protein interactions in neurodegenerative diseases

Lizzie Glennon, Heledd Griffiths, Jo Humphrey, Vicki Lewis, Kate Kellet, Harry King, Nicole Watt, Isobel Whitehouse and Nigel Hooper

Introduction/Background

Alzheimer's disease (AD) is the commonest neurodegenerative disease of old age. Currently, there are no drugs available to halt or slow the progression of this devastating disease which is placing a huge burden on patients and carers. AD is characterised by the deposition in the brain of senile plaques that are composed of the amyloid-beta peptide (Abeta). Through mechanisms that are poorly understood, Abeta oligomers, fibrils and/or aggregates are toxic to nerve cells. Abeta is derived from the larger transmembrane amyloid precursor protein (APP) through proteolytic cleavage by the beta- and gamma-secretases. The beta-secretase (BACE1) cleaves within the APP sequence at the N-terminus of the Abeta peptide, with the gamma-secretase complex cleaving the resulting membrane-bound stub at the C-terminus of the Abeta sequence. Inhibition of both the beta- and gamma-secretases are being considered as potential therapeutic approaches to combat AD.

The prion protein is probably best known for its role in the transmissible spongiform encephalopathies or prion diseases, such as Creutzfeldt-Jakob disease in humans and bovine spongiform encephalopathy in cattle. In these diseases the normal cellular for of the prion protein (PrPC) undergoes a conformational conversion to the infectious form, PrPSc. In addition, we have shown that PrPC inhibits the beta-secretase cleavage of APP, lowering the amount of Abeta produced and, therefore, potentially protecting against AD. In both cell models and mice, reduction of PrPC levels resulted in an increase in Abeta production. BACE1 co-immunoprecipitated with PrPC from cells and brain samples, suggesting a direct interaction between the two proteins.

Proteolysis in prion disease

PrPC is bound to the plasma membrane via a glycosyl-phosphatidylinositol (GPI) anchor, although a secreted, soluble form has also been identified. We used gain-of-function (over expression) and loss-of-function (siRNA knockdown) experiments in cells to identify the ADAMs (a disintegrin and metalloproteinases) involved in the ectodomain shedding of PrPC. These experiments revealed that ADAM9 and ADAM10, but not ADAM17, are involved in the shedding of PrPC, and that ADAM9 exerts its effect on PrPC shedding via ADAM10. Using dominant negative, catalytically inactive mutants, we showed that the catalytic activity of ADAM9 is required for its effect on ADAM10. Mass spectrometric analysis revealed that ADAM10, but not ADAM9, cleaved PrP between Gly228 and Arg229, three residues away from the site of GPI anchor attachment. The shedding of another membrane protein BACE1 by ADAM9 was also mediated via ADAM10. Furthermore, we showed that pharmacological inhibition of PrPC shedding or activation of both PrPC and PrPSc shedding by ADAM10 overexpression in scrapie-infected neuroblastoma N2a cells did not alter the formation of proteinase K-resistant PrPSc. Collectively, these data indicated that whilst PrPC can be shed through the action of ADAM family members, modulation of PrPC or PrPSc ectodomain shedding does not regulate prion conversion.

Protein:protein interactions in prion disease

PrPC associates with lipid rafts through its glycosyl-phosphatidylinositol (GPI) anchor and a region in its N-terminal domain which also binds to heparan sulfate proteoglycans (HSPGs). We showed that heparin displaces PrPC from rafts and promotes its endocytosis, suggesting that heparin competes with an endogenous raft-resident HSPG for binding to PrPC. We then utilised a transmembrane-anchored form of PrP (PrP-TM), which is targeted to rafts solely by its N-terminal domain, to show that both heparin and phosphatidylinositol-specific

phospholipase C can inhibit its association with detergent-resistant rafts, implying that a GPI-anchored HSPG targets PrPC to rafts. Depletion of the major neuronal GPI-anchored HSPG, glypican-1, significantly reduced the raft association of PrP-TM and displaced PrPC from rafts, promoting its endocytosis. Glypican-1 and PrPC colocalised on the cell surface and both PrPC and PrPSc co-immunoprecipitated with glypican-1. Critically, treatment of scrapie infected N2a cells with glypican-1 siRNA significantly reduced PrPSc formation. These data indicate that glypican-1 is a novel cellular cofactor for prion conversion and we proposed that it acts as a scaffold facilitating the interaction of PrPC and PrPSc in lipid rafts.

Protein:protein interactions in Alzheimer's disease

Several other proteins, in addition to PrPC, have been reported to regulate the proteolytic processing of APP. For example, some proteins bind to APP and/or alter its subcellular trafficking to modulate its proteolytic processing, including F-spondin and ApoER2. Thy-1, contactin and neurofascin, along with PrPC, were recently identified to interact with APP in vivo, i.e. be components of the brain interactome of APP. From these studies, it is evident that APP processing and Abeta generation can be modulated by a diverse number of interacting proteins in various cellular compartments. This modulation could involve direct binding to BACE1 or APP itself, thereby influencing enzyme activities or the susceptibility of APP to cleavage. Alternatively, the mode of action may be indirect, involving the segregation of the secretases and APP into either the same or different membrane domains or cellular compartments. The molecular and cellular mechanisms underlying the modulation of APP processing in this way clearly need to be understood in order to provide a complete knowledge of AD pathogenesis. The components of the APP and BACE1 interactomes could potentially be exploited therapeutically to modulate Abeta production.

Publications

Kellett K. and Hooper N. (2009) Prion protein and Alzheimer disease. *Prion*, **3**:190-4.

Mok, N, Chadwick, J. Kellett, K., Hooper, N., Johnson, P., Fishwick, C. (2009) Discovery of novel non-peptide inhibitors of BACE-1 using virtual high-throughput screening. *Bioorg Med Chem Lett*, **19**:6770-6774.

Taylor, D., Parkin, E., Cocklin, S., Ault, J., Ashcroft, A. Turner, A. and Hooper, N. (2009) Role of ADAMs in the ectodomain shedding and conformational conversion of the prion protein. *J Biol Chem*, **284**:22590-22600.

Taylor D., Whitehouse I. and Hooper N. (2009) Glypican-1 mediates both prion protein lipid raft association and disease isoform formation. *PLoS Pathog*, **5**:e1000666.

Vardy, E., Rice, P., Bowie, P., Holmes, J., Catto, A. and Hooper, N. (2009) Plasma angiotensin-converting enzyme in Alzheimer's disease. *J Alzheimers Dis*, **16**:609-618.

Walmsley, A., Watt, N., Taylor, D., Perera, W., Sumudhu S. and Hooper, N. (2009) α -cleavage of the prion protein occurs in a late compartment of the secretory pathway and is independent of lipid rafts. *Mol Cell Neurosci*, **40**:242-248.

Funding

This work was funded by the MRC, Wellcome Trust, Alzheimer's Research Trust and BBSRC.

Collaborators

Tony Turner, Colin Fishwick, Alison Ashcroft

Biomolecular modeling and structural bioinformatics

James Dalton, Joel Dockray, Christopher Fallaize, Jonathan Fuller, Sarah Kinnings, Joseph Ward and Richard Jackson

1. A multiple structure-based ligand matching method for 3D virtual screening

We have developed a new virtual screening (VS) method called LigMatch and evaluated its performance on 13 protein targets using a filtered and clustered version of the directory of useful decoys (DUD). The method uses 3D structural comparison to a crystallographically determined ligand in a bioactive 'template' conformation, using a geometric hashing method, in order to prioritize each database compound. We show that LigMatch outperforms several other widely used VS methods on the 13 DUD targets. We go on to demonstrate that improved VS performance can be gained from using multiple, structurally diverse templates rather than a single template ligand for a particular protein target. In this case, a 2D fingerprint-based method is used to select a ligand template from a set of known bioactive conformations. Furthermore, we show that LigMatch performs well even in the absence of 2D similarity to the template ligands, thereby demonstrating its robustness with respect to purely 2D methods and its potential for scaffold hopping (Kinnings *et al*., 2009).

2. A genome-wide protein-ligand interaction network of *Mycobacterium tuberculosis*

The continuing emergence of M.tuberculosis strains resistant to all existing, affordable drug treatments means that the development of novel, effective and inexpensive drugs is an urgent priority. However, de novo drug discovery is a time-consuming and expensive process that is poorly equipped in the battle against tuberculosis. Drug repositioning provides a promising solution to reduce both the time and costs associated with drug development. We have developed a computational method to compare the binding sites of existing drugs approved for human use against the entire M.tb structural proteome. The resulting protein-ligand interaction network reveals not only that many existing drugs show the potential to be repositioned to treat tuberculosis, but also that many currently unexploited M.tb proteins may be highly druggable and could therefore serve as novel antitubercular targets. We are currently in talks with collaborators with regards to experimental testing of our hypotheses.

3. Virtual screening of transthyretin amyloid inhibitors

Amyloid aggregates and fibrils are a product of deviant protein-protein interactions and assembly of conformational intermediates found along the unfolding pathway of certain proteins. These aggregates and fibrils are at the source of cytotoxicity in diseases such as Alzheimer's disease, Familial Amyloid Polyneuropathy (FAP), Type 2 Diabetes and several others. Inhibition of fibril formation by stabilization of the native form of the protein transthyretin (TTR) is an appealing approach for the treatment of FAP. We undertook an extensive benchmark of five protein- and ligand-based virtual screening (VS) methods for identifying novel TTR stabilizers: (1) 2D similarity searches with chemical hashed fingerprints, pharmacophore fingerprints and UNITY fingerprints, (2) 3D similarity searches based on shape, chemical and electrostatic similarity, (3) LigMatch, a new ligand-based method which uses multiple templates and combines 3D geometric hashing with a 2D pre-selection process, (4) ligand- and receptor-based 3D-pharmacophore searches, and (5) molecular docking to consensus X-ray crystal structures of TTR. Validation of methods was conducted on a test set comprised of known TTR stabilizers and criteriously selected decoy molecules. By combining the best-performing VS protocols, a narrow subset of small molecules was retrieved from a tailored library of 2.3 million commercially available compounds and identified as representative of multiple series of potential new leads. According to our predictions, the identified molecules possess distinctive features from the

TTR stabilizers discovered to date, holding better solubility, fraction of halogen atoms and binding affinity.

4. Design of high affinity protein-protein-interaction inhibitors using molecular docking structure-based design and free energy calculations.

Protein-protein interactions play an essential role in many biological processes. Loss of control of these interactions can, therefore, cause disease. For this reason, efforts are underway to develop drug-like protein-protein interaction inhibitors for therapeutic use or simply for use as laboratory tools. There has been considerable success where one of the interacting partners binds via an alpha-helix.

We have been developing a general method of identifying replacement side chains that would be likely to increase the binding affinity of a protein-protein interaction inhibitor mimicking an alpha-helix. Current efforts have focussed on oligobenzamide inhibitors of the paradigmatic p53-Mdm2 interaction. Mdm2 is a negative regulator of the tumour suppressor protein p53 and aberrant upregulation of Mdm2 is responsible for the anti-apoptotic activity of many tumours.

4.1 Structure-based design and docking

Potential side chains for screening are generated by in silico cleavage of molecules obtained from the Chemical Structural Database (http://www.ccdc.cam.ac.uk/products/csd/) or ZINC (http://zinc.docking.org/). Database molecules are initially screened for desirable properties and to ensure that the resulting molecules will be synthetically accessible. Ensuring ease of synthesis is essential because, for the purpose of method validation, selected inhibitors will be made by the group of Dr Wilson (Department of Chemistry) and will then be tested in collaboration with Dr Edwards' group to determine *in vitro* efficacy.

After initial filtering, ultra-high-throughput screening using a pharmacophore model precedes more detailed fitting and scoring. The detailed scoring combines both ligand-based and structure-based methods; docking is used primarily to rank but high-scoring results are also evaluated in the context of known antagonists. A novel clustering method has been excogitated with the hope that by grouping similar structures it will be possible to reduce the number of side chains that must be tested for high-affinity substituents to be found.

The similarity between alpha-helix-mediated interactions in terms of the spacing and orientation of the interacting residues means that inhibitors such as our oligobenzamide, which have the potential for combinatorial chemistry, could theoretically be developed, using our methods, to inhibit any such protein-protein interaction. Although initial testing has been on p53 and Mdm2, we have plans to apply our methods to the Mdm2 homologue, MdmX and then to two other apoptosis-related interactions, that of Bcl-xL and BAK and that of Mcl-1 and NOXA-B, both of which are also of chemotherapeutic interest.

4.2 Free energy calculations

It would be also desirable to gain accurate predicted binding affinities that can not only determine whether a compound is a non-binder or binder, but additionally rank a list of compounds by there relative binding affinities. In collaboration with Prof. Michael Shirts from the University of Virginia we have applied state of the art free energy calculations on aromatic oligoamide compounds designed to mimic a portion of alpha helix from the p53 transactivation domain thus inhibit the MDM2/p53 interaction. The calculations were

performed using molecular dynamics simulations carried out with the Desmond software package on the new ARC computer cluster and analysed using the Bennett Acceptance Ratio (BAR).

Publications

Fuller, J., Burgoyne, N. and Jackson, R. (2009) Predicting druggable binding sites at the protein-protein interface. *Drug Discov Today*, **14**:155-161.

Kinnings, S. and Jackson, R. (2009) Binding site similarity analysis for the functional classification of the protein kinase family. *J Chem Inf Model*, **49**:318-329.

Kinnings, S. and Jackson, R. (2009) LigMatch: a multiple structure-based ligand matching method for 3D virtual screening. *J Chem Inf Model*, **49:**2056-2066.

Kulharia, M., Bridgett, S., Goody, R. and Jackson, R. (2009) InCa-SiteFinder: A method for structure-based prediction of inositol and carbohydrate binding sites on proteins. *J Mol Graph Model,* **28**:297-303.

Funding

This work is funded by the BBSRC, EPSRC, FCT, Worldwide Universities Network

Visiting Researchers

Mr. Carlos Simoes (University of Coimbra, Portugal)

Collaborators

Dr. Thomas Edwards (FBS, UoLeeds)
Dr. Andrew Wilson (Chemistry, UoLeeds)
Prof. Kanti Mardia (Maths, UoLeeds)
Dr. Stuart Barber (UoLeeds)
Prof. Rui Brito (University of Coimbra, Portugal)
Prof. Michael Shirts (University of Virginia)
Prof. Philip Bourne (Skaggs School of Pharmacy, University of California San Diego)

Electrodes to study membrane proteins

Sophie Weiss, Duncan McMillan, Nikolaos Daskalakis, Lukasz Krzeminksi, James Kendall, Steve Evans, Richard Bushby, Peter Henderson and Lars Jeuken

Introduction

Membrane proteins, which are estimated to account for a third of the human genome, perform a myriad of functions in biology. They perform key roles in signal processing and bioenergetics. Our lab develops new techniques to study membranes and membrane proteins and we focus on ion channels and redox enzymes. Ion channels have key roles in signal transduction, while redox enzymes catalyse redox reactions in many vital processes, including photosynthesis and metabolism. We aim to link membranes and membrane proteins to electrode surfaces, which allows us to probe electron consumption/production (redox enzymes) or transmembrane charge transport (ion channels) using electrochemical methods.

Cholesterol tethers to 'wire' membranes

We have prepared electrode surfaces which enables the characterisation of redox-active membrane enzymes and ion-channels in a native-like environment. For this, we have used the methodology of tethered bilayer lipid membranes (tBLM), in which the lipid bilayer is attached to the electrode surface via special chemical anchors that are bound to the surface on one side and insert into a bilayer leaflet at the other (Figure 1). Cholesterol derivatives have been synthesised, which, via a hydrophilic linker, are connected to a thiol group that form self-assembled monolayers (SAMs) on gold electrodes. These cholesterol-lipids have been mixed with small thiols to provide space for transmembrane proteins. The surfaces of these mixed SAMs have been characterised in detail and shown to exhibit a complex pattern of phase separation, confirming the demixing of the two thiols schematically shown in Figure 1.

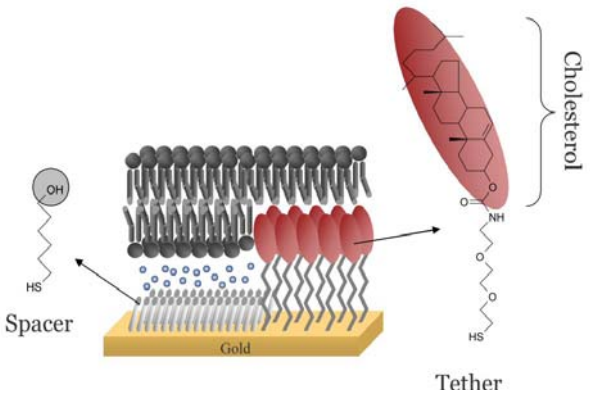

Figure 1: Chemical structures of 6-mercaptohexanol (spacer) and the cholesterol tether molecule used to form tBLMs.

tBLM from bacterial membrane extracts

New protocols have been developed to prepare tBLMs from inner membranes extract from *E. coli*. In contrast to the systems prepared previously with purified membrane proteins, these systems are easier to prepare and more robust in nature. The membrane-bound quinones in these tBLM systems still act as substrates for quinone enzymes that are co-immobilised (Figure 2, left). Using this novel membrane system, the activity of an ubiquinol oxidase from *Escherichia coli*, cytochrome bo_3 (cbo_3) is studied using voltammetry techniques. Cbo_3 reduces oxygen and the apparent K_M of cbo_3 for oxygen was determined to be 1.1±0.4 μM, in good agreement with literature values for whole cell experiments and for purified cbo_3. Last year we reported initial evidence that suggested that increasing the concentration of lipophilic UQ-10 beyond 10 pmol/cm^2 in the membrane leads to an decrease in cbo_3 activity. In 2009 we have further developed our methodology and by titrating UQ-10 directly into the tBLM from a DMSO stock we have confirmed and elaborated on our earlier findings (Figure 2, right). The activity of cbo_3 with long chain ubiquinones appears to be different to literature, which mainly describes short-chain substrate analogues such as UQ-1. Furthermore, detailed analysis of the voltammetry data with the lipophylic UQ shows that cbo_3 is inhibited by ubiquinol (substrate), but not by ubiquinone (product).

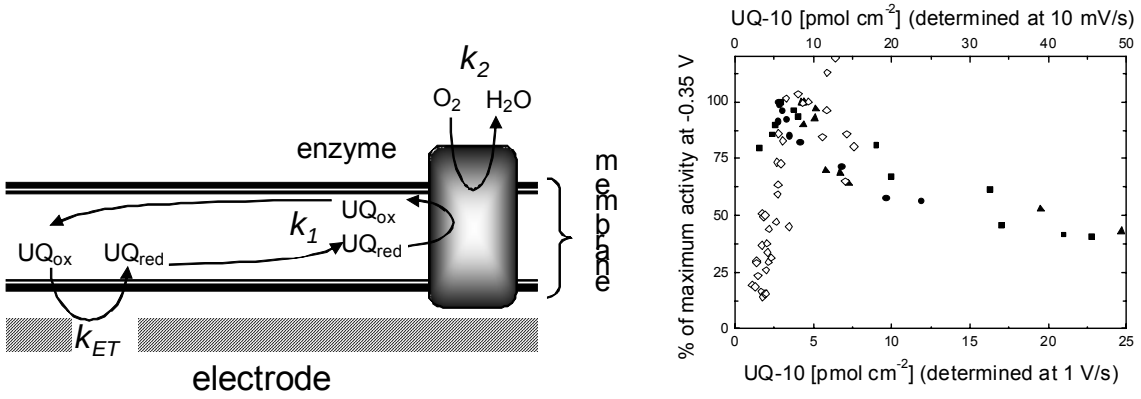

Figure 2: (left) schemetic representation of the tBLM systems in the electrochemical, diffusion and enzymatic reaction taking place. **(right)** Enzymatic activity of cytochrome *bo*$_3$ obtained using the tBLM system prepared from inner membrane extracts from c*bo*$_3$. The maximum reduction activity (at high oxygen concentration) of inner membranes (1:9 mixed with *E. coli* lipid extract) is plotted as a function of ubiquinol-10 present in the membrane. The line is included as a guide to the eye.

Ion channels

Studies were performed to provide a proof-of-principle that our tBLM system can be used to characterise ligand gated ion-channels. For this purpose, tBLMs were formed on either (a) pure tether lipid or on (b) mixed self-assembled monolayers (SAMs) of tether and spacer molecules (see Figure 1). While the tether lipid is required to form a tBLM with high resistivity, the spacer molecule dilutes the cholesterol content in the lower leaflet of the bilayer forming "ionic reservoirs" required for the sub-membrane hydration. By using simple ion-channels (gramicidin) and ionophores (valinomycine) we have shown that these ionic reservoirs are required for ion transport through the membranes (Figure 3). This is most likely due to the thermodynamic requirements of ions to be solvated once transported through the membrane. Unexpectedly, electrochemical impedance spectroscopy (EIS) shows an increase of capacitance upon addition of gramicidin, while valinomycin addition decreases the membrane resistance in the presence of K^+ ions. We hypothesise that this is due to previously reported phase separation of tether-lipid and spacer molecule on the surface.

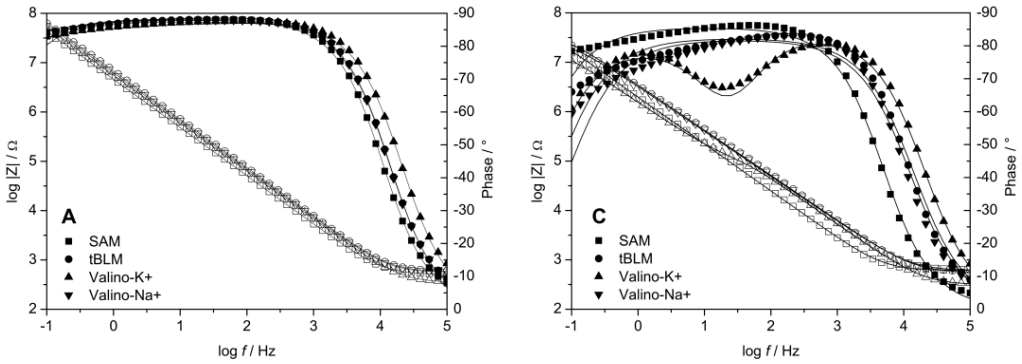

Figure 3: Electrochemical impedance data (Bode plots) of tBLMs formed on **(left)** pure tether lipids and **(right)** mixtures of tether lipids and spacer molecules. **(Left)** With the tBLM formed without spacer molecules no effect is seen after the addition of the ionophore valinomycin. **(Right)** When spacer molecules are present the resistance of the membrane decreases when valinomycin is added, but only in the presence of K^+ which is the substrate of valinomycin.

Future directions

We aim to continue to study the enzyme mechanics of c*bo*$_3$ and other quinone enzymes with particular focus on properties that made UQ a special substrate when compared to aqueous solutes. Besides c*bo*$_3$ we will use UQ-converting membrane proteins that have a less 'membrane-integral' nature. The proteins CymA and NapC both have a single α-helix that

binds them to the membrane and for NapC a mutant is made that misses this membrane-spanning sequence. In a second project, intact vesicles with fluorescent pH indicators are adsorbed on the surface in order to monitor simultaneously the electron and proton transfer properties of c*bo*$_3$. The work with ion channels will be continued by testing more complex ligand-gated ion-channels. The tBLMs are also tested for their suitability to bind soluble proteins via his-tags that bind to synthetic NTA-lipis. Finally, EU funding has been obtained to study if the tBLM platform can be used to study the interaction between nanoparticles and lipid membranes, with the aim to characterise potential toxicological effects of nanoparticles.

Publications

Jeuken, L. (2009) Electrodes for integral membrane enzymes. *Nat Prod Rep*, **26**:1234-1240.

Weiss, S., Bushby, R., Evans, S., Henderson, P. and Jeuken, L. (2009) Characterization of cytochrome bo3 activity in a native-like surface-tethered membrane. *Biochem J* **417**:555-560.

Weiss, S. and Jeuken, L. (2009) Electrodes modified with lipid membranes to study quinone oxidoreductases. *Biochem Soc Trans*, **37**:707-712.

Kendall, J., Johnson, B., Symonds, P., Imperato, G., Bushby, R., Gwyer, J., van Berkel, C., Evans, S. and Jeuken, L. (2010) Effect of the structure of cholesterol-based tethered bilayer lipid membranes on ionophore activity, *ChemPhysChem.*, in press

Weiss, S. A., Bushby, R. J., Evans, S. D., Jeuken, L. J. C. (2010) A study of cytochrome **bo**3 in a tethered bilayer lipid membrane, *BBA - Bioenergetics*, in press**.**

Funding

This work is funded by an ITN (FP6), EU (FP7), BBSRC, EPSRC, Royal Society and Philips.

A stable single α-helix can act as a lever in myosin

Thomas Baboolal, Scott Jackson, Michelle Peckham and Peter Knight

Introduction

The α-helix (first identified by W. T. Astbury) is a secondary structure commonly found in proteins, either as part of globular proteins or paired with one or more adjacent α-helices in coiled coils, such as in the 'leucine zipper' of the transcriptional regulator GCN4. It is generally thought that single α-helices are inherently unstable in aqueous solution. We recently discovered that secondary structure prediction software incorrectly assigns as coiled coils, sequences that lack the hydrophobic seam that holds the chains together. Several such sequences occur in members of the myosin family of motor proteins. We found that one such sequence from myosin 10 instead forms a monomeric α-helix that is more stable against denaturation by heat or salt than the α-helices of coiled coils. A characteristic of this single α-helix (SAH domain) appears to be large numbers of both acidic and basic amino acid residues that are able to form salt bridges between successive turns of the helix and thus compensate effectively for the tendency of water to disrupt the H-bond network that stabilises the α-helical fold. We have since found that such sequences are widely distributed both across the biome and in proteins of diverse compartments of the cell. However the roles of the SAH domain in proteins remain obscure. In myosins the SAH domain is located adjacent to the lever that amplifies the small, ATP-driven changes in the motor domain into large movements of cargo, and we suggested that it might act as a lever extension. We have recently put this proposal to the test.

Properties of a chimeric myosin

Our test consisted of replacing a large part of the lever of the well-studied myosin 5 with a putative, long SAH domain from a different myosin (MyoM from the slime mould *Dictyostelium discoideum*), and then determining to what extent this chimeric protein behaved like wild type myosin 5 in a battery of test assays.

Myosin 5 is a dimeric myosin in which two heads each consisting of a motor domain and a lever are linked together by a coiled-coil tail (Figure 1). The lever of myosin 5 consists of 6 calmodulin molecules bound close together along an α-helical extension from the motor (which, unlike a SAH domain, collapses if the calmodulins dissociate). The calmodulin-binding sites on this helix are called IQ motifs (because they contain a consensus sequence IQxxxRGxxxR). We deleted 4 of the 6 IQ motifs (creating Myo5-2IQ) and spliced in the putative SAH domain between the IQ motif and the tail to create Myo5-2IQ-SAH (Figure 1).

Electron microscopy of Myo5-2IQ-SAH showed the SAH domain was straight and 17-nm long as predicted from the number of amino acid residues and the rise per residue of an α-helix (0.15 nm), restoring the truncated lever to the length of wild type (Myo5-6IQ). The powerstroke (21.5 nm) produced by single molecules interacting with a single actin filament, as measured in the optical trap, was slightly less than that for Myo5-6IQ but much greater than for Myo5-2IQ, indicating that the SAH domain can indeed extend the mechanical lever action. Myo5-2IQ-SAH moved processively along actin at physiological ATP concentrations with similar step and run lengths to Myo5-6IQ during in-vitro Total Internal Reflection Fluorescence Microscopy assays. In comparison, Myo5-2IQ is not processive under these conditions.

In wild type myosin 5 walking along an actin filament, the trailing head inhibits release of ADP from the leading head (i.e. acts as a gate), and this is presumed to occur by mechanically-preventing the shape change in the leading head that is required for ADP release. For the Myo5-2IQ-SAH chimera, solution biochemical experiments indicated that the

rear head did not mechanically gate the rate of ADP release from the lead head, unlike Myo5-6IQ. These data show that the SAH domain can form part of a functional lever in myosins although its mechanical stiffness might be lower. More generally, we conclude that SAH domains can act as stiff structural extensions in aqueous solution and this structural role may be important in other proteins.

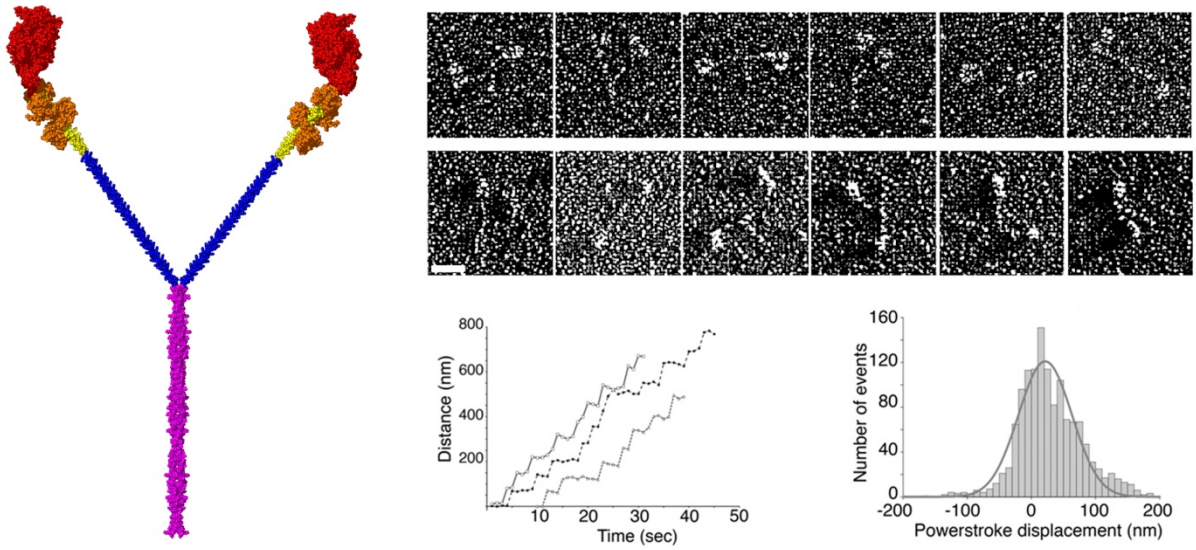

Figure 1: Chimera of myosin 5-2IQ with SAH domain of MyoM. **Left**: atomic model of the chimera; myosin 5 motors red, IQ helix yellow, calmodulins orange, coiled-coil tail mauve; SAH domain blue. **Top right**: EM of single molecules seen by metal shadowing; the thin SAH domains can be seen; scale bar is 25 nm. **Bottom centre**: TIRF assays show strides taken by molecules along actin, that average 70 nm. **Bottom right**: Powerstroke in optical trap averages 22 nm.

Publications

Baboolal, T., Sakamoto, T., Forgacs, E., White, H., Jackson, S., Takagi, Y., Farrow, R., Molloy, J., Knight, P., Sellers, J. and Peckham, M. (2009) The SAH domain extends the functional length of the myosin lever. *Proc Natl Acad Sci USA*, **106**:22193-22198.

Peckham, M. and Knight, P. (2009) When a predicted coiled coil is really a single α -helix, in myosins and other proteins. *Soft Matter*, **5**:2493-2503.

Funding

This work was funded by the BBSRC, Wellcome Trust and NIH.

Collaborators

E. Forgacs and H.D. White, East Virginia Medical School, Norfolk, VA, USA
T. Sakamoto, Y. Takagi and J.R. Sellers, NIH, Bethesda, MD, USA
R.E. Farrow and J.E. Molloy, MRC NIMR, Mill Hill, London, UK

Structural studies of innate immune signalling proteins and viral oncogenes

Laura Wetherill, Kathryn Richards, Sayaka Sato, Rebecca Ross, Lynne Cherriman, Shruti Nandha, Arwen Pearson, Steven Griffin, Eric Blair and Andrew Macdonald

Introduction.

Virus infections are associated with chronic pathologies and are the causative agents of various cancers. For example 78% of biopsies from patients with cervical cancer are positive for human papillomavirus (HPV) and new cancer-associated viruses are being discovered including the Merkel cell carcinoma polyomavirus (MCV). Our ability to control virus infection is often inadequate due to the limited availability of drugs that target many pathogenic viruses and an incomplete understanding of the host response to virus infection. As such there is a pressing need to increase our understanding of the host response to virus infection. To be effective it requires rapid and appropriate activation of inflammatory cytokine messengers to eliminate the spread of infection as quickly as possible. However, as this response often evolves at the cost of tissue damage, failure of resolution can result in inflammatory disorders and the further development of disease. Due to this inherent danger of an inappropriate response, the crucial steps are regulated by a growing number of cellular proteins. There remains a poor understanding of the molecular mechanisms utilised by these proteins. Additionally, it is clear that these signalling pathways are target for viral subversion and often deregulated by virus-encoded proteins to affect the anti-viral or inflammatory response. Thus, a clearer understanding of this area will arm us with better strategies to fight viral infection through the development of novel therapeutics.

Biophysical characterisation of viral oncogenes.

The human papillomaviruses are causative agents of a range of ano-genital and head and neck cancers. The E5 onco-protein transforms primary keratinocytes and causes cancerous lesions in the cervix of transgenic mice. The mechanism of E5 mediated transformation is not well understood. As E5 is theorised to function in the early stages of HPV persistence, we focussed on characterising the biochemical nature of E5 in an attempt to expose a drugable function. E5 is a highly hydrophobic membrane bound protein. We designed the first successful bacterial purification system for E5. Using a multifaceted approach consisting of biophysical characterisation, cell based assays and *in silico* modelling we demonstrate that E5 exists as a hexamer (Figure 1). Furthermore, we are the first to describe E5 as a novel viroporin or virally encoded ion channel. E5 is the first oncoprotein to be described as a viroporin. Collaborating with Prof. Colin Fishwick we are adopting a rational approach to E5 inhibitor design incorporating virtual screening of compounds tailored against our molecular model. This approach successfully produced the first small molecule inhibitor against E5 and represents a breakthrough in rational drug design against an *in silico* target.

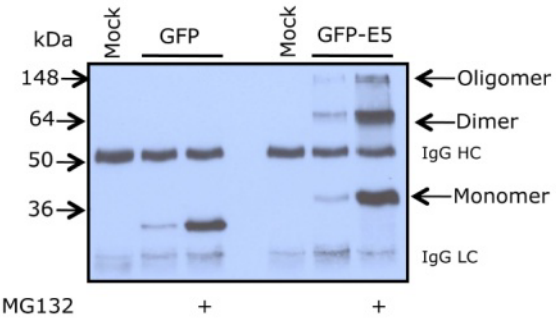

Figure 1: HPV16 E5 oligomerises in cells. SDS-PAGE and immunoblotted for anti-FLAG demonstrating E5 monomer, dimer and oligomer and levels of protein were enhanced in the presence of the proteasome inhibitor MG132. Non-specific IgG heavy and light chain are indicated.

Studies on regulators of the innate immune response

Studies from our laboratory have identified the protein optineurin as a negative regulator of the anti-viral response. The mechanism by which optineurin regulates the anti-viral response is currently unknown, although it may require an interaction with the protein kinase TBK1 and upstream signalling proteins that are ubiquitylated. Preliminary experiments demonstrated that optineurin forms a higher molecular weight oligomeric structure in response to viral nucleic acids (Figure 2). Our Royal Society funded studies are analysing the structural and molecular biology of optineurin in greater detail, with the eventual aim of solving the three dimensional structure of this critical mediator of signalling.

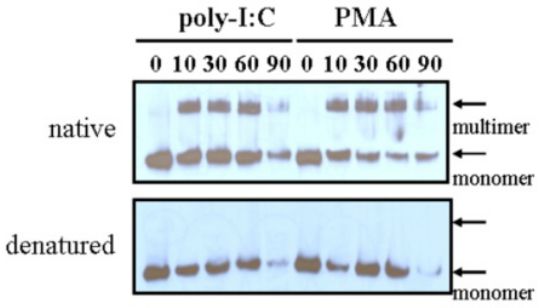

Figure 2: Formation of higher order structures by optineurin. Cells expressing optineurin were stimulated with the viral dsRNA mimic poly-I:C or treated with the mitogen PMA and lysed at the indicated time-point. Lysates were analysed either by non-denaturing native electrophoresis (top) or by denaturing.

Publications

Poole, E., Groves, I., Macdonald, **A.,** Pang, Y., Alcami, A. and Sinclair, J. (2009) Identification of TRIM23 as a co-factor involved in the regulation of NFκB by the Human cytomegalovirus gene product UL144. *J Virol* **83**:3581-90.

Short, J. and Macdonald, A. (2009). Viral evasion of interferon-stimulated genes. *Bio-Science Horizons,* **2:** 212-224.

Wittmann, M., Macdonald, A. and Renne, J. (2009) IL-18 and inflammation. *Autoimmun Rev*,**9**:45-48.

Gamlen, T., Richards, K., Mankouri, J., Hudson, L., McCauley, J., Harris, M. and Macdonald, A. (2010) Cytopathogenic BVDV NS3/4A induces apoptosis but is not required for inhibition of IFNβ induction. *J Gen Virol*, **91**:133-44.

Mankouri, J., Fragkoudis, R., Richards, K., Wetherill, L., Harris, M., Kohl, A., Elliott, R. and Macdonald, A. (2010) The nemo-related protein optineurin is a regulator of innate antiviral signalling. *PLoS Pathogens,* **19**:e1000778.

Funding

This work is funded by EPSRC, Yorkshire Cancer Research, MRC, BBSRC, The Royal Society and the University of Leeds.

The yin and yang of gene expression

Louise Kime, Stefanie Jourdan, David Romero and Kenneth McDowall

The degradation of transcripts and transcription can be considered the yin and yang of gene expression. In this report, we outline our recent advances in understanding both of these processes using bacteria as model systems. Last year, we reported how we had used SELEX to identify sequences that are recognised by a transcription factor, called AtrA that controls the production of an antibiotic in *Streptomyces coelicolor*. Using bioinformatics, this had led to the identification of a target, *nagE2* that encodes the transporter of a key nutrient. This work has now been published. In an exciting twist, further refinement of the weighted matrix used for *in silico* scanning revealed multiple links to the metabolism of acetyl-CoA, the precursor of actinorhodin, and to additional morphogenes. The emerging picture is one of AtrA as a central coordinator of metabolism and morphological development. This has stimulated sufficient interest to initiate a collaboration to study AtrA on a systems/genome-wide level using chromatin-immunoprecipitation and transcriptomics.

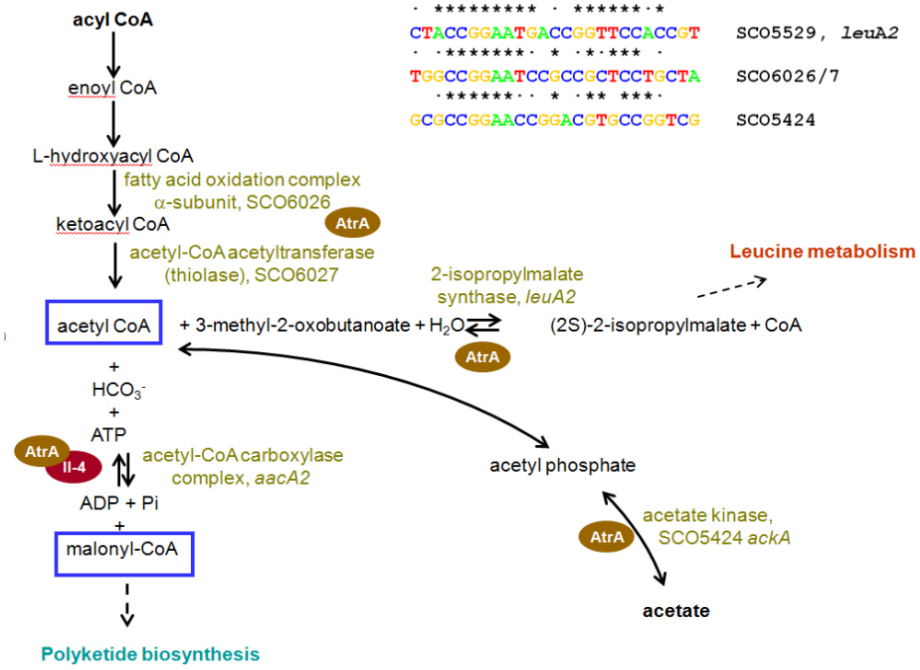

Figure 1: AtrA links to acetyl-CoA metabolism. Binding to promoters has been confirmed using electrophoretic mobility shift assays. The sequence of the binding sites is shown top right.

The degradation of mRNA is more than just a counterbalance; for example, it is the basis of the close coupling of translation to programs of transcription. Previously, we proposed here that the initiation of the degradation of many transcripts in *E. coli* is not dependent on "decapping", but endonucleolytic cleavages that are facilitated by the ability of the corresponding nuclease, RNase E to interact cooperatively with multiple single-stranded regions. This work has also now been published. This mode of recognition offers a simple explanation for the finding that in the absence of translating ribosomes many transcripts are highly susceptible to RNase E. We suggest that it might provide quality control by ensuring the rapid removal of defective mRNAs and reinforce the effects of small antisense RNAs that block translation.

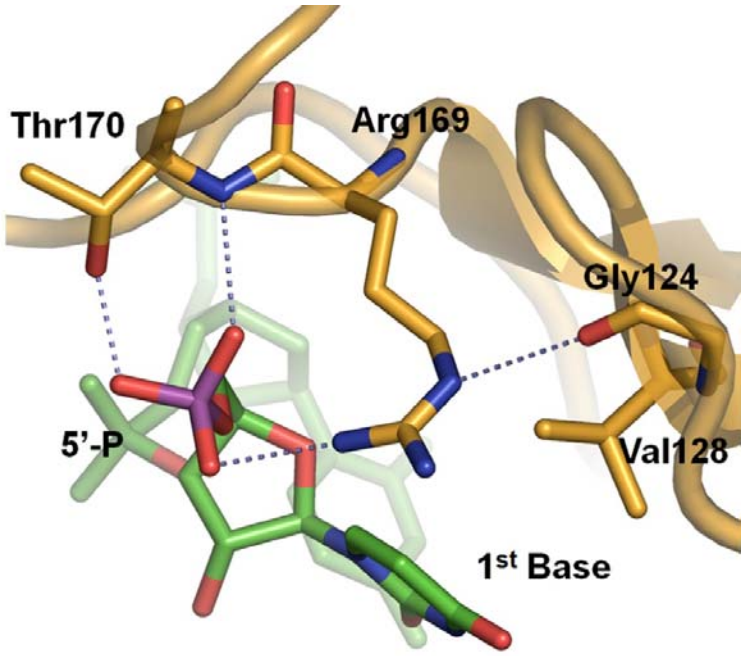

Figure 2: The interaction between the 5' end of an RNA substrate and RNase E. It now appears that this interaction can serve primarily as an additional foothold. While important for efficient cleavage in some circumstances, this interaction appears not to be universally required and not to serve as a critical allosteric switch.

Publications

Carpousis, A., Luisi, B. and McDowall, K. (2009) Endonucleolytic initiation of mRNA decay in *Escherichia coli*. *Prog Mol Biol Transl Sci*, **85**:91-135.

Jourdan, S., Kime, L. and McDowall, K. (2010) The sequence of sites recognised by a member of the RNase E/G family can control the maximal rate of cleavage, while a 5'-monophosphorylated end appears to function cooperatively in mediating RNA binding. *Biochem Biophys Res Commun* **391**:879-83.

Kime, L., Jourdan, S., Stead, J., Hidalgo-Sastre, A. and McDowall, K. (2010) Rapid cleavage of RNA by RNase E in the absence of 5'-monophosphate stimulation. *Mol Microbiol* **76**:590-604.

Nothaft, H., Rigali, S., Boomsma, B., Swiatek, M., McDowall, K., van Wezel, G. and Titgemeyer, F. (2010) The permease gene *nagE2* is the key to N-acetylglucosamine sensing and utilization in *Streptomyces coelicolor* and is subject to multi-level control. *Mol Microbiol* **75**:1133-1144.

Collaborators

Prof. Gilles P. van Wezel (Leiden Institute of Chemistry, The Netherlands)
Prof. Ben F. Luisi (Biochemistry, Cambridge, UK).

Funding

This work was funded by the European Union through the Marie Curie Actions and a BBSRC grant to K. J. M.

Biophysics of lipid bilayers

Richard J. Bingham, Chinmay Das, Brett Donovan, Khizar Sheik, Simon Connell, Stephen Smye, Nigel Hooper, and Peter Olmsted

Introduction

Lipid bilayer membranes are an essential component of all biological systems, forming a functional barrier for cells and organelles from the surrounding environment. The advent of many new experimental techniques has led to an explosion in work on the basic physical mechanisms behind membranes. Over the past year our group has studied a number of these properties.

Lipid bilayers in electric fields

Electric field-induced formation of pores in bilayers is widely exploited as an experimental protocol (*e.g.* for drug delivery), although a complete theory of the process does not yet exist. The lipid molecules that form membranes contain both permanent and induced dipoles, and an electric field can induce the formation of pores when the transverse field is sufficiently strong (electroporation). Here, a phenomenological free energy is constructed to model the response of a bilayer to a transverse static electric field. The model contains a continuum description of the membrane dipoles and a coupling between the headgroup dipoles and the membrane tilt. The membrane is found to become unstable through buckling, rather than peristaltic, modes. The instability occurs on a length scale (nm) that similar to that of pore formation and at a critical transmembrane voltage of order 0.3V, similar the magnitude reported in experiments. The instability is found to depend strongly on the strength of the coupling between the dipolar headgroups and the membrane tilt as well as the degree of dipolar ordering in the membrane.

Stratum corneum bilayers

Stratum corneum, the outermost layer of skin, consists of keratin-filled rigid non-viable corneocyte cells surrounded by multilayers of lipids; it is responsible for the barrier properties of skin.

We performed atomistic molecular dynamics of fully hydrated bilayers comprising ceramide NS-24:0, free fatty acid 24:0 and cholesterol, to address the effect of the different components in the stratum corneum (the outermost layer of skin) lipid matrix on its structural properties. Bilayers containing ceramide molecules show higher in-plane density and hence lower rate of passive transport compared to phospholipid bilayers. At physiological temperatures, for all composition ratios explored, the lipids are in a gel phase with ordered lipid tails. However, the large asymmetry in the lengths of the two tails of the ceramide molecule leads to a fluidlike environment at the bilayer midplane. The lateral pressure profiles show large local variations across the bilayer for pure ceramide or any of the two-component mixtures. Close to the skin composition ratio, the lateral pressure fluctuations are greatly suppressed, the ceramide tails from the two leaflets interdigitate significantly, the depression in local density at the interleaflet region is lowered, and the bilayers have lowered elastic moduli. This indicates that the observed composition ratio in the stratum corneum lipid layer is responsible for both the good barrier properties and the stability of the lipid structure against mechanical stresses.

To address permeability, we calculated the excess chemical potential and diffusivity of water as a function of depth in lipid bilayers with compositions representative of the stratum corneum using atomistic molecular dynamics simulations. The maximum in the excess free energy of water inside the lipid bilayers is found to be twice that of water in phospholipid bilayers at the same temperature. The permeability, which decreases exponentially with the

free energy barrier, is reduced by several orders of magnitude as compared with phospholipid bilayers. The average time it takes for a water molecule to cross the bilayer is calculated by solving the Smoluchowski equation in the presence of the free energy barrier. For a bilayer composed of a 2:2:1 molar ratio of ceramide NS 24:0, cholesterol and free fatty acid 24:0 at 300 K, we estimate the permeability P =0.037 nm/s and the average crossing time to be 0.69 ms. The permeability is about 30 times smaller than existing experimental results on mammalian skin sections.

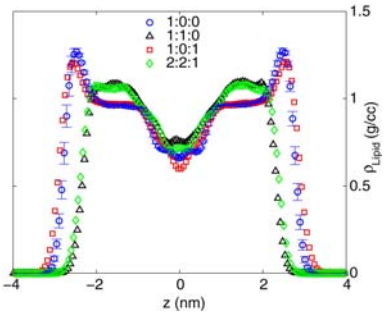

Figure 1: Total lipid density through the stratum corneum bilayers of different compositions at 340K from atomistic simulations. The compositions are shown as a molar ratio of Ceramide:Cholesterol:Free Fatty Acid.

Coarse-grained models for lipid bilayers

We have developed a new off-lattice coarse grained implicit solvent model for membranes which exhibits phase separation in mixtures that mimic saturated and unsaturated lipids. The model is computationally efficient, while allowing for self assembly and calculation of membrane mechanical properties. We develop model detergent molecules, and study the effects of asymmetrically inserted detergent molecules: this induces macroscopic behaviour such as pore formation, pore closing, and budding, depending on the packing paremeter of the detergent. We also devised models for amphipathic peptides (which are of crucial importance in fighting infection), and use this to study their orientation within the lipid matrix as a function of their hydrophobicity and relative length.

Publications

Das, C., Noro, M. and Olmsted, P. (2009) Simulation studies of stratum corneum lipid mixtures. *Biophys J*, **97**:1941-1951.

Das, C., Olmsted, P. and Noro, M. (2009) Water permeation through stratum corneum lipid bilayers from atomistic simulations. *Soft Matter*, **5**:4549-4555.

Evans, R., Simha, R., Baule, A. and Olmsted P. (2010) Statistical mechanics far from equilibrium: prediction and test for a sheared system. *Phys Rev E Stat Nonlin Soft Matter Phys* **81**:051109.

Bingham, R., Olmsted, P. and Smye, S. (2010) Undulation instability in a bilayer lipid membrane due to electric field interaction with lipid dipoles, *Phys Rev E Stat Nonlin Soft Matter Phys* **81**:051909.

Funding

This work was funded by the EPSRC, Yorkshire Forward, the EU (FP7 Network of Excellence SOFTCOMP), and Unilever.

Collaborators

The stratum corneum work was carried out in close collaboration with Massimo Noro, Robert Marriot, Barry Stidder, Andrea Ferrante, and Alex Lips at Unilever Research Port Sunlight; and with Jamshad Anwar, Michael Bonner, and Raj Periasamy at Bradford University.

Simulations are instrumental in interpreting single-molecule experiments and determine free-energy landscapes of proteins

Zu Thur Yew and Emanuele Paci

The study of mechanical unfolding, through the combined efforts of atomic force microscopy and simulation, is yielding fresh insights into the free-energy landscapes of proteins. Thus far, experiments have been mostly analyzed with one-dimensional models of the free-energy landscape. We have recently found that, as the two ends of a protein (**filamin** in this case) are pulled apart at a speed tending to zero, the measured mechanical strength plateaus at ~30 pN instead of going toward zero, deviating from the almost universally assumed *Bell model*. The deviation can only be explained by a switch between parallel pathways. Insightful analysis of mechanical unfolding kinetics needs to account for the multidimensionality of the free-energy landscapes of proteins, which are crucial for understanding the behavior of proteins under the small forces experienced *in vivo*.

Ankryin repeat proteins comprise tandem arrays of a 33-residue, predominantly α-helical motif that stacks roughly linearly to produce elongated and superhelical structures. They function as scaffolds mediating a diverse range of protein-protein interactions, and some have been proposed to play a role in mechanical signal transduction processes in the cell. Atomic force microscopy and molecular-dynamics simulations show that the natural 7-ankyrin repeat protein gankyrin unfolds under force via multiple distinct pathways in a non-cooperative manner. The peeling away of half an ankyrin repeat, or one or more ankyrin repeats, occurs at low forces but, intermediate species stabilized by nonnative interactions are formed that are resistant to high forces. The unfolding of individual ankyrin repeats generates a refolding force never observed before for globular proteins. But the most remarkable finding is that the mechanics of natural occurring ankyrin repeat proteins and those of designed consensus ankyrin repeat differ remarkably, which is a clear indication that nature does not design proteins like humans do.

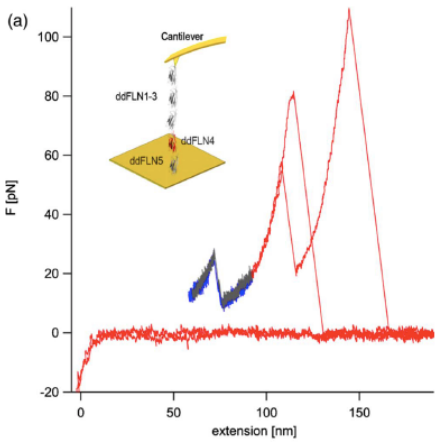

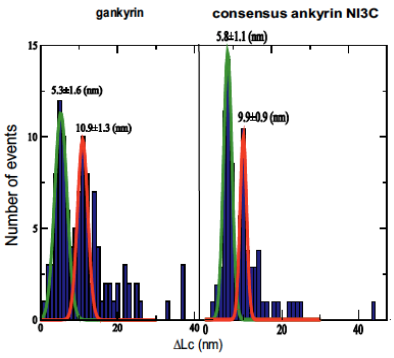

Figure 1: (top) typical force-extension profiles obtained for filamin when using the protein construct depicted (inset). **(bottom)** Histograms of the extension length increments between consecutive metastable states for gankyrin (left panel) and designed ankyrin (right panel). Both show two major increments, corresponding to ~6 nm (half of an ankyrin repeat) and ~11 nm (one ankyrin repeat). However, gankyrin shows other high frequency increments ranging from 13 to 36 nm.

Like filamin, the **PKD domains of polycystin-1** challenge the assumption that that native state protein topology is the principle determinant of mechanical strength: they are stronger than predicted from their native structure. Molecular dynamics simulations suggest that force induces rearrangement to an intermediate structure, with nonnative hydrogen bonds, that resists unfolding. This hypothesis was tested directly by our collaborator Jane Clarke in Cambridge by introducing mutations designed to prevent formation of these nonnative interactions. These mutations, which only moderately destabilize the native state, were found to reduce the mechanical stability dramatically. The results demonstrate that nonnative interactions impart significant mechanical stability, necessary for the mechanosensor function of polycystin-1. Remarkably, such nonnative interactions result from force-induced conformational change: the PKD domain is strengthened by the application of force.

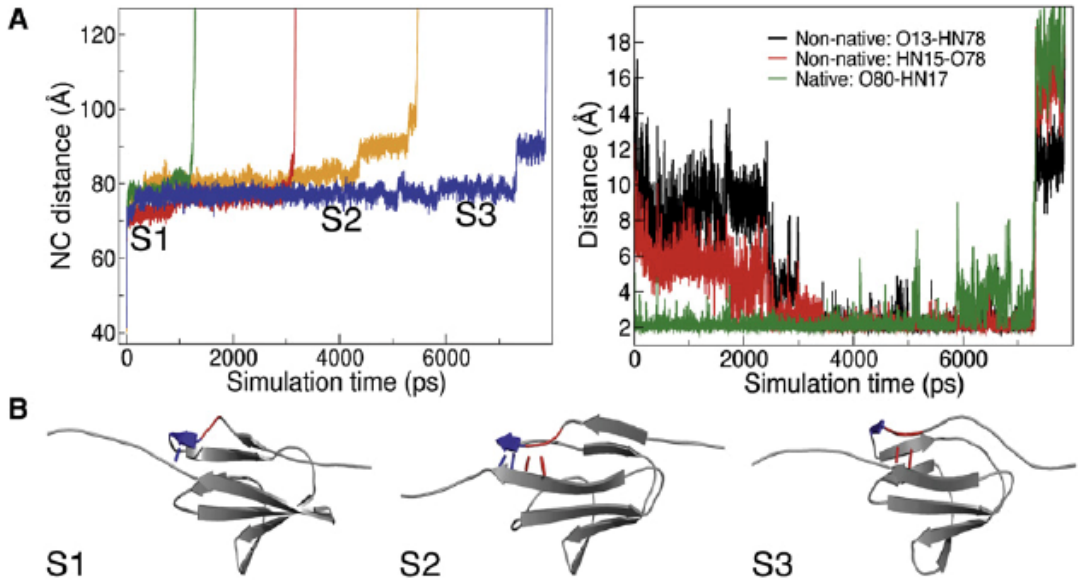

Figure 2: Unfolding Mechanism of ArPKD **(A)** Left: Plot of N-C extension against simulation time (ps) as ArPKD is pulled with a constant force of 200 pN in SMD simulations (data from four different simulations shown). The extension of the native state is 4 nm. The N to C extensions corresponding to the major states, S1-S3, along the unfolding pathway of ArPKD are indicated. in some of the simulations, an additional state with an extension of 9-10 nm appears just prior to full unfolding (see, for example, blue line). The lifetime of this state is much shorter than the unfolding time, which is dominated by states S2 and S3. As such, this minor state is unlikely to be detected experimentally and merely reflects the increased resolution of the simulations. Right: Hydrogen bond formation as a function of the simulation time for one of the simulations. The native HN17 to O80 hydrogen bond (green) lengthens and breaks before the unfolding event, but new nonnative hydrogen bonds form between residues 13 (black) and 15 (red) in the new A' strand and residue 78 in the G-strand, which only break when the protein unfolds. **(B)** Structures of the major states, S1-S3, along the unfolding pathway of ArPKD in simulations where a constant force of 200 pN is applied to the termini of the protein. Native and nonnative hydrogen bonds, including the regions that are involved, are colored blue and red, respectively.

Publications

Allen, L., Krivov, S. and Paci, E. (2009) Analysis of the free-energy surface of proteins from reversible folding simulations. *PLoS Comput Biol*, **5**:e1000428.

Allen, L. and Paci, E. (2009) Orientational averaging of dye molecules attached to proteins in Forster resonance energy transfer measurements: Insights from a simulation study. *J Chem Phys*, **131**:065101/1-065101/6.

Forman J., Yew Z., Quamar S., Sanford R., Paci E. and Clarke J. (2009) Non-native interactions are critical for mechanical strength in PKD domains**.** *Structure*, **17**:1582-1590.

Serquera D., Lee, W., Settanni, G., Marszalek, P., Paci , E. and Itzhaki, L. (2010) Mechanical unfolding of an ankyrin repeat protein. *Biophys J* **98**: 1294-1301.

Yew, Z., Schlierf, M., Rief, M. and Paci, E. (2010) Direct evidence of the multi-dimensionality of the free-energy landscapes of proteins revealed by mechanical probes. *Phys Rev E Stat Nonlin Soft Matter* **81**: 031923.

Funding
This work was funded by EPSRC and Wellcome Trust.

Collaborators
Laura Itzhaki, Cambridge Cancer Centre, Cambridge, UK.
Jane Clarke, Department of Chemistry, University of Cambridge, UK.
Michael Schlierf and Matthias Rief, Center for Integrated Protein Science Munich, Physics Department, Munich, Germany.

Structure based design of inhibitors of human and *Plasmodium falciparum* dihydroorotate dehydrogenase

Matthew Davies, Timo Heikkila, Deborah Cowen, Paul Beddingfield, Paul Acklam, Glenn McConkey, Colin Fishwick, Peter Johnson and Mark Parsons

Introduction/Background

Pyrimidine biosynthesis presents an attractive drug target in a variety of organisms, including humans and the malaria parasite *Plasmodium falciparum*. Dihydroorotate dehydrogenase (DHODH), an enzyme catalyzing the only redox-reaction of the pyrimidine biosynthesis pathway, is a well characterized target for chemotherapeutical intervention. We are using an interdisciplinary approach to design, synthesise, characterise and determine crystal structures of novel and improved inhibitors of DHODH from several species.

Main body

DHODHs catalyses the conversion of dihydroorotate to orotate in the key rate-limiting step in pyrimidine biosynthesis. They contains a bound FMN cofactor and the Class 2 enzymes from both human (HsDHODH) and *P. falciparum* (PfDHODH) utilise respiratory quinones as terminal electron acceptors. The enzymes have a conserved $(\alpha/\beta)_8$ barrel fold and are membrane-associated via an amino-terminal extension. All well-characterised inhibitors of DHODH bind in the putative quinone binding site. This is a cleft that lies between two helices of the membrane-association domain and a loop region between strand 8 and helix 8 of the barrel and terminates close to the bound FMN cofactor. Whilst the cleft is predominantly hydrophobic around its opening, it contains a number of polar sidechains at its inner end, that are proposed to interact with the quinone and may play key roles in electron transport from $FMNH_2$.

Through the use of SPROUT, a Leeds-developed software suite for structure-based inhibitor development, we have evaluated a large number of candidate inhibitors of both HsDHODH and PfDHODH. Some of these have been developed by lead optimisation based upon existing inhibitors and others have been developed *de novo* using fragment-based approaches. Compounds predicted to bind tightly to either enzyme have been chemically synthesised and their ability to inhibit DHODH evaluated in an *in vitro* biochemical assay. Our best compounds (unpublished work which is currently being patented) have apparent inhibitory constants (K_I) of approximately 10 nM against PfDHODH and are essentially inactive against HsDHODH.

The tightest binding inhibitors of PfDHODH have also been tested *in vivo*, in a parasite viability assay. This confirms that not only do these compounds inhibit PfDHODH *in vitro*, but they also halt growth of the parasite (IC_{50} of 3.5 nM for the best compound).

A number of the tightest binding inhibitors of HsDHODH have been co-crystallised with the enzyme and there structures determined to high resolution (Figure 1). Such structures allow the specific interactions between enzyme and inhibitor to be analysed. In general these confirm the SPROUT-predicted binding modes although with occasional subtle differences.

(A)

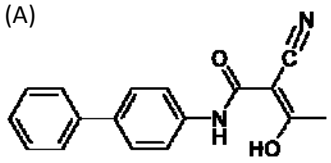

(B)

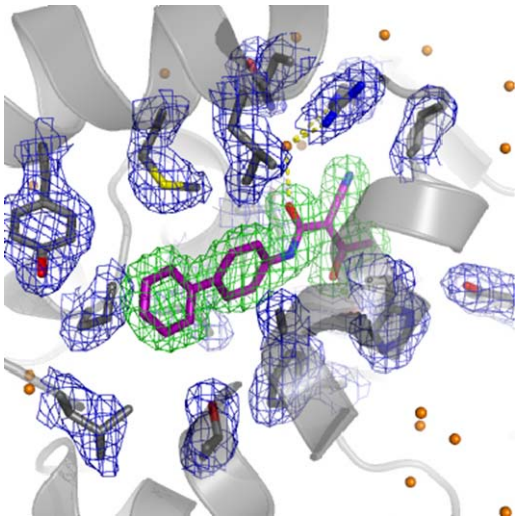

Figure 1: (A) chemical structure of MD250, a potent inhibitor of HsDHODH. **(B)** Crystal structure of HsDHODH with clear electron density (green) indicating the location of bound MD250.

Publications

Davies, M., Heikkilä, T., McConkey, G., Fishwick, C., Parsons, M. and Johnson, P. (2009) Structure-based design, synthesis, and characterization of inhibitors of human and *Plasmodium falciparum* dihydroorotate dehydrogenases. *J Med Chem* **52**:2683-2693.

Terahertz spectroscopy of single crystal proteins

Katarzyna Tych, Andrew Burnett, John Cunningham, Christopher Wood,
Edmund Linfield, Giles Davies and Arwen Pearson.

Intoduction

Over the past decade, the use of terahertz time-domain spectroscopy (THz-TDS) has become routine for the investigation of low-frequency inter-molecular vibrations in polycrystalline small organic molecular systems. THz spectroscopy has been shown to be particularly sensitive to long-range order and chemical environment in small organic systems. In particular, a number of normal modes observed at THz frequencies can be attributed to external vibrations present only when the molecule is fixed within a crystalline lattice; these vibrations arise because of the lack of free rotation of molecules within the crystal. THz frequency range studies of proteins reported to date have been performed in solution, or using amorphous hydrated thin protein films. The data from these studies reveal broad absorption spectra, without sharp absorption features. It is likely that the reason for this is a combination of the large number of low frequency normal modes within a macromolecule, and the lack of external modes in non-crystalline materials. We are developing broadband THz-TDS techniques to investigate the low-frequency spectra of protein single-crystals.

THz-TDS measurements of protein crystals

The THz region of the electromagnetic spectrum extends between 100 GHz (3.33 cm^{-1}) and 10 THz (333.3 cm^{-1}). THz radiation is non-ionising, and has been used to characterise a broad range of crystalline materials, since it can reveal unique ('fingerprint') absorption spectra, indicative of the chemical structure of the material studied. The timescales usually accessible to THz-TDS, covering the range from pico– to micro– seconds, relate to both the intra-molecular (internal) motions arising from the chemical structure of the molecule studied, and intermolecular (external or collective) motions, which arise from the way in which molecules interact within a crystal. In proteins, these low frequency collective modes are thought to be related to the large scale conformational motions responsible for functions such as electron transfer and enzymatic action.

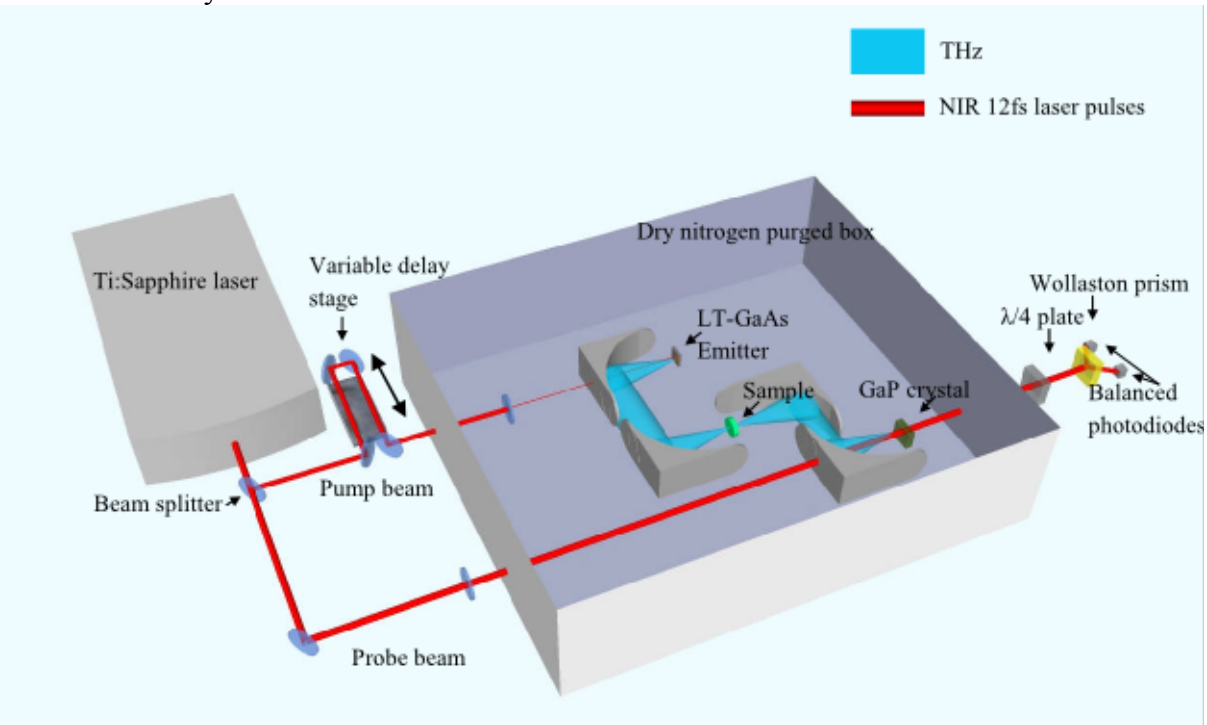

Figure 1: Schematic of the broadband THz-TDS experimental used for spectroscopy of protein crystals.

Figure 1 shows the experimental arrangement used for THz-TDS in this work. A diode-pumped 76 MHz repetition rate Ti:Sapphire laser (Femtosource, Femtolasers) provides near infra-red (NIR) pulses of 12 fs duration at a centre wavelength of 812 nm. This is split into pump (~330 mW) and probe (~40 mW) component beams. The pump beam is focused onto a THz emitter, comprising titanium/gold electrodes (biased with a 10 kHz, 110 V pk-pk square wave), with a 400 μm gap between them, formed on a low-temperature-grown gallium arsenide (LT-GaAs) photoconductive substrate. The THz radiation is collected from the front surface of the emitter, in order to maximise bandwidth by avoiding dispersion and absorption within the LT-GaAs substrate, before being collimated and focused onto the protein crystal sample using off-axis parabolic mirrors. Since the protein crystals are usually smaller than the focal diameter of the THz beam (~1 mm), a 500 μm aperture is placed in front of the sample at the focal point of the beam, ensuring that transmitted THz radiation interacts fully with the protein crystal. The transmitted THz signal is collected and focused onto a 150-μm-thick GaP electro-optic crystal, spatially overlapped with the probe beam, enabling lock-in detection by electro-optic sampling of the THz radiation in the time-domain.

THz-TDS sample cells are formed using 500-μm-thick windows of THz-transparent polymethylpentene (TPX), separated by a nitrile o-ring spacer (1 mm thick). The sample cell is filled with an ultra-violet (UV) activated epoxy, and a sample chamber of diameter 7.5 mm and capillary channel formed using UV photolithography. Protein crystals are placed, using the capillary channel, on the inside surface of one of the TPX windows within the sample chamber. A small amount of reservoir solution is then placed in the capillary channel, and the cells sealed to prevent dehydration of the crystals.

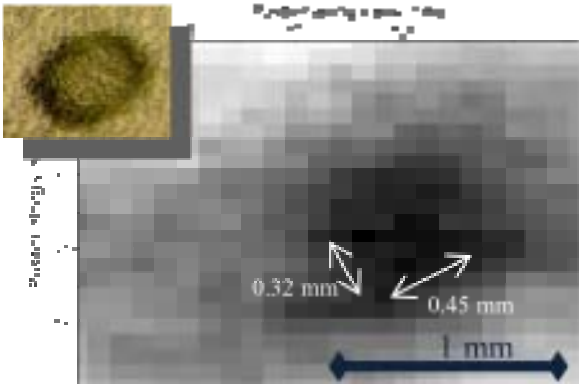

Figure 2: Terahertz absorption image of a lysozyme crystal obtained with contrast indicating the peak to peak amplitudes at each pixel of signals transmitted through the sample cell, and (inset) an optical micrograph of the same crystal, taken through the TPX window.

The sample cells are placed in the broadband (0.3 – 8.0 THz) THz-TDS system described above, and raster scanned in the *x*,*y* plane, perpendicular to the THz beam. Figure 2 shows an image of the change in THz peak-to-peak amplitude as a function of this *xy* position (the dark area of high absorption shows the crystal position). This is the first image of a protein crystal made using the technique of THz-TDS. We have recently shown that the technique is highly sensitive to the hydration state of the crystal, finding a decreased THz absorption as water is removed from the crystal.

Funding
This work is supported by the EPSRC and the Leverhulme Trust.

Activation and inhibition of purified intact membrane sensor kinases involved in virulence and antibiotic resistance in *Enterococcus faecalis*

Pikyee Ma, Hayley Yuille, Lianne M. Davis, Peter Henderson and Mary Phillips-Jones

Introduction

Enterococcus faecalis is the fourth most important agent of hospital-acquired and other infections in the UK, causing bacteremia, endocarditis, urinary tract infection and endophthalmitis. Of particular concern is the intrinsic and increasing resistance to most currently approved antibacterial agents, including the 'last-line' glycopeptide vancomycin (Depardieu *et al*. (2007) *Clin Microbiol Revs* **20**:79-114).

E. faecalis possesses sixteen membrane-bound sensor kinases, which constitute the sensory components of the sixteen regulatory two-component signal transduction systems of this bacterium. Recently we reported the successful expression and purification of twelve of these membrane proteins as intact active proteins. Some of these sensors have been implicated in the regulation of virulence and antibiotic resistances, including EF1820 (FsrC, the sensor of the Fsr quorum-sensing system that responds to the autoinduced peptide GBAP and has roles in both virulence and biofilm formation) and EF2298 ($VanS_b$, which is involved in activating VanB-type vancomycin resistance genes). In light of their importance in virulence and antibiotic resistance, these proteins constitute promising targets for new and novel anti-enterococcal drugs. Here we report on recent progress in our ongoing molecular and structural studies to identify inhibitors as well as activators of intact FsrC and $VanS_b$ proteins, including the identification of a direct inhibitor of FsrC autophosphorylation activity and the development of successful strategies for optimising the production of $VanS_b$, which previously proved difficult to produce in sufficient quantities for future activity, ligand-protein interactions and structural studies.

Results

Activation and inhibition of intact purified FsrC.

In vitro autophosphorylation activity assays were performed in triplicate over a 60 min period using purified FsrC in the presence and absence of 2-fold molar excess of the activating pheromone ligand GBAP (10.7 μM) and in the presence or absence of a 5-fold molar excess of a candidate inhibitor (50 μM). The results are shown in Figure 1. The presence of GBAP produced an approximately 7-fold increase in FsrC-P levels after 60 min compared to the control assays containing FsrC alone, as expected for this activating pheromone 'signal' (Ma et al., 2008). The presence of 50 μM candidate inhibitor in addition to 10.7 μM GBAP in the assays reduced the levels of phosphorylated FsrC by approximately 50 % (Figure 1). A similar level of inhibition of non-GBAP stimulated FsrC activity (in the absence of added GBAP) by the inhibitor was obtained numerically, though this does not appear to be statistically significant presumably because of the relatively low levels of FsrC-P that are produced under such conditions. We therefore conclude from these data that

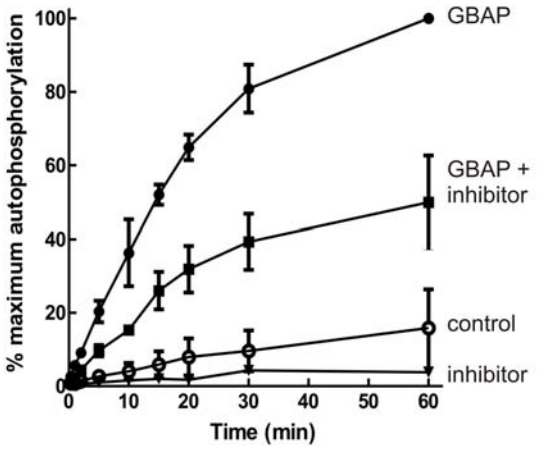

Figure 1: Time course autophosphorylation activity assays for FsrC in the presence and absence of a 2-fold molar excess of the activating pheromone ligand GBAP and/or a 5-fold molar excess of candidate inhibitor. Values represent the mean ± standard deviation of triplicate determinations.

our activity assays are suitable for inhibitor studies and that the candidate inhibitor used here is a significant and direct inhibitor of the GBAP-stimulated activity of FsrC.

Optimised production of purified and active intact $VanS_b$.

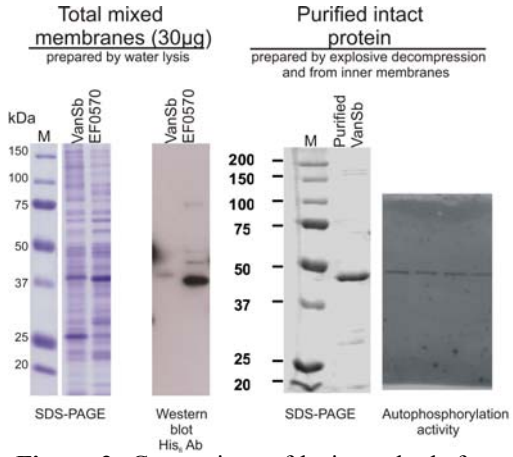

Figure 2: Comparison of lysis methods for subsequent purification of active, intact $VanS_b$ from *Escherichia coli* BL21 [DE3]/pTTQ18-$VanS_b$ lysates.

In previous studies using non-optimised expression and purification trials for intact $VanS_b$, low yields of purified protein were obtained. Therefore several modifications to the methodology have been introduced for $VanS_b$ purification, including methods that reduce protein degradation (Figure 2), resulting in intact undegraded protein (as revealed by mass spectrometry, N-terminal sequencing and Western blotting). The protein is now being used to identify activators and inhibitors of its activity.

Funding
This work was funded by the BBSRC.

Collaborators
Professor Jiro Nakayama and Dr Kenzo Nishiguchi, Kyushu University.

Fibril fragmentation in amyloid assembly and cytotoxicity

Wei-Feng Xue, Andrew Hellewell, Steve Homans, Eric Hewitt and Sheena Radford

Amyloid assemblies are associated with several debilitating human disorders including type II diabetes mellitus and Alzheimer, Parkinson and Creutzfeldt-Jakob diseases. Understanding the intra- and extracellular assembly of normally soluble proteins and peptides into amyloid aggregates and how they disrupt normal cellular functions is therefore of paramount importance. In recent years, pre-fibrillar oligomers have been implicated as the primary cytotoxic species associated with amyloid formation. However, various reports have implicated the fibrillar products of assembly as the primary cytotoxic species, suggesting that they should not be dismissed as merely the inert products of amyloid assembly. The physical attributes of fibrillar aggregates, that influence surface interactions and biological availability, may therefore play an important role in amyloid disease.

To investigate the impact of fibrils on the cellular responses to amyloid, in particular how the responses are related to the physical dimensions of the fibrils, we characterised the length distribution of fibrils formed *in vitro* from β_2-microglobulin (β_2m). Using a custom built precision stirrer we generated fibril samples containing an identical monomer equivalent concentration that had indistinguishable molecular architecture, but distinct length distributions (Figure 1A).

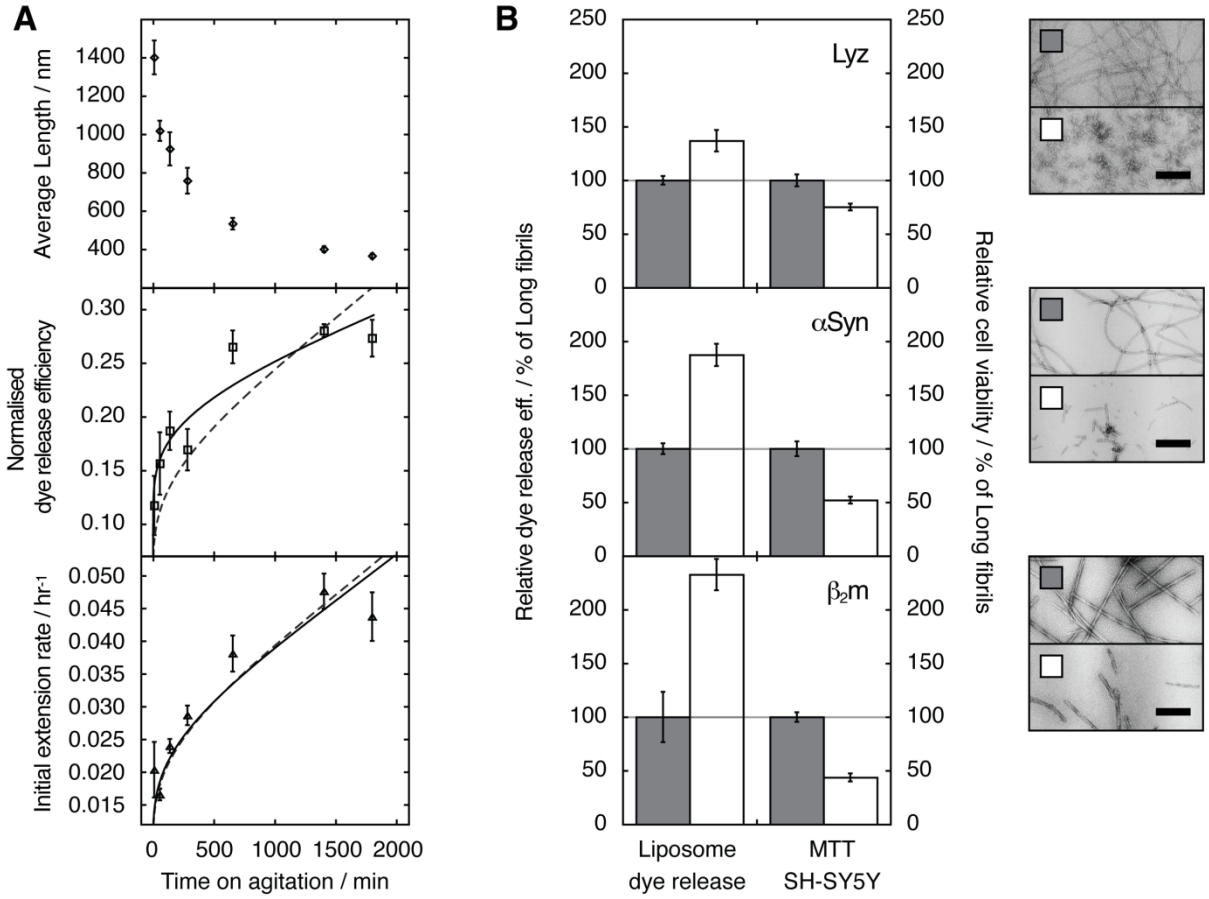

Figure 1: The effect of fibril fragmentation on length, seeding capability, capacity to cause membrane disruption and cytotoxic potential of fibril samples. **(A)** Change in weight average fibril length as measured using TM AFM single particle image analysis (upper), ability to disrupt a model lipid membrane (middle) and initial fibril extension rate when added to fresh monomer solutions (lower). **(B)** Ability to disrupt liposome membranes (dye release assay), and to decrease cell viability (MTT assay) by samples containing short (white bars) or long (grey bars) fibrils of lysozyme (top), α-synuclein (middle) or β_2m (bottom). The error bars represent one standard error. Negative stain transmission electron micrographs of the fibril samples (top: lysozyme, centre: α-synuclein, bottom: β_2m) are shown to the right, with scale bars representing 200 nm.

When fibril growth of β_2m was seeded by each of these samples, the initial rate of fibril growth was shown to be enhanced for fibril samples containing short fibrils compared with their longer counterparts (Figure 1A). Importantly, when added to liposomes, the fibril samples were found to be able to cause membrane disruption. Most remarkably, however, the samples containing shorter fibrils were found to disrupt the liposome membranes more efficiently than their longer counterparts (Figure 1B). The ability of fibril samples to cause a reduction in cell viability was assayed using 3-(4,5-dimethylthiazol-2yl)-2,5-diphenyltetrazolium bromide (MTT) assays. The MTT assays showed that samples containing shorter fibrils reduced cell viability of SH-SY5Y and RAW 264.7 cells to a greater extent than samples containing longer fibrils (Figure 1B). The same length-dependent effect on liposome membrane integrity and on cell viability assayed by MTT was also observed for fibrils formed from lysozyme or α-synuclein. The results therefore demonstrate the striking finding that shorter fibrillar samples show an enhanced cytotoxic potential compared with their longer counterparts, despite possessing indistinguishable molecular architecture (Figure 1).

These findings bring fragmentation, and the dimensions and surface interactions of amyloid fibrils into focus as potential key properties affecting the behaviours of amyloid fibrils in disease. The combined effects of decreasing the length of individual fibrils and increasing the number of fibrillar particles caused by fibril fragmentation may together contribute to enhance the cytotoxic potential of fibrillar material. Reduction in the dimensions of fibrils following fragmentation could result in enhanced fibril-membrane surface interactions and/or reduced fibril-fibril interactions that may increase the biological availability and overall surface activity of fibril deposits. Reducing the overall fibril size could also lead to increased internalisation by cells or increased membrane penetration of extracellular fibrils, giving them an access to potentially more vulnerable internal membranes. Our study has indicated that the hallmarks of amyloid disease do not only depend on the quantity of amyloid deposits, or the nature of amyloid precursors, but also on the physical size of fibrils, possibly by affecting the biological availability of amyloid aggregates and/or their surface properties. Thus, strategies that reduce the amount of aberrant surfaces presented by amyloid fibrils, or which reduce their biological availability could be successful in limiting the rate of amyloid deposition, as well as reducing the cytotoxic effects of amyloid itself.

Publications

Xue, W.-F., Homans, S. and Radford, S. (2009) Amyloid fibril length distribution quantified by atomic force microscopy single-particle image analysis. *Protein Eng Des Sel* **22**:489-496.

Xue, W.-F., Hellewell, A., Gosal, W., Homans, S., Hewitt, E. and Radford, S. (2009) Fibril fragmentation enhances amyloid cytotoxicity. *J Biol Chem*, **284**:34272-34282.

Xue W.-F., Hellewell AL, Hewitt EW and Radford SE (2010), Fibril fragmentation in amyloid assembly and cytotoxicity – When size matters, *Prion*, **4**:20-25.

Funding

We are grateful to the University of Leeds, BBSRC and The Wellcome Trust for financial support.

Collaborators

This project was performed in collaboration with Walraj Gosal (now at the University of Texas, Dallas).

Towards a structure of β_2-microglobulin amyloid fibrils

Carol Ladner, Timo Eichner, John Hodkinson, Eva Petrik, Geoffrey Platt, Katy Routledge, Alessandro Sicorello, David Smith, Ricardo Tome, Nathalie Valette, Lucy Woods, Wei-Feng Xue and Sheena Radford

Introduction

Amyloid fibrils with characteristic cross-β structure are formed by various proteins with unrelated structures. The structure of amyloid fibrils is of great importance for developing a molecular interpretation of amyloidosis and for the rational development of therapies against amyloid disease. High resolution structures have been obtained for cross-β fibril structures formed from peptide and protein fragments, but no all-atom model has been obtained for fibrils composed of a full-length protein. Our approach to determine an all-atom model of β_2m fibril structure is to combine biophysical and biochemical techniques. We have recently probed the structural organisation, sidechain mobility and sidechain accessibility of the 99 residue β_2m protein in amyloid fibrils using continuous wave electron paramagnetic resonance (CW-EPR) spectroscopy.

Parallel in-register structure of β_2m in amyloid fibrils

Site-directed spin labelling at 19 positions in β_2m was used to probe the organisation of the polypeptide sequence in amyloid fibrils formed at pH 2.5. Spin labelled positions in the polypeptide sequence that are in a parallel, in-register arrangement (labels <7 Å apart) give rise to EPR spectra characterised by exchange-narrowing, exemplified by position 81 (Figure 1A). This analysis revealed a core involving residues 19-50 and 55-91 organised in a parallel in-register arrangement.

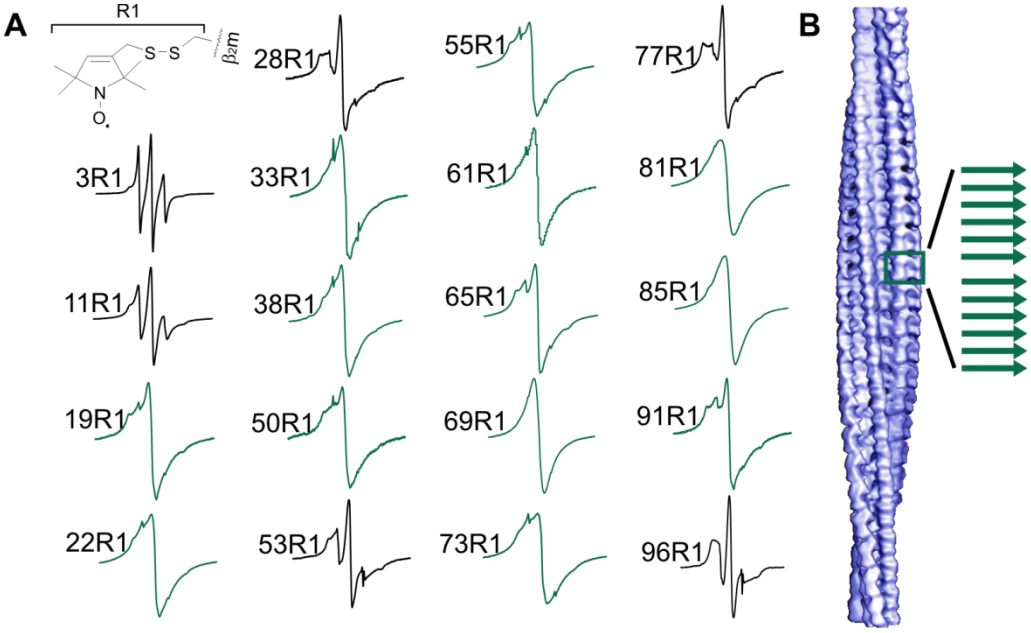

Figure 1: EPR spectroscopy of spin labelled β_2m fibrils reveals a parallel, in-register organisation. **(A)** EPR Spectra of β_2m fibrils are shown for 19 single cysteine β_2m variants labelled with 1-oxyl-2,2,5,5-tetramethyl-D-pyrroline-3-methyl-methanethiosulfonate (R1). **(B)** The organisation of β_2m in the cryo-EM 3D reconstruction structure is shown as two sets of *ca.* six β-strands arranged in a stacked array.

Stacked sets of parallel in-register structure

A continuous array of parallel, in-register β-strands involving most of the polypeptide sequence is inconsistent with the cryo-electron microscopy (cryo-EM) structure which reveals an architecture based on subunit repeats. To reconcile these data, the number of spins in close

proximity required to give rise to spin exchange was determined. Systematic studies of a model protein system indicated that juxtaposition of four spin labels is sufficient to generate exchange narrowing. Based on the data presented we proposed that the subunit repeat observed in the cryo-EM structure of β_2m fibrils, which varies from 5.2 to 6.5 nm in height in different fibrils, is composed of two stacks of *ca.* six β-strands organized in a parallel and in-register array along the fibril axis (Figure 1B). Furthermore, information obtained from the sidechain mobility and accessibility results suggest an organisation more complex than the accordion-like β-sandwich structure commonly proposed for amyloid fibrils.

Future Perspectives

In addition to determining the structure and dynamics of β_2m fibrils, our research group is investigating the broad molecular interpretation of amyloidosis. This involves using NMR to characterize the early steps, mass spectrometry to investigate oligomeric intermediates and ssNMR, cross-linking and FRET to further probe fibril structure. Together our aim is to provide an atomistic map of protein fibrilization and to understand its consequences on cellular function.

Publications

Eichner, T. and Radford, S. (2009) A Generic Mechanism of beta2-Microglobulin amyloid assembly at neutral pH involving a specific proline switch. *J Mol Biol*, **386**:1312-1326.

Platt, G., Xue, W.-F., Homans, S. and Radford, S. (2009) Probing Dynamics within amyloid fibrils using a novel capping method. *Angew Chem Int Ed Engl*, **48**:5705-5707.

Routledge, K., Tartaglia, G., Platt, G., Vendruscolo, M. and Radford, S. (2009) Competition between intramolecular and intermolecular interactions in an amyloid-forming protein. *J Mol Biol*, **389**:776-786.

White, H., Hodgkinson, J., Jahn, T., Cohen-Krausz, S., Gosal, W., Müller, S., Orlova, E., Radford, S. and Saibil, H. (2009) Globular tetramers of beta$_2$-microglobulin assemble into elaborate amyloid fibrils. *J Mol Biol* **389**:48-57.

Ladner, C., Chen, M., Smith, D., Platt G., Radford, S. and Langen, R. (2010). Stacked sets of parallel, in register β-strands in β_2-microglobulin amyloid fibrils revealed by site-directed spin labelling and chemical labeling. *J Biol Chem*, **285**:17137-17147.

Funding

We are grateful to the University of Leeds, Fundacao para a Ciencia e Tecnologia - MCTES - Portugal, BBSRC and The Wellcome Trust for financial support. We thank Keith Ainley for technical assistance.

Collaborators

This project was performed in collaboration with Ralf Langen from University of Southern California and Prof. Helen Saibil from Birkbeck College, as well as with Alison Ashcroft, Steve Homans and Stuart Warriner of the Astbury Centre for Structural Molecular Biology.

Exploring the folding energy landscape of immunity protein 7

Alice Bartlet, Stuart Knowling, Gareth Morgan, Clare Pashley, Sara Pugh, David Brockwell and Sheena Radford

Introduction

The fundamental problem of how an amino acid sequence determines protein structure is still not fully reconciled. Towards this aim, the folding of small, relatively simple proteins are being studied in atomistic detail to characterise all species encountered during the folding process. Over the last decade the folding mechanism of the colicin immunity protein, Im7, has been extensively interrogated by a range of biophysical approaches. Although we now have a detailed understanding of how this four-helical protein folds to its native stave, via a transiently populated intermediate ensemble, there are still many unexplored areas of this complicated mechanism. Current research has focussed applying new experimental approaches to glean new information about protein folding and exploring the relationship between in vivo and in vitro protein folding.

A three- helix intermediate is a necessary feature on the folding landscape

Although previous work demonstrated that Im7 folding proceeds via transient population of a three helix intermediate, it had not been clear whether this is a necessary feature on the folding landscape or simply a consequence of a sub-optimal amino acid sequence. Helix III is not fully formed, or docked, in the intermediate ensemble of Im7, and is only fully formed and correctly docked after the rate limiting transition state. However, helix III is also is also the shortest helix in Im7 and has a very low helical propensity. A polyalanine region was introduced into helix III, to extend and increase its helical propensity. Structural data indicates that the protein is still able to fold to the native state, and furthermore this alteration appears to have negligible effects on the kinetics of protein folding. These results show the three-helix intermediate is a necessity in the folding process, and even when the denatured state contains a preformed helical structure in this region, the protein folding mechanism is preserved.

Development of specific hydrophobic core packing during Im7 folding

Over-packing substitutions, in which side chain size is increased, were created to probe the specificity and malleability of core-packing during Im7 folding. In parallel, polar groups were introduced into the Im7 core to determine the solvation status of core residues at different stages of folding. Φ-value analysis demonstrated that the major changes in Im7 core solvation occur prior to the population of the folding intermediate, with key regions involved in docking of the short helix III remaining solvent exposed until after the rate-limiting transition state has been traversed. When these regions are over-packed Im7 fails to fold correctly and the intermediate species becomes highly populated at equilibrium indicating that Im7 does not achieve a specifically packed core until the very last step in the folding mechanism.

In vivo stability

Im7 has been used to develop a system that allows protein stability to be measured in vivo, allowing the directed evolution of protein stability independently of function. By fusing Im7 into the antibiotic resistance protein β-lactamase, we can infer the stability of the inserted protein by measuring the antibiotic resistance of cells expressing the fusion construct. The in vivo measurements of protein stability were compared with the in vitro measurements of the thermodynamic and kinetic stability of isolated Im7 variants. A striking correlation between in vivo and in vitro stability was observed. Evolved mutations that stabilized the protein were predominantly involved in the binding site of Im7 to its cognate nuclease, colicin E7. The results demonstrate a stark trade-off between stability and function in the evolution of Im7.

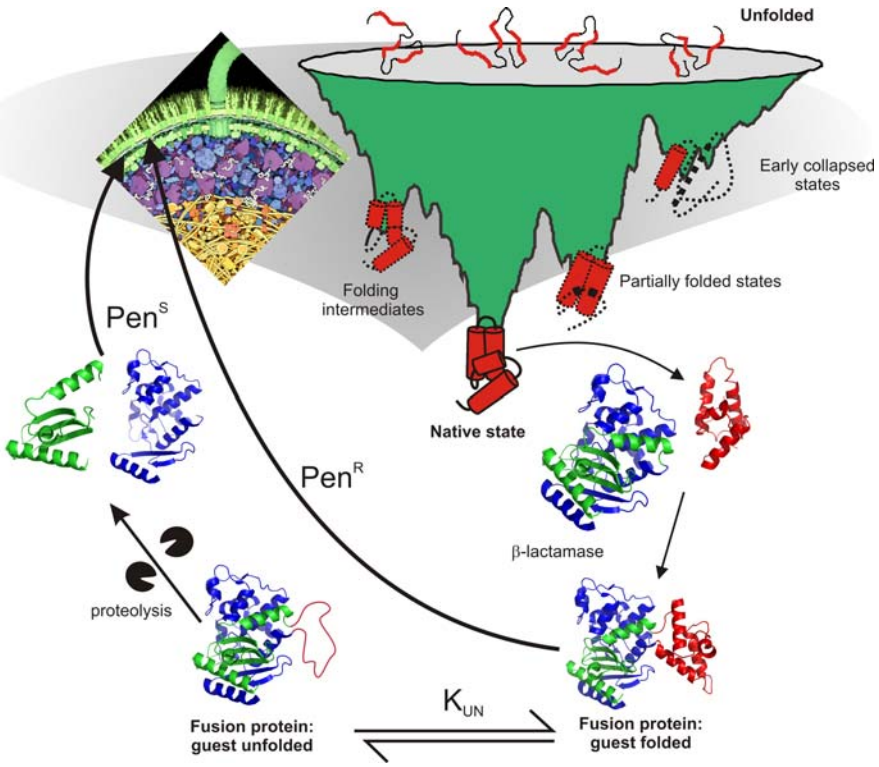

Figure 1: whilst much of our research is focused on dissecting protein folding events *in vitro*, we have recently developed a system to allow us to compare *in vivo* and *in vitro* measurements of protein stability. The β-lactamase enzyme tolerates insertions into a loop between its two domains, and hence a "guest" protein sequence can be inserted into the construct to create a fusion protein. The enzyme activity (against penicillin-type antibiotics) is used to report on the stability the guest protein, within *E. coli* cells. Inserts which do not fold correctly will be cleaved by the host's protein quality control machinery, severing the peptide chain between the two domains of the β-lactamase and inhibiting its activity. Hence, the resistance of the *E.coli* to penicillin is directly related to the stability of the guest protein within the cell, and in turn to its expression levels. This system offers us a convenient method to compare the stability of a protein *in vivo* with *in vitro* measurements of protein stability We can use this system to measure the stabilities of guest proteins, or to evolve proteins for increased stability *in vivo*.

Single molecule FRET studies of Im7 folding

Cysteine mutations were introduced into Im7 to allow fluorescent dye labelling of the protein for single molecule studies. The FRET efficiency of the dyes increases as the distance between the dyes decrease. The dyes are likely to, on average, have longer distances between them in unfolded species, compared with more compact states. Hence, this method allows the distributions of the unfolded, intermediate and native state to be assessed, and the protein folding of Im7 to be characterised at a single molecule level for the first time. A remarkable observation from these experiments was that the unfolded state of Im7 in the absence of denaturant was significantly more compact than the urea-denatured state, suggesting that significant structure could be present in the unfolded ensemble. How this structure influences folding and its precise nature are currently under investigation.

Current work

Although the correlation between *in vivo* and *in vitro* stability was striking, there were notable exceptions. In some cases a protein is more stabile *in vitro*, but apparently less well tolerated by the cell. How well a protein is tolerated by the cell is likely to have a fundamental affect on protein expression, and we are attempting to use the β-lactamase system to dissect the factors

involved in this process. We intend to further investigate the single molecule observations of the unfolded ensemble. The unfolded ensemble contains all conformations sampled at the beginning of the folding process, and is therefore crucial to our understanding of further folding events. However since the unfolded state is not significantly populated at equilibrium, it is difficult to characterise by biophysical methods. Mutations have been introduced into the Im7 sequence to destabilise the intermediate and native states, such that the unfolded state becomes the most stable species at equilibrium. Using this rationale, we have successfully created an unfolded variant of Im7, which populates an unfolded state under conditions favouring folding. Biophysical studies are on-going to characterise this ensemble in atomistic detail.

Publications

Foit L., Morgan, G., Kern, M., Steimer. L., von Hacht, A.-K. , Titchmarsh, T., Warriner, S., Radford, S. and Bardwell, J. (2009) Optimizing protein stability *in vivo*. *Mol Cell,* **36**: 861-871.

Knowling, S., Figueiredo, A., Whittaker, S., Moore, G. and Radford, S. (2009) Amino-acid insertion reveals a necessary three-helical intermediate in the folding pathway of the colicin E7 immunity protein Im7. *J Mol Biol*, **392**:1074-1086.

Bartlett, A. and Radford, S. (2010) Desolvation and development of specific hydrophobic core packing during Im7 folding. *J Mol Biol* **396**:1329-1345.

Pugh, S., Gell, C., Smith, D., Radford, S. and Brockwell, D. (2010) Single-molecule studies of the Im7 folding landscape. *J Mol Biol* **398**:132-145.

Funding

This work is funded by the BBSRC. We thank Keith Ainley for technical support.

Collaborators

Jim Bardwell (University of Michigan, USA), Christopher Gell (Max Planck Institute of Molecular Cell Biology & Genetics, Germany), Alastair Smith (Avacta Group Plc, York)

Biomimetic production of precise nanomagnetic particles using magnetic bacteria and their biomineralisation proteins

Johanna Galloway, Masayoshi Tanaka, Jonathan Bramble, Stephen Baldwin, Stephen Evans and Sarah Staniland

Introduction

Scientific and economic interest in nanotechnology has grown in recent years. Within this the quest to produce tiny and highly tailored magnetic particles, or nanomagnets is crucial. Nanomagnets have a range of practical uses such as: the development of 3D information storage systems providing high density data storage; medical applications site specific targeted therapies and image enhancers for diagnostic medicine.

However, as nanotechnology grows, so does the need to develop precisely engineered nanomagnets. Different applications demand different shapes and sizes of particles and different magnetic properties. Producing nanomagnets with highly controlled; composition, size and shapes, in large enough amounts to be of use to these industries, has therefore become a key goal of researchers.

Magnetotactic bacteria are the simplest organisms that perform biomineralisation. They take up iron ions from solution and produce nanoparticles of magnetite (Fe_3O_4) within lipid vesicles (which are termed magnetosomes) under precise control, resulting in a strain specific uniform size and morphology (Figure 1).

The aim of this group's research is to investigate the microbiology and proteomics of these bacteria and to manipulate the biomineralisation process to enable the production of high-yields of customised nanomagnets for nanotechnological application using the genetic precision of nature.

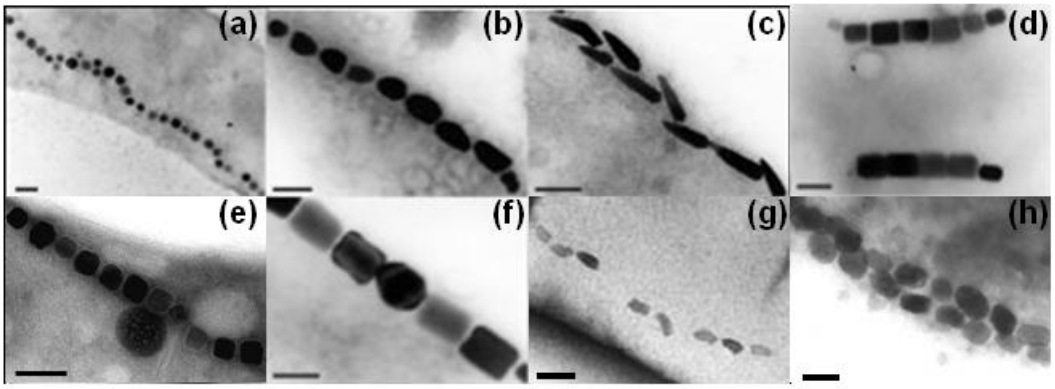

Figure 1: TEM images of different magnetosome morphologies. **(a)** and **(e)** show cubo-octahedral magnetosomes, **(b)** bullet shaped magnetosomes, **(c)** tooth-shaped magnetosomes. **(d)** and **(f)** are elongated magnetosomes and **(g)** and **(h)** irregular bullet shaped magnetosomes. Scale bars are 100 nm.

The Research

The magnetic composition of magnetosomes as been sucessfully altered *in vivo* by doping the magnetosomes with cobalt resulting in magnetosomes with an increased magnetic coecivity compared to control magnetosomes. This was acheived with the addition of cobalt ions into the bacterial growth media which were taken up and incorperated into the magnetite mineral in approximately 1% quanities. This could not be increased *in vivo* due to the restriction imposed by the organism. We thus sought an *in vitro* route to offer more flexibility and higher-yields. Here, in collaboration with the lab of Prof. Matsunaga we build on their original method and developed a biomimetic route to more precise nanomagnets synthesied at

room temperature using a protein mediated precipitation of particles. The protein used was Mms6 (magnetosome membrane specific, 6 KDa) which was found to be unique to the magnetosome mebrane and tightly bound to the crystal. When this protein was expressed and purified and used in vitro it was found to control particle size and shape. This protein was located along with 3 others (Mms 5, 7 & 13) and all of them have charactierstic similar to other biomineralisation templating proteins such as and LG repeat sequence.

Research is now being conducted in two paraellel and complementary directions. Firstly, the physical investigation of how these proteins interact with the forming mineral and control the magnetite's formation and morphology is being investigated. Several new proteins are being identified and expressed while their interaction with magnetite is being assessed using a range of spectroscopy, electron/force microscopy and neutron scattering techniques (schematic of project is shown in Figure 2).

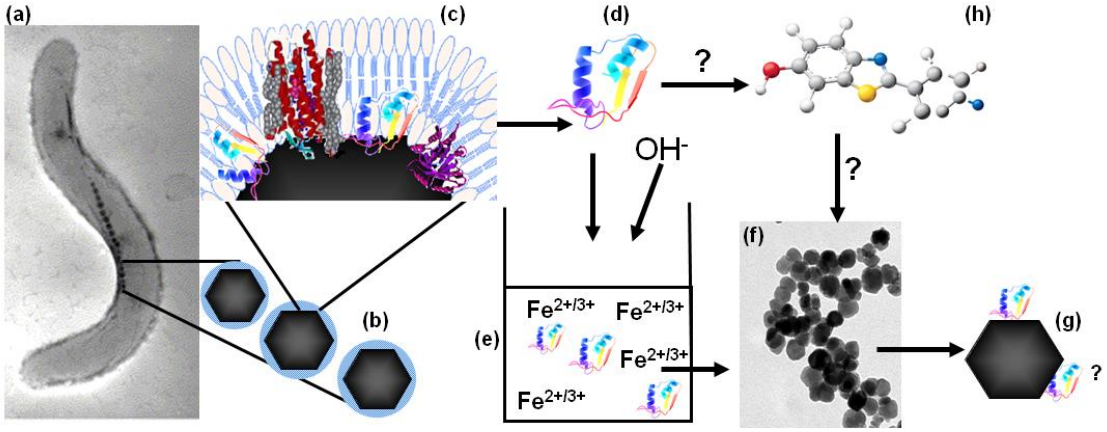

Figure 2: Schematic of research, showing; **(a)** *Magnetospirillum magneticum* AMB-1, **(b)** extracted magnetosomes, **(c)** biomineralisation proteins in the magnetosome membrane, **(d)** purified biomineralisation protein Mms6, **(e)** protein mediated *in vitro* precipitation of magnetite, **(f)** resultant nanoparticles **(g)** particle/protein analysis, **(h)** potential synthetic protein mimic.

Once key motifs, peptide and binding sites can be identifed we could begin to design tailored addatives for high-yield industrial nanomagnet production. Secondly, we are developing a range of methods using the expressed Mms proteins *in vitro* for more advanced synthesis. We are enhancing this with the addition of membranes and vesicles to the systems. This is being furthered by experimenting with different proteins that affect the fucntionality of membranes. For example we are investigating novel metal ion transport proteins and vesicle deformation proteins which can be incorperation into vesicles along with Mms proteins to develop a range of novel, flexible biomimetic systems. For example we are patterning surfaces with Mms6 to attempt to form customised nanomagnetic arrays. This is just one of many biomimetic systems we are developing to create several novel mineral/membrane assemblies, some tethered/free and attached to surfaces.

Additionally a recent TEM study has revealed how mangetic bacteria divide and what happens to the magnetosome chain within them duing this process.

Publications

Staniland, S. (2009) Magnetosomes: bacterial biosynthesis of magnetic nanoparticles and potential biomedical applications. In Magnetic nanomaterials: Nanomaterials for the life sciences series Vol. 4 (Kumar, C., ed), pp 399, Wiley-VCH, Weinheim

Staniland S., Ward F. and Harrison, A. (2009) Biomineralisation of magnetite nanoparticles by microbes. In Neutron applications in earth, energy, and environmental sciences (Liang, L., Rinaldi, R. and Schober, H., eds), pp 595-619, Springer, London.

Staniland, S., Moisescu, C. and Benning, L. (2010) Cell division in magnetotactic bacteria splits magnetosome chain in half. *J Basic Microbiol*, in press.

Staniland, S., Coppock, M., Tuffin, M., van Zyl, L., Roychoudhury, A. and Cowan. D. (2010) Cobalt uptake and resistance to trace metals in *Comamonas testosteroni* isolated from a heavy-metal contaminated site in the Zambian copperbelt. *Geomicrobiol J*, in press.

Funding
This work has been funded by the EPSRC (Overseas Postdoctoral Life-science Interface Fellowship Scheme 2005-2008 EP/C53204X/1) and is now being funded by the BBSRC (2010-1014 BB/H005412/1)

Collaborators
C. Moisescu and Prof. L. Benning, School of Earth and Environment. University of Leeds.
Dr. B. Ward, University of Edinburgh.
Prof. A. Harrison, ILL, Grenoble, France
Prof. T. Matsunaga, Tokyo University of Agriculture and Technology, Tokyo, Japan
Prof. D. Cowan, University of the Western Cape, Cape Town, South Africa
Prof. A. Roychoudhury, University of Stellenbosch, Stellenbosch, South Africa

Induced bending of a plasmid origin of replication by its cognate replication initiator protein, RepD, and the helicase PcrA

Gerard Lynch, Neil Thomson and Christopher Thomas

Background

The *pcrA* gene is ubiquitous in Gram-positive bacteria and encodes an essential but poorly processive helicase. Although the role of PcrA in Gram-positive bacteria such as the human pathogen *Staphylococcus aureus* remains unclear, it has been shown to be important for the rolling circle replication of the pT181 family of staphylococcal plasmids.

Previously work has focused on the interaction of PcrA helicase with the replication initiator protein of the staphylococcal plasmid pC221, RepD. Here we show by Atomic Force Microscopy (AFM) how RepD induces a bending of its cognate origin of replication, *oriD*. Recruitment of PcrA further modifies the distribution of bending of *oriD*. Finally, there is a re-modelling of the protein:DNA complex in the presence of the non-hydrolysable ATP analogue, AMPNP. These findings highlight the sequential nature of initiating plasmid replication and the need to remodel the *oriD* at different stages of the process.

Recent Findings

To maintain supercoiling effects and ensure efficient binding, all complexes were first assembled on the negatively supercoiled plasmid, pCER*oriD*. The *oriD* was then excised with the restriction endonuclease PvuII, and the resultant *oriD*:protein complexes deposited on a mica surface for imaging by AFM. Naked DNA was uniform in appearance, however in the presence of RepD a high, globular feature can be seen bound asymmetrically to the DNA (see Figure 1). The angle between the DNA arms, exiting from the globular feature were measured for three different *oriD*:protein complexes: RepD only; RepD and PcrA; and RepD, PcrA and the non-hydrolysable nucleotide, AMPNP. Two principle types of complex were seen: one characterised by a sharp bend in the DNA (less than 110°), and the other a shallow bend (110° or greater). In the presence of RepD, bending of DNA focuses tightly around the 80-90° angle and there is also a broader distribution around 140-150°. The

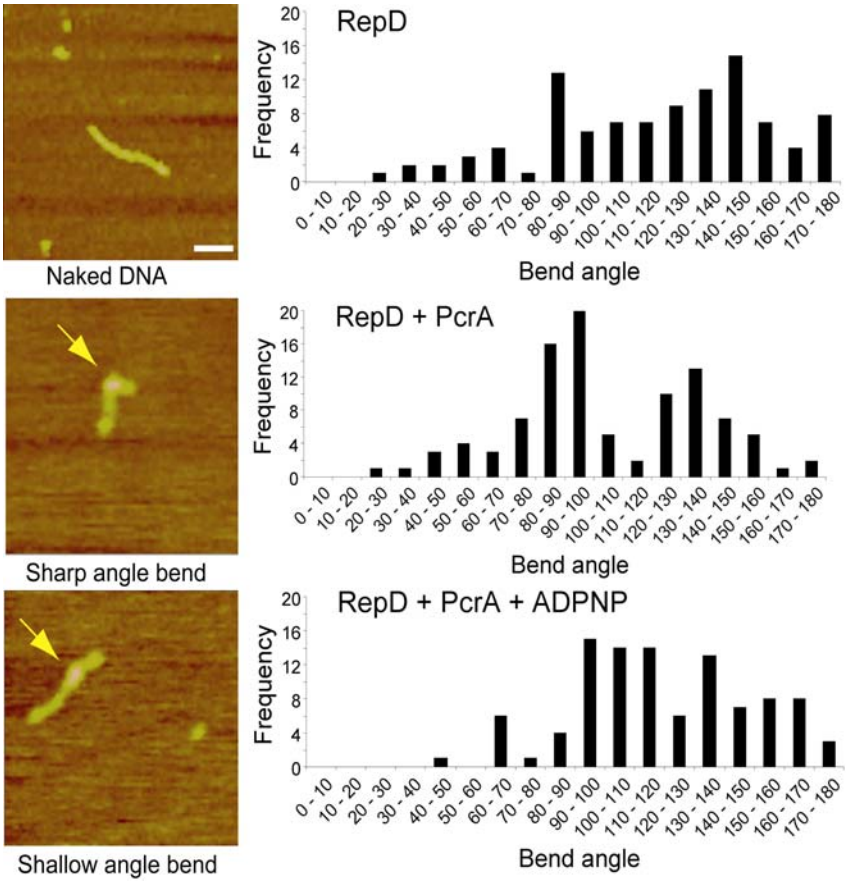

Figure 1: Representative AFM images and bend angle distributions of *oriD* in the presence of RepD; RepD and PcrA; and RepD, PcrA and AMPNP. Bound protein is seen as a globular feature on the DNA (yellow arrow). One hundred samples were imaged for each combination, and the bend angles were measured. Histograms depicting the distributions are shown. The white scale bar represents 50 nm.

proportion of sharply-bent fragments was 39%. In the presence of PcrA with RepD the number of sharply-bent fragments observed increased to 60%. The distribution also became more focused around the principle angles, suggesting an decrease in the flexibility of the *oriD*:protein complex. Finally, when AMPNP was included, the number of sharply-bent fragments decreased again, to 41%, and the bend angle distribution broadened. This increase in intermediate angled fragments is perhaps indicative of a remodelling of the *oriD*:RepD:PcrA complex by binding of AMPNP, into a more flexible structure. Remodelling of the *oriD* by RepD, PcrA and bound nucleotide seem important in preparing the origin for duplex separation and subsequent replication.

Publications

Machon, C., Lynch, G., Thomson, N., Scott, D., Thomas, C. and Soultanas, P. (2010) RepD-mediated recruitment of PcrA helicase at the *Staphylococcus aureus* pC221 plasmid replication origin, *oriD*. *Nucleic Acids Res* **38**:1874-1888.

Funding

This work was funded by the BBSRC.

Acknowledgements

We thank Sergio Santos Hernandez for assistance with the AFM work.

Mechanical response of collagen fibrils measured by atomic force microscopy

Colin Grant, David Brockwell, Sheena Radford and Neil Thomson

Introduction

Collagen is the most abundant protein in the mammalian body, accounting for up to 35% of whole-body protein content. It is predominantly found in tissues such as cartilage, bone, skin, tendons and ligaments; all of which are vital for the large degree of locomotion that we currently have. Most collagenous tissues, e.g. tendons, have a structural hierarchy in that bundles of fascia and collagen fibres are made up from collagen fibrils, which themselves are made up from collagen monomers. Knowledge of collagen fibril biomechanics is an essential part of understanding the mechanics of tissues at the nano-level, giving us an insight to fracture behaviour. Furthermore, fibrils are an ideal re-enforcing material in a gel-like matrix, similar to composite materials like carbon-fibre and plywood, giving them huge potential for tissue engineering applications such as biomimetic tissue replacements.

Effect of hydration on the mechanical properties of collagen fibrils

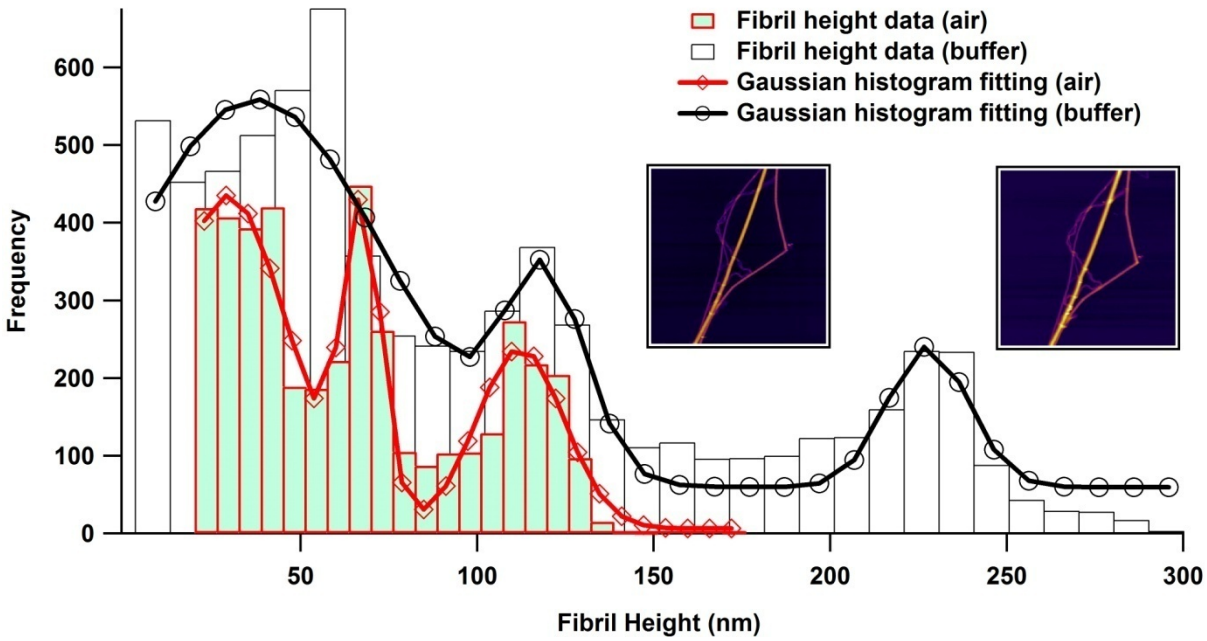

Figure 1: Swelling of collagen fibrils associated with re-hydration from an air environment. The AFM image on the left is taken in air while the image on the right is taken after re-hydrating for 1 hour in buffer. The height histograms of the same areas of the sample show that although there are fibrils of three different diameters all of them increase their height by a factor of approximately two.

The atomic force microscope (AFM) is capable of measuring mechanical properties of samples at nanoscale resolution. We have used it in nanoindentation mode to study the elastic properties of individual collagen fibrils reconstituted from bovine Achilles tendon. Comparison of the behaviour of dehydrated fibrils in air and those in aqueous buffer shows that the elastic modulus drops from around 1 GPa to 1 MPa, a three orders of magnitude change. On rehydration, swelling of the fibrils occurs, leading to almost a two fold increase in fibril diameter as measured using tapping-mode AFM imaging (Figure 1). In the dehydrated

state, larger loads can create plastic indents in the surface enabling the hardness of the fibrils in air to be estimated.

Tuning the collagen fibril modulus in electrolytic environments

In fully hydrated environments, the ionic strength, composition and pH of the surrounding solution can be systematically varied. We found that the elastic modulus could be increased from around 1 MPa in a reproducible and time-dependent reversible manner. Increasing the monovalent salt concentration to 1M raised the modulus to about 5 MPa. Decreasing the pH from 7 to 5 raised the modulus by another 4 to 5 fold. This behaviour led us to the idea that the elastic properties of collagen fibrils and collagenous materials can be tuned through variation of the electrolyte composition. The molecular interactions between tropocollagen monomers are complex and depend on many sources. Modulation of interactions such as salt-bridging, H-bonding, electrostatic and hydrophobic interactions are thought to be responsible for variations in the mechanical behaviour. More work is needed to understand which forces dominant the intermolecular interactions during changes in electrolyte strength and composition. Collagen contains a large amount of water as we see from the swelling behaviour going from the dehydrated to hydrated state. The protein component, therefore, accounts for only one quarter to one third of the volume of the fibril. This point is highlighted on the front cover of the December 2nd 2009 issue of Biophysical Journal where the collagen fibrils are likened to corrugated water pipes (Figure 2).

Figure 2: "Collagen Water Pipes". Front cover of *Biophys J* (2009), Volume 97, Issue 11.

Publications

Grant C., Brockwell D., Radford S. and Thomson N. (2008) Effects of hydration on the mechanical response of individual collagen fibrils. *Appl Phys Lett* **92**:233902.

Grant C., Brockwell D., Radford S. and Thomson N. (2009) Tuning the elastic modulus of hydrated collagen fibrils. *Biophys J* **97**:2985-92.

Funding

This work was funded by the BBSRC, grant number BB/D011191.

Shape and flexibility in the titin 11-domain super-repeat

Larissa Tskhovrebova, Nasir Khan, Andy Baron and John Trinick

Introduction

Titin is a giant protein of striated muscle with important roles in the assembly, intracellular signalling and passive mechanical properties of sarcomeres. The molecule consists principally of <300 immunoglobulin and fibronectin domains arranged in a chain more than 1 μm long. The isoform dependent N-terminal part of the molecule forms an elastic connection between the end of the thick filament and the Z-line. The larger, constitutively expressed C-terminal part is bound to the thick filament. Through most of the thick filament part, the immunoglobulin and fibronectin domains are arranged in a repeating pattern of 11 domains termed the 'large super-repeat'. There are 11 contiguous copies of the large super-repeat making up a segment of the molecule nearly 0.5 μm long. We have studied a set of two-domain and three-domain recombinant fragments from the large super-repeat region by electron microscopy, synchrotron X-ray solution scattering and analytical ultracentrifugation, with the goal of reconstructing the overall structure of this part of titin.

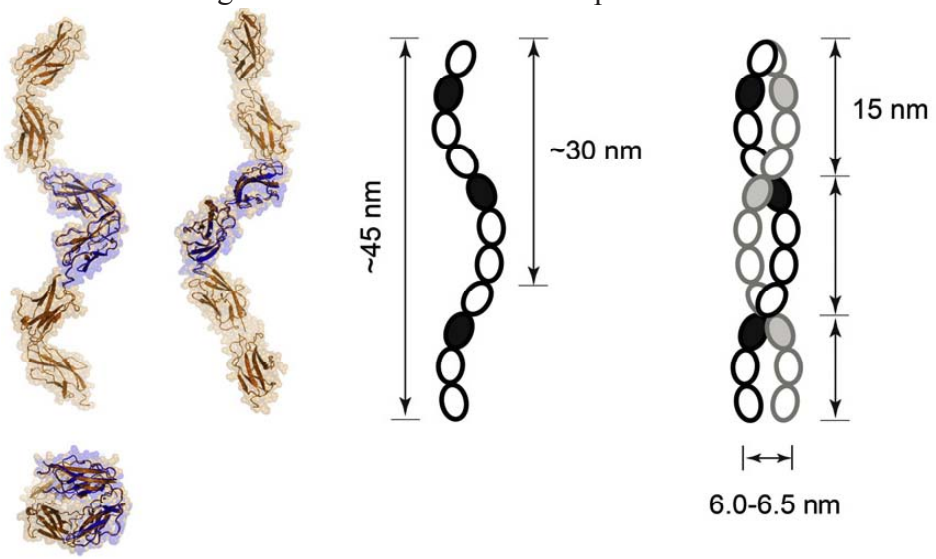

Figure 1: (left panel) Model of the six-domain segment corresponding to the first two subdivisions of the large super-repeat reconstructed from solution scattering models. (**middle and right panels)** Schematic representations of large super-repeat structure in monomeric (middle) and dimerised (right) states. Ig domains are black.

Results

The data illustrate different average conformations in different domain pairs, which correlate with differences in interdomain linker lengths. They also illustrate interdomain bending and flexibility around average conformations. Overall, the data favour a helical conformation in the large super-repeat. They also suggest that this region of titin is dimerised when bound to the thick filament.

Publications

Tskhovrebova, L., Walker, M., Grossmann, G. Khan, G., Baron, A. and Trinick, J. (2010) Shape and flexibility in the titin eleven domain super-repeat. *J Mol Biol* **397**:1092-105.

Funding

Supported by the British Heart Foundation.

Collaborators

Matt L. Walker (Newton Abbott) and J. Gunter Grossmann (Daresbury Laboratory).

Structural Investigation of a Fibronectin Type III Domain Tandem from A-band Titin

Andras Czajlik, Gary Thompson, Arnout Kalverda, Ghulam Khan, Larissa Tskhovrebova, Steve Homans and John Trinick

Single molecules of the giant protein titin extend over one half muscle sarcomeres, from the Z-disk boundary to the central M-band and have key roles in muscle assembly and elasticity. A-band titin sequence shows a regular pattern of eleven fibronectin type III and immunoglobulin-like domains, arranged in what are called the large super-repeats. The large super-repeat occurs eleven times and forms nearly half of the titin moecule. It is likely to be involved in sarcomere assembly through interactions with A-band proteins, especially myosin. We are determining the atomic structure and dynamic properties of overlapping double and triple domain fragments of the large super-repeat (in this case A59-A69) from human heart muscle by NMR spectroscopy and will combine the folds and dynamics of the individual subunits to model the structure and dynamics of the complete super repeat.

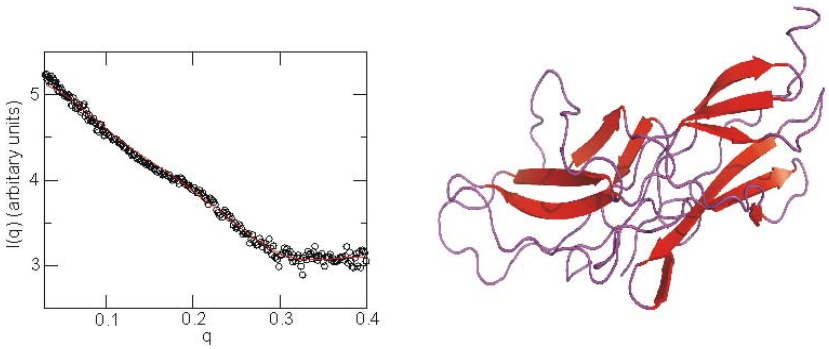

Figure 1: Fit of SAX data to the most consistent NMR trial structure **(left)**. The NMR structure showing the best consistency with the SAX data **(right)**.

While A59-A60 has a well resolved ^{1}H-^{15}N HSQC spectrum at 750 MHz, even with a per-deuterated sample ^{1}H-^{15}N nOe spectra of the protein were poor. Therefore, the A59-A60 domain tandem was investigated by a mixture of chemical shift based structure determination and homologous NMR structures. The fold of A59 was determined using CS23D based on ^{1}H, ^{15}N and ^{13}C chemical shifts. For A60 we used the NMR structure of A71 (1BPV), as this is the domain present at the same position as A60 in the next super-repeat. ^{1}H-^{15}N residual dipolar couplings (RDCs) in a C12E6-hexanol liquid crystal system (750MHz, pH=6.5, 0.5M NaCl) were used to validate the structures. A good correlation (R> 0.9) between the back-calculated and the measured RDC values was observed for all resonances from secondary structure elements, clearly showing that the structural models in use are valid. RDC data only describe domain orientations up to an inversion Cartesian axes which does not change the handedness of alignment tensor frame; giving four possible structural solutions. Structures were calculated using rigid body minimization in XPLOR-NIH using RDC results as an energy term. Only two of the four possible structures were physically possible and of these one was found to give the best fit to when back calculating SAX data with CRYSOL (Figure 1A), assuming an inter-domain linker of 7.5-17Å. Thus the approach chosen resulted in a single unique structure (Figure 1B).

Funding
We thank the British Heart Foundation for financial support

Collaborators
J. Gunter Grossman from the University of Liverpool for the SAX data.

Influence of lever structure on myosin 5a walking

Olusola Oke, Stan Burgess, Peter Knight and John Trinick

Introduction

The myosin 5a molecular motor occurs widely and is especially abundant in neurons, forming ~0.3% of brain protein. The two heads in a molecule walk hand-over-hand along actin filaments pulling diverse vesicle cargoes. Heads attach to actin through their motor domains, which also contain ATPase activity. Extending from the motor domains are levers that produce force and movement by swinging through ~80°, brought about by movement of the converter region of the motor domain.

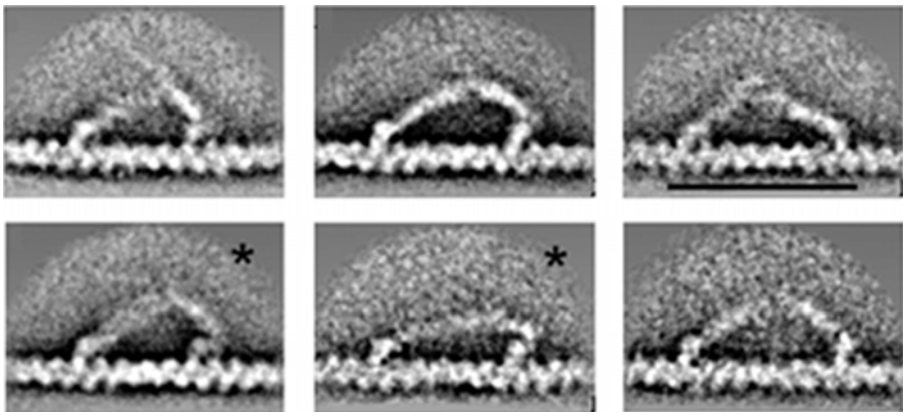

Figure 1: The panels show image averages of negatively stained myosin 5a walking to the right along actin filaments. In the two asterisked panels the lever arm of the lead head has completed its powerstroke. This demonstrates a new attached head state of myosin.

Results

We used electron microscopy, image processing and stopped-flow fluorescence to study binding to actin of wild type and mutant myosin 5a molecules. We observed a new attached head state of myosin, where the lead head has completed its powerstroke at the expense of severe distortion of its lever arm (asterisked panels above). Post-powerstroke lead heads were seen in both wild type and modified lever molecules, mostly where there was least strain. The data allow the strain dependence of the equilibrium between pre- and post-powerstroke conformations to be measured. Slow rates of ADP dissociation observed from lead heads of these molecules can be explained by the unfavorable equilibrium between the pre-and post-powerstroke conformations preceding ADP loss.

Publications

Oke, O., Burgess, S., Forgacs, E., Knight, P., Sakamoto, T., Sellers, J., White, H. and Trinick, J. (2010). Influence of lever structure on myosin 5a walking. *Proc Natl Acad Sci USA* **107**:2509-2514.

Funding

Supported by NIH EB00209

Collaborators

Takeshi Sakamoto and James R Sellers (NIH-Bethesda) and Eva Forgacs and Howard White (Eastern Virginia Medical School).

Structure of self-assembling bacteriochlorophyll nanostructures

Roman Tuma

Introduction

Chlorosomes from green photosynthetic bacteria are large light harvesting complexes containing self-assembling aggregates of bacteriochlorophylls, carotenoids and quinones. The pigments within chlorosomes are organized in lamellar structures. Purified pigments self-assemble *in vitro* into nanostructured aggregates with similar optical properties. These nanostructures constitute promising photonic material with potential use in photovoltaic and optoelectronic applications.

Results

We prepared nanostructures from purified bacteriochlorophyll c by precipitation in hexane and examined the product by X-ray scattering and absorption spectroscopy. Based on the optical properties and scattering patterns we concluded that the nanostructures exhibited lamellar pigment arrangement identical to that of native chlorosomes. Thus, the self-assembly of these pigments does not require additional factors (e.g. proteins) and is fully encoded by their chemical structure. Next, we transesterified bacteriochlorophyllides with alcohols exhibiting different chain lengths and established a linear relationship between the esterifying alcohol length and the lamellar spacing. The results provide a structural basis for lamellar spacing variability observed for native chlorosomes from different species. A plausible physiological role of the variable spacing is to accommodate additional pigments and photoprotective molecules (e.g. carotenoids, quinones) in response to different light conditions.

The X-ray scattering also confirmed the assignments of peaks, which arise from the crystalline baseplate in the native chlorosomes. The baseplate, which is composed of pigment-protein complexes, mediates excitation energy transfer to the photosynthetic reaction centres. We have studied ultrastructure of the baseplate in the intact chlorosomes from green filamentous bacterium *Chloroflexus aurantiacus* by electron microscopy and cryo-tomography.

Publications

Psencik, J., Collins, A., Liljeroos, L., Torkkeli, M., Laurinmäki, P., Ansink, H., Ikonen, T., Serimaa, R., Blankenship, R., Tuma, R. and Butcher, S. (2009) Structure of chlorosomes from the green filamentous bacterium *Chloroflexus aurantiacus*. *J Bacteriol*, **191**:6701-6708.

Psencik, J., Torkkeli, M., Zupcanova, A., Vacha, F., Serimaa, R. and Tuma, R. (2010) The lamellar spacing in self-assembling bacteriochlorophyll aggregates is proportional to the length of the esterifying alcohol. *Photosynth Res* **104**:211-219.

Funding

This work was funded by Academy of Finland, University of Leeds, Czech Science Foundation and the Department of Energy, USA.

Collaborators

This is an ongoing collaboration between several groups: Profs. Sarah Butcher and Ritva Serimaa, Drs. M. Torkkeli and Teemu Ikonen, Pasi Laurinmäki at the University of Helsinki, Finland; Dr. Jakub Psencik at Charles University, Prague; Prof. Frantisek Vacha and Anita Zupcanova from University of Southern Bohemia, Czech Republic. The work on native chlorosomes from filamentous bacteria was done in collaboration with Prof. Robert Blankenship at Washington University, St. Louis, USA.

Studies on bacterial toxins

Thomas Branson, Simon Connell, Martin Fascione, Edward Hayes, Steve Homans, Peter Johnson, Arnout Kalverda, Pintu Mandal, Premanand Patil, Arwen Pearson, Neil Ranson, Cristina Sisu, Gary Thompson and Bruce Turnbull

Introduction

Diarrhoeal diseases such as cholera are still life threatening diseases in many parts of the world. Many diarrhoeal diseases are caused by protein toxins that have an AB_5 hetero-oligomeric structure. The proteins comprise a single toxic A-subunit and a pentameric B-subunit that interacts with specific cell surface glycolipids. Inhibitors of such protein-carbohydrate interactions could provide prophylactic treatments for these debilitating diseases. We have adopted a multidisciplinary approach to develop ligands and inhibitors for the B-subunits of three bacterial toxins: cholera toxin, *E. coli* heat-labile toxin, and verotoxin.

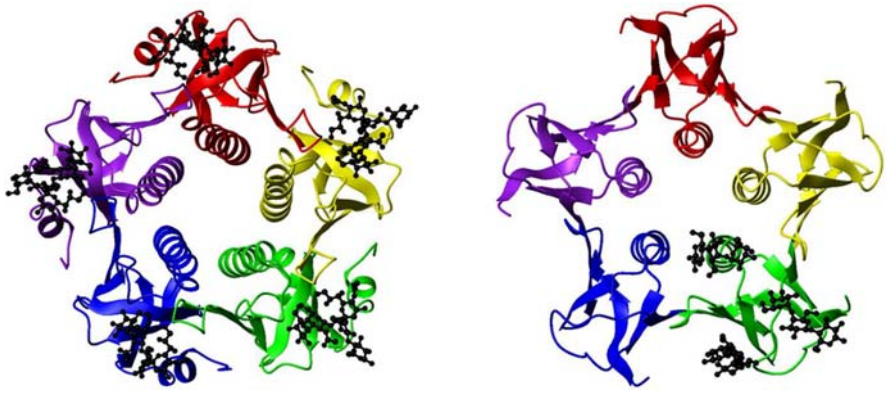

Figure 1: The B-subunits of cholera toxin (left) and verotoxin (right) bound to their carbohydrate ligands.

We are investigating the binding properties of blood group oligosaccharides for a secondary binding site on *E. coli* heat-labile toxin. It is believed that these interactions can influence how susceptible patients are to travellers' diarrhoea and certain strains of cholera. We are also using a combination of virtual screening, molecular modelling, NMR spectroscopy, X-ray crystallography and synthetic chemistry for fragment-based design of small molecule inhibitors of cholera toxin. A similar approach is also being used to develop inhibitors against verotoxin that also possess anti-bacterial activity for use as dual-acting drugs. We have shown that these bifunctional compounds can cause the toxins to form discrete aggregates that should not be able to bind to a cell surface. We have also studied the aggregative properties of multivalent carbohydrate inhibitors of cholera toxin and *E. coli* heat-labile toxin using analytical ultracentrifugation, dynamic light scattering and atomic force spectroscopy. These studies have revealed different aggregation mechanisms that depend on the valency of the inhibitors. We are now aiming to control these aggregative processes to direct the assembly of proteins into discrete three-dimensional structures to provide a general bottom-up strategy for synthetic biology.

Publications

Sisu, C., Baron, A., Branderhorst, H., Connell, S., Weijers, C., de Vries, R., Hayes, E., Pukin, A., Gilbert, M., Pieters, R., Zuilhof, H., Visser, G. and Turnbull, B. (2009) The influence of ligand valency on aggregation mechanisms for inhibiting bacterial toxins. *ChemBioChem*, **10**:329-337.

Collaborators

Gerben Visser, and Han Zuilhof Wageningen University, The Netherlands.

Roland Pieters, Utrecht University, The Netherlands.
David Andrews and Andrew Leach, AstraZeneca, UK.
Ute Krengel, University of Olso, Norway.
Ravindranathan Kartha, National Institute of Pharmaceutical Education and Research, India.

Funding
This work is funded by the Royal Society, EPSRC, Commonwealth Scholarships, Newton International Fellowships, AstraZeneca and the University of Leeds.

Development of LC-MS-MS assays for the directed evolution and characterisation of aldolase enzymes

Lucy Chappell, Nicole Timms, Adam Daniels, Jennifer Stockwell, Thomas Harman, Adam Nelson, Alan Berry and Stuart Warriner

Introduction

N-Acetyl neuraminic acid lyase (NAL) is a Class I aldolase that catalyses the reversible aldol condensation between *N*-acetyl mannosamine, **1**, and pyruvate to yield *N*-acetyl neuraminic acid, **2** (Scheme). We have previously demonstrated that directed evolution is a powerful tool in the discovery of synthetically valuable aldolase variants. For example, we discovered the aldolase variant E192N whose substrate specificity was switched towards the alternative aldehyde substrate **3**; condensation of the aldehyde, **3**, with pyruvate yields the product, **4**, which is a potential precursors of some influenza A sialidase inhibitors. In addition, we have used directed evolution to create a pair of stereoselective aldolase enzymes that may be used to prepare stereoselectively the 4*S* and 4*R* diastereomers of **4**.

Scheme

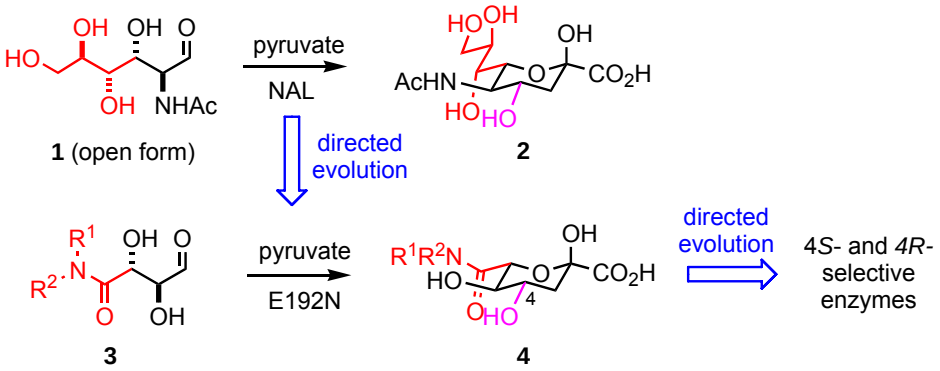

Throughout our directed evolution programme, we have used a coupled enzyme assay to identify variant enzymes with promising activity. We have also used the same coupled enzyme assay to characterise variant enzymes at each stage of evolution. The coupled enzyme assay relies on the reversibility of the aldol condensation, and allows the retro-aldol reaction to be assayed. Thus, aldolase-catalysed *cleavage* of condensation products (e.g. **4**) yields pyruvate whose reduction may be catalysed by lactate dehydrogenase and, thus, consumption of NADH. A drawback of this approach is that it is necessary to prepare, using chemical synthesis, the required products of aldolase-catalysed reactions; significant quantities of these products are generally required for directed evolution, and the characterisation of promising aldolase variants.

Development of LC-MS-MS methods for assaying aldolase-catalysed condensation reactions

We have developed LC-MS-MS methods that allow aldol *condensations* to be assayed. The assay is amenable to operation in reasonably high-throughput format, and may be used to identify active variants in directed evolution experiments. In addition, the assay may be used to explore rapidly the substrate specificity of specific aldolase variants. We have also used the method to characterise the kinetics of aldolase-catalysed condensation reactions.

The assay involves the analysis of samples are analysed using a Bruker HCT-Ultra ion trap detector. The sensitivity is greatly increased by operating in MS-MS mode in which identification of the compound is obtained by selective ion acquisition. In the case of compound **4**, we were able to detect, in negative ion mode, concentrations down to ~50 nM in a solution containing crude cell lysate. Fragmentation of the molecular ion [M̃H] (*m/z* = 304)

yielded a fragment at *m/z* = 129 which was used to quantify the analyte. By using this selective fragmentation pathway, sensitivity is greatly increased because random noise at *m/z* = 304 is very unlikely to give a fragment at 129, whereas virtually all the intensity in the analyte is transferred to *m/z* = 129 and 87. Using this approach, we have been able to calibrate the response of the instrument over 4 orders of magnitudes of analyte concentration. We have used this method to follow the complete time-course of the reaction catalysed by E192N NAL (Figure 1).

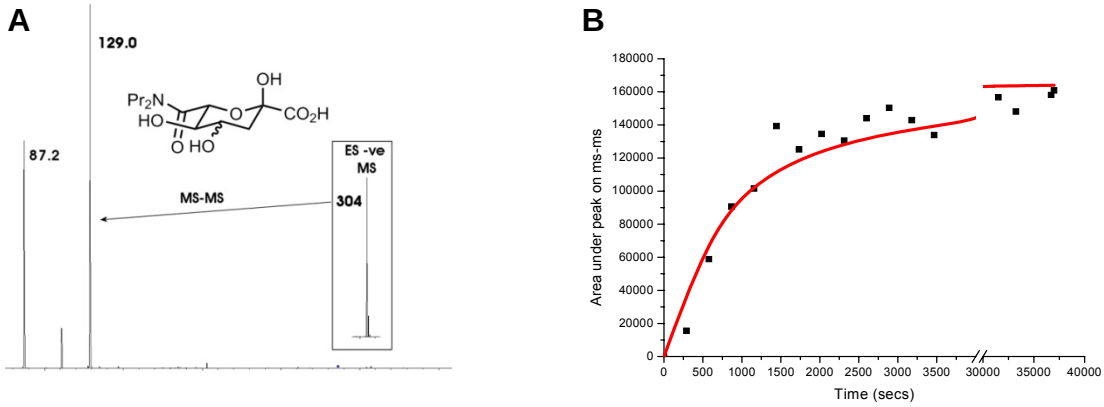

Figure 1: an LC-MS-MS assay for the characterisation of aldolase-catalysed reactions in the forward direction. **(A)** MS-MS of compound **4** showing the molecular ion at 304 yields fragments at 129 and 87. **(B)** Peak intensity at *m/z* = 129 used to follow the time-course of an NAL-catalysed reaction to give **4**.

We have also used the assay to characterise the kinetics of NAL-catalysed reactions in forward (condensation) direction. The initial rates of condensation were determined, for a range of aldehyde concentrations, at fixed pyruvate concentration. The kinetic parameters for the wild type and E192N variants were determined for the aldehydes **1** and **3**, and are summarised in the Table.

Enzyme	Aldehyde **1**			Aldehyde **3**			$(k_{cat}/K_m)_3$ / $(k_{cat}/K_m)_1$
	k_{cat} /s^{-1}	K_m / mM	k_{cat}/K_m / $s^{-1}mM^{-1}$	k_{cat} /s^{-1}	K_m / mM	k_{cat}/K_m / $s^{-1}mM^{-1}$	
WT	0.63 ± 0.02	22.5 ± 1.4	0.028	15.0 ± 0.95	34.1 ± 4.1	0.44	16
E192N	0.23 ± 0.04	510 ± 150	0.00044	94.2 ± 7.5	6.2 ± 0.9	15.3	34 000

Table: Kinetic parameters for aldolase-catalysed condensation reactions

The wild type enzyme was shown to be a better catalyst than the E192N variant, in terms k_{cat}/K_m, for the condensation of the aldehyde **1** and pyruvate. Similarly, the variant E192N was a better catalyst than the wild-type enzyme for the condensation of the aldehyde **3** and pyruvate. The substrate specificity of the E192N variant, relative to the wild-type enzyme, was switched 2100-fold from *N*-acetyl mannosamine, **1**, towards the alternative aldehyde substrate **3** (in terms of the ratio of the k_{cat}/K_m parameters for the two substrates). Surprisingly, however, *both* the wild type and E192N variant enzymes catalysed the condensation of the aldehyde **3** more effectively than that of the natural substrate **1**. This observation is likely to stem from the fact that an unfavourable ring-opening process is required before the substrate **1** can undergo an aldol reaction with pyruvate. In contrast, the **3** does not exist in a cyclic form and is, thus, primed to undergo aldol condensation. It was only possible to glean these novel insights because the mass spectrometry assay allowed kinetic parameters for the condensation process to be obtained.

In summary, we have developed a novel LC-MS-MS method for assaying aldolase-catalysed reactions in the forward direction. The method will find application in the directed evolution of aldolases with new activities; in the determination of the substrate specificity of aldolase

variants; and in the kinetic characterisation of aldolase-catalysed condensation reactions. Applications of the new method will be disclosed in due course.

Publications

Campeotto, I., Carr, S., Trinh, C., Nelson, A., Berry, A., Phillips, S. and Pearson, A. (2009) Structure of an *Escherichia coli* N-acetyl-D-neuraminic acid lyase mutant, E192N, in complex with pyruvate at 1.45 angstrom resolution. *Acta Crystallogr Sect F Struct Biol Cryst Commun* **65**:1088-1090.

Funding

We thank BBSRC, EPSRC, the Wellcome Trust and AstraZeneca for support.

Mechanistic study of an ADP-dependent kinase

Zhenlian Ling, Jeffrey Hollins, Tom McAllister, Andrew Grimes, James Blaza, Arwen Pearson and Michael Webb

Introduction

Pyruvate, orthophosphate dikinase (PPDK) regulatory protein (PDRP) is responsible for the light/dark regulation of PPDK in C_3 and C_4 plants[1]. This enzyme supplies phosphoenolpyruvate for temporary fixation of CO_2 in the mesophyll before shuttling to the bundle sheath cells for fixation by Rubisco. In the dark *in planta*, PDRP inactivates PPDK *via* an ADP-dependent phosphorylation of a threonine residue adjacent to the catalytic phosphohistidine residue; in the light, PDRP reactivates PPDK *via* a pyrophosphate-generating phosphotransferase activity. At present the mechanistic basis of neither reaction has been identified.

We are taking a multidisciplinary approach to our initial study of PDRP. We have recombinantly overexpressed and purified homologues from maize, Arabidopsis and *E. coli* and we are now using biophysical techniques including calorimetry, analytical ultracentrifugation and surface plasmon resonance to characterise the interactions of these proteins with their substrates, ADP and PPDK, and to define the binding order for the inactivation reaction. Using this approach we have demonstrated that this protein has a single binding site for ADP and are currently attempting to obtain further structural information. We are also synthesizing peptides incorporating new non-hydrolysable analogues of phosphohistidine as model substrates for the enzyme. These may have wider application as haptens for selection of phosphohistidine-specific immunochemical reagents in addition to use as probes of the structural basis for ADP-dependent phosphorylation in this system.

Funding

We acknowledge funding from the EPSRC and the BBSRC.

Collaborators

We gratefully acknowledge on-going collaborations with Holly Astley and Dr Julian Hibberd (Cambridge), Dr Chris Chastain (Minnesota State Moorhead) and Dr Jim Burnell (James Cook, Aus). We would also like to acknowledge assistance from Dr Ryan Mehl (Franklin and Marshall, PA) in compound testing.

Identification of the ribonucleoprotein complex required for efficient export and translation of herpesvirus intronless mRNAs

Brian Jackson, Adam Taylor, Marko Norenberg and Adrian Whitehouse

Introduction

The nuclear export of mRNA composes one part of a larger network of molecular events that begin with transcription of the mRNA in the nucleus and end with its translation and degradation in the cytoplasm. During trafficking to the cytoplasm, a nascent mRNA undergoes numerous co-transcriptional processing steps, including 5' capping, splicing to remove introns and 3' polyadenylation. Of these events it has become clear that splicing is particularly important for mRNA nuclear export, as recruitment of multiprotein complexes required for mRNA export are bound to mRNA in a splicing dependent manner. Two multiple protein complexes, namely, hTREX and the EJC bind at separate locations on spliced mRNA. hTREX, which comprises Aly, UAP56 and the multiprotein ThoI complex, is recruited exclusively to the 5' end of the first exon, providing 5'-polarity and therefore directionality observed in mRNA export.

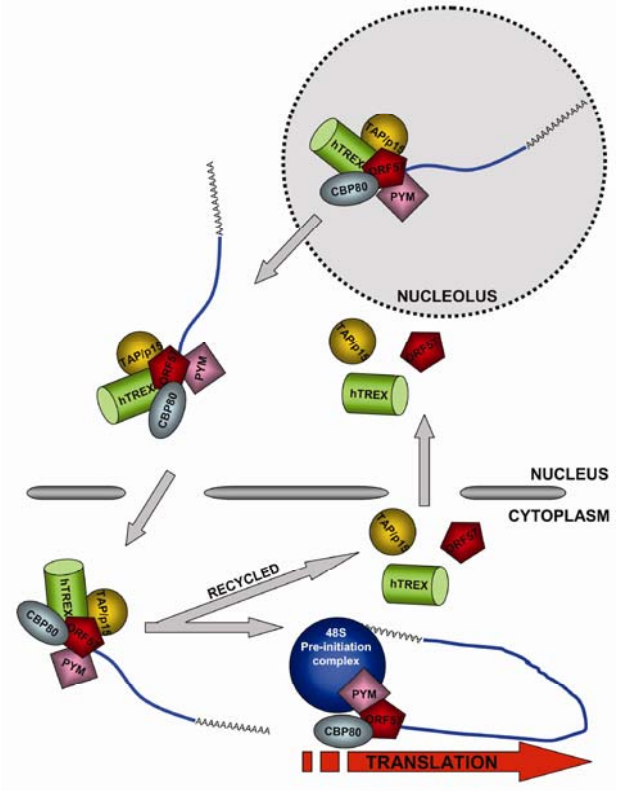

Figure 1: KSHV ORF57 mimics splicing to recruit the necessary nuclear export factors onto viral intronless transcripts and also mimics an EJC to enhance their translation.

However, in contrast to the majority of mammalian genes, analysis of herpesvirus genomes has highlighted that most lytically expressed viral genes lack introns. Herpesviruses replicate in the nucleus of the host mammalian cell, and therefore require their intronless mRNAs to be exported out of the nucleus to allow viral mRNA translation in the cytoplasm. This therefore leads to an intriguing question concerning the mechanism by which the viral intronless mRNAs are exported out of the nucleus in the absence of splicing. To circumvent this problem, and to facilitate viral mRNA export, γ-2 herpes viruses encode the ORF 57 protein. ORF 57 interacts with Aly, binds viral RNA, shuttles between the nucleus and the cytoplasm and promotes the nuclear export of viral mRNA.

We are currently investigating how an intronless viral mRNP is assembled in KSHV and what role ORF57 plays in that process. We have shown that ORF57 interacts with hTREX and is essential for the recruitment of hTREX onto intronless viral mRNA transcripts. Importantly,

ORF57 does not recruit the EJC to intronless viral transcripts. Moreover, we are currently determining how ORF 57 recognises the viral mRNA and allows recruitment of hTREX. This is the first system that has distinguished between hTREX and EJC *in vivo* and demonstrates that recruitment of hTREX alone to mRNA transcripts is sufficient for their nuclear export. Therefore, we believe this viral system is an exciting model to further study mRNA export mechanisms. We propose a model for herpesvirus mRNA export, whereby ORF57 mimics splicing in order to recruit the mRNA export machinery to intronless viral mRNAs.

Moreover, the inability of ORF57 to recruit the EJC may have implications for the efficiency of translation of the viral intronless mRNAs, as recent data suggests that the EJC promotes efficient translation of spliced mRNAs by several mechanisms. One such mechanism involves the cellular protein, PYM, which links the EJC to the 48S pre-initiation complex. Therefore, we have investigated whehter KSHV ORF57 has any role in enhancing translation as well as nuclear export. We have shown that ORF57 sediments predominantly with the 40S ribosomal subunit and enhances translation of viral intronless transcripts. Moreover, we have demonstrated that ORF57 interacts with PYM and components of the 48S pre-initiation complex and functions to recruit PYM onto a viral intronless mRNA. Significantly, siRNA-mediated depletion of PYM ablates the interaction between ORF57 and components of the 48S pre-initiation complex and dramatically decreases the translation of KSHV intronless mRNAs. Therefore, we propose a model whereby ORF57 also mimics an EJC enabling efficient translation of intronless KSHV transcripts.

Publications

Boyne, J. and Whitehouse, A. (2009) Nucleolar disruption impairs Kaposi's sarcoma-associated herpesvirus ORF57-mediated nuclear export of intronless viral mRNAs. *FEBS Lett*, **583**:3549-3556.

Colgan, K., Boyne, J. and Whitehouse, A. (2009) Uncoupling of hTREX demonstrates that UAP56 and hTHO-complex recruitment onto herpesvirus saimiri intronless transcripts is required for replication. *J Gen Virol* **90**:1455-1460.

Colgan, K., Boyne, J. and Whitehouse, A. (2009) Identification of a response element in a herpesvirus saimiri mRNA recognized by the ORF57 protein. *J Gen Virol*, **90**:596-601.

Boyne, J., Jackson, B., Taylor, A., Macnab, S. and Whitehouse, A. (2010). Kaposi's sarcoma-associated herpesvirus ORF57 interacts with PYM to enhance viral intronless mRNA translation. *EMBO Journal,* 29:1851-1864.

Acknowledgements

This project is funded by the BBSRC, Wellcome Trust and Yorkshire Cancer Research.

Repressosome formation and disruption regulates the KSHV latent-lytic switch

Faye Gould, Jennifer Wood and Adrian Whitehouse

Introduction

The etiological agent of Kaposi's Sarcoma, Kaposi's sarcoma associated herpesvirus virus (KSHV), is the most recently identified human tumour virus. KSHV has two distinct forms of infection, latent persistence and lytic replication. The switch between these phases is important as lytic replication plays an essential part in the pathogenesis and spread of KSHV infection. The KSHV Rta protein is the key gene product which regulates viral lytic gene expression as sustained transient expression of Rta in a KSHV-latently infected cell line leads to the stimulation of its own expression and consequently viral lytic replication. This implicates the Rta protein as the molecular switch for reactivation and initiation of the KSHV lytic replication cycle.

We are currently investigating the host cell-Rta interactions to further understand the role of KSHV Rta in the latent-lytic switch. We have demonstrated that KSHV Rta interacts with the cellular protein, Hey-1. Hey-1 functions as a transcriptional repressor, acting as adapter protein that binds to specific DNA binding sites within gene promoters, and subsequently recruits transcriptional repressosome complexes. The interaction between KSHV Rta and the transcriptional repressor protein Hey-1 is a particular intriguing one. Why would Rta interact with a transcriptional repressor protein, given the role of Rta in transcriptional activation and initiating the lytic replication cycle? However, we have shown that the Hey-1- Rta interaction is an essential interaction playing a pivotal role in regulating the KSHV latent-lytic switch.

Recently, it has been shown that Rta is a novel E3 ubiquitin ligase that targets a number of transcriptional repressor proteins for degradation by the ubiquitin-proteasome pathway. Therefore, we believe we have identified a novel target for Rta's ubiquitin ligase activity. We have demonstrated that Hey1 is a target for Rta-mediated ubiquitination is degraded by the proteasome. Moreover, a Cys plus His-rich region within RTA is important for Rta-mediated degradation of Hey1. We also showed that Hey1 represses the Rta promoter and binds to the RTA promoter. An interaction was also observed between Hey1 and the co-repressor mSin3A and this interaction was abolished in the presence of Rta. Additionally, mSin3A associated with the Rta promoter in unreactivated, but not reactivated, BCBL1 cells. Moreover, siRNA knockdown of Hey1 in KSHV-latently infected rKSHV.219 HEK 293T cells led to increased levels of Rta expression upon reactivation, but was insufficient to induce complete lytic reactivation. These results suggest that other additional transcriptional repressors are also important in maintenance of KSHV latency. Taken together our results suggest a contributory role for Hey1 in the maintenance of KSHV latency, and that disruption of the Hey1 repressosome by Rta-targeted degradation may be one step in the mechanism to regulate lytic reactivation. This project will provide valuable information on KSHV reactivation that may ultimately lead to the identification of specific antiviral targets to inhibit ORF 50–host cell interactions which may be developed as a novel treatment for this important human pathogen.

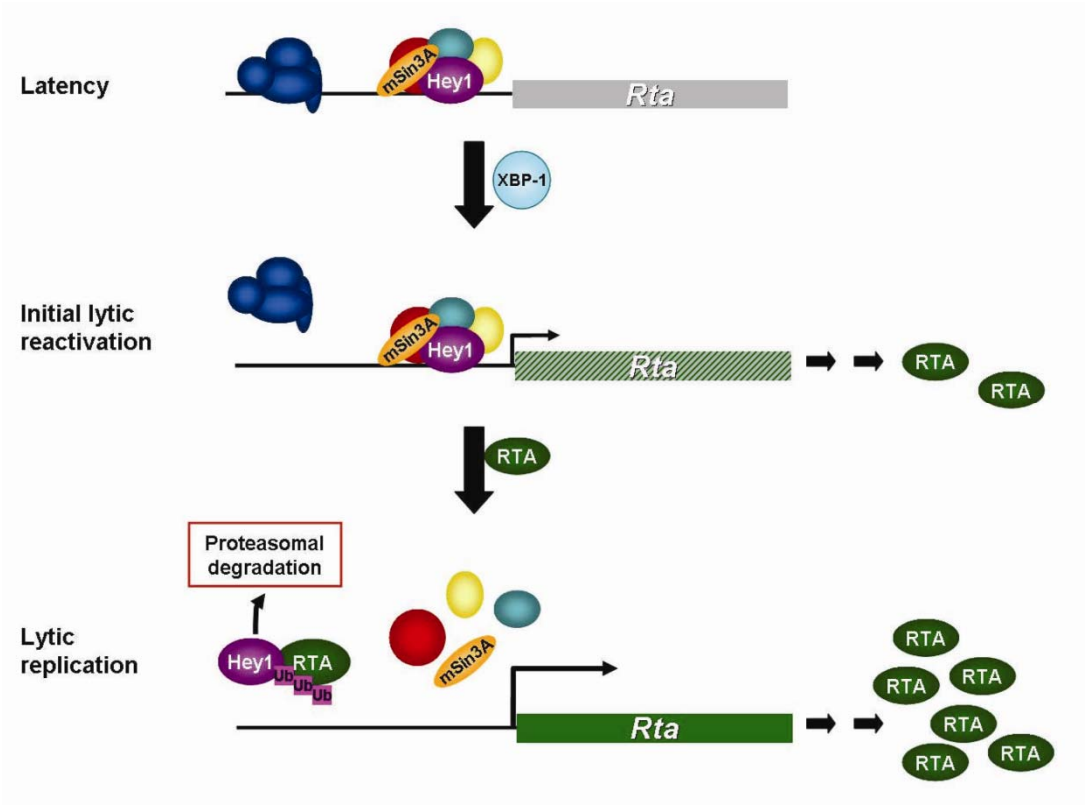

Figure 1: Proposed role of Hey1 in KSHV reactivation and lytic replication. During latency the RTA promoter is tightly repressed by the Hey1-induced repressosome and other repressors (indicated as a complex to the left of the Hey1 repressosome), preventing RTA expression. Upon plasma cell differentiation, XBP-1s is expressed and activates the RTA promoter, causing low-level RTA expression and thus triggering initial lytic reactivation. Once a small amount of RTA is expressed, it ubiquitinates Hey1, leading to proteasomal degradation of Hey1 and dissociation of the repressosome from the RTA promoter. Loss of the Hey1-induced repressosome from the RTA promoter enhances RTA expression, allowing complete lytic replication to proceed.

References

Gould, F., Harrison, S., Hewitt, E. and Whitehouse, A. (2009) Kaposi's sarcoma-associated herpesvirus RTA promotes degradation of the Hey1 repressor protein through the ubiquitin proteasome pathway. *J Virol*, **83**:6727-6738.

Funding

This project is funded by the Wellcome Trust and BBSRC.

Protein-surface recognition using synthetic agents

Fred Campbell, Maria Filby, James Muldoon, Jeffrey Plante, Michael Webb,
Alison Ashcroft, Thomas Edwards, Stuart Warriner and Andrew Wilson

Introduction

Protein-protein interactions (PPIs) play a pivotal role in diseased states and so there is a pressing need for synthetic agents that selectively target these interfaces. Several general approaches tailored to particular protein topologies are emerging for the design of scaffolds that inhibit PPIs including: *proteomimetics* and *surface mimetics*. *'Proteomimetics'* replicate the spatial projection of key binding residues from a secondary structural motif important in the target protein-protein interaction whilst *'surface mimetics'* present recognition domains from a core scaffold in a multivalent manner to achieve high affinity protein surface recognition. This report will summarise our work in both areas

α-Helix Mimetics

We have set out to design and synthesize libraries of small molecules that recapitulate the key structural and recognition features of an α–helix. We have elaborated two scaffolds (Figure 1a) based upon an aromatic oligoamide template and have developed solution and solid-phase syntheses of both. The later approach places us in a position to assemble libraries for screening against a diverse array of helix mediated protein-protein interactions. In order to demonstrate such compounds act as helix mimetics, we have testing our compounds against the p53-*h*DM2 protein-protein interaction which represents an importance cancer target. Our fluorescence anisotropy displacement screen (Figure 1b) has identified μM inhibitors of this interaction (blue trace) with comparable affinity to the control p53 peptide (red trace) as significantly compounds that bind with poor affinity (green trace) implying a certain level of specificity. ^{1}H-^{15}N HSQC chemical shift perturbation analyses (Figure 1c) suggest our compounds indeed mimic the p53 helix and occupy the same cleft on hDM2. Future studies are focused towards generation of larger libraries and screening against additional helix-mediated PPIs *in vitro* and *ex vivo*.

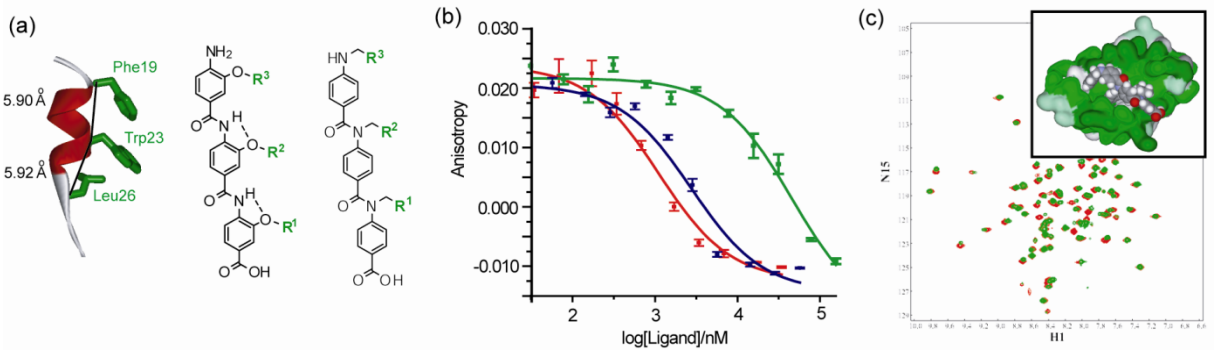

Figure 1: (a) structure of p53-helix with key hDM2 binding residues shown in green aromatic oligoamide helix mimetics **(b)** fluorescence anisotropy titrations ($p53_{15-29}$Flu 54 nM, *h*DM2 50 nM, 40 mM sodium phosphate, pH 7.4, 200 mM NaCl and 0.02 mg/ml of bovine serum albumin) **(c)** ^{1}H-^{15}N HSQC spectra in presence and absence of helix mimetics (inset: manually docked structure)

Design and synthesis of ruthenium complexes for recognition of protein surfaces

Alongside our interest in controlling α-helix mediated PPIs, we have synthesised a series of ruthenium complexes designed to act as protein surface mimetics. These are designed to recognise less well defined protein surfaces with high affinity and selectivity by multivalent presentation of recogntion arms from the core $Ru(Bipy)_3$ scaffold onto the protein-surface (Figure 2a). The system offers significant advantages for fundamental studies of protein

surface recognition as binding to metalloproteins and non-metalloproteins can be detected using simple fluorescence quenching or anisotropy changes respectively. We have demosntrated this strategy works through a panel of experiments (fluorescence titration (Figure 2b), ascorbate reduction and non-covalent mass spec) that illustrate our compounds recognize cytochrome c with low nM affinity and selectivity over other proteins of comparable surface composition (e.g. lysozyme). Furthermore, structure affinity studies with a range of ruthenium complexes indicate affinity can be tuned in a predicatable manner. Current and future studies are focused towards demonstrating these large macromolecules have biological relevance through cell based experiments.

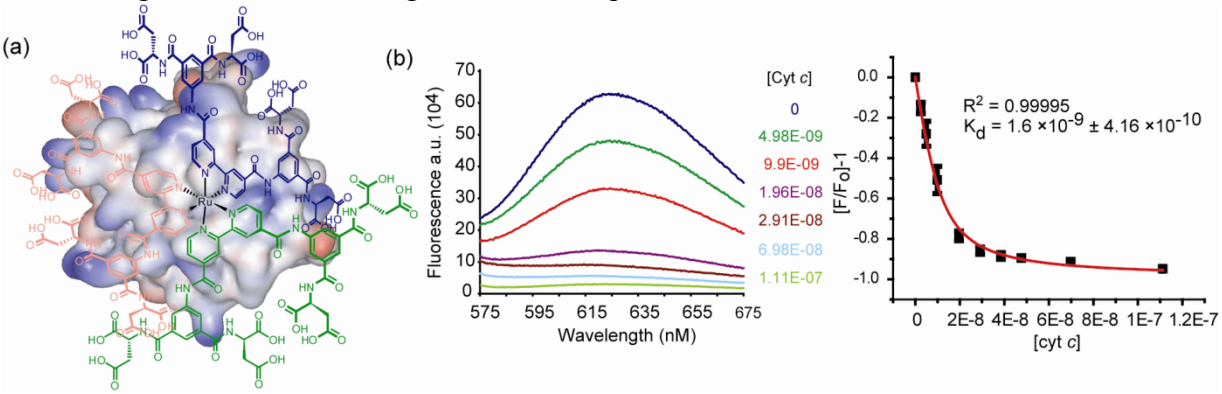

Figure 2: (a) structure and cartoon representation of $Ru(bipy)_3$ compound bound to cytochrome c **(b)** fluorescence titration of $Ru(bipy)_3$ with cytochrome c (10 nM receptor, 5 mM sodium phosphate buffer, pH 7.4, ex 467 nm).

Publications

Plante, J., Burnley, T., Malkova, B., Webb, M., Warriner, S., Edwards, T. and Wilson, A. (2009) Oligobenzamide proteomimetic inhibitors of the p53-hDM2 protein-protein interaction. *Chem Commun (Camb)*, **34**:5091-5093.

Wilson, Andrew J. (2009) Nanonose for sniffing out proteins. *Nat Chem*, **1:**429-430.

Wilson, Andrew J. (2009) Inhibition of protein-protein interactions using designed molecules. *Chem Soc Rev*, **38**:3289-3300.

Campbell, F., Plante, J., Edwards, T., Warriner, S. and Wilson, A. (2010) *N*-Alkylated Oligoamide α-Helical Proteomimetics. *Org Biomol Chem*, **8**:2344-2351.

Muldoon, J. Ashcroft, A. and Wilson, A. (2010) Selective protein-surface sensing using ruthenium(II) Tris-(bipyridine) complexes. *Chem Eur J*, **16**:100-103.

Funding

We gratefully acknowledge EPSRC, the University of Leeds, The Wellcome Trust, Yorkshire Cancer Research and The European Research Council for financial support of this research.

Collaborators

We gratefully acknowledge Nicholas Fletcher and Serin Dabb (University of Belfast) for synthesis of bypyridine precursors.

A pH-driven, fast-responding DNA hydrogel

Dejian Zhou

Introduction

Over the past twenty years, DNA has been demonstrated to be an excellent building material for the assembly of functional nanostructures, molecular motors, two-dimensional grids to isolated three-dimensional nanostructures. Recently, DNA assembly has been expanded to unconstrained three-dimensional structures, e.g. 'DNA hydrogel'. The previous DNA gel which is based on DNA duplex formation followed by enzyme-catalyzed ligation is rather slow, requiring overnight ligation. Besides, the release of the entrapped materials is also very slow, requiring over 10 days to release the entrapped insulin for example. This may limit its applications where fast trapping and releasing process is required. Here we report the preparation of a fast, pH-responsive DNA hydrogel with three-armed DNA nanostructure (Y-unit, Figure 1A) assembled together *via* the formation of inter-unit i-motif structures. The DNA gel can be switched to non-gel state in one minute by using environmental pH changes.

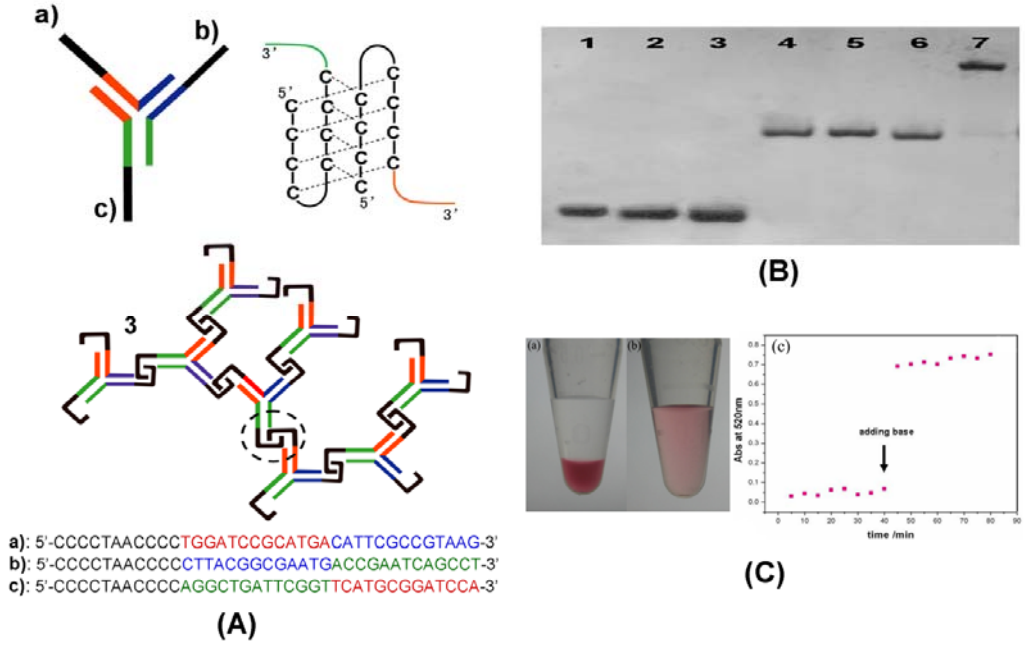

Figure 1: (A) Principle of the pH-responsive DNA gel. (**B**) Native gel electrophoresis analysis of the formation of the hierarchical self-assembly: Lane 1, 2 and 3 are strands a, b and c; lane 4 (a+b), 5 (a+c), 6 (b+c) are partial complementary structures; and Lane 7 is the fully assembled DNA Y-unit (a+b+c). **(C)** pH-induced gel transition visualized by gold nanoparticles (GNPs): (a) GNPs trapped in DNA hydrogel with the upper covered by pH 5.0 MES buffer; (b) after changing the buffer pH to 8.0, GNPs were released to form a uniform solution; (c) time trace of absorption at 520 nm for upper part of the solution before and after NaOH addition.

Figure 1A shows our priciple: a Y-unit is formed by three 37 mer single-stranded DNA, each containing two functional domains: a 11-mer interlocking domain with two cytosine (*C*)-rich stretches (black) and a 26 mer double-stranded 'Y' shape domains (red, green and blue, see **A** for their sequences). The Y-shape domains are carefully designed to have two half-complimentary sequences such that equal amount of the three DNA strands will hybridize to each other to produce the Y-unit with three interlocking domains sticking out. At high pH (> 6.5), the interlocking domains are random coils, so the Y-units are isolated. As the pH is lowered to slightly acidic, the *C*s in the *C*-rich domains become partially protonated, leading to the formation of $C{\equiv}CH^+$ triple hydrogen bonds between hemi-protonated *C*-pairs (Figure 1A, top-right). Accumulation of the Y-unit assembly leads to an extended three-dimensional DNA network structure, producing the DNA hydrogel.

To verify our design, stoichiometric amount of the DNA strands, **a**, **b** and **c**, was mixed in 50 mM MES buffer (pH 8.0, 50 mM NaCl) to give a final concentration of 40 μM for each strand. The DNA assembly was characterized by native polyacrylamide gel electrophoresis. Figure 1B shows that all three DNAs can assemble to their complementary strands to form the expected DNA structural units with the expected gel mobility. A single dominant band in lane 7 is observed, confirming the efficient assembly of the designed DNA Y-unit.

To visualize the gel transition, we used gold nanoparticles (GNPs) as a "tracer agent" which were added to DNA solution before the gelling process. Addition of HCl to lower the system pH to 5.0 initiates the gel formation, so that the GNPs are trapped within the gel and cannot be dispersed into the upper pH 5.0 buffer. The resulting GNP containing gel is very stable, no GNPs release was observed over several days without stirring. However, on addition of NaOH to render the upper buffer solution slightly basic (i.e. pH 8), the DNA gel is quickly disassembled. The trapped GNPs are released and dispersed into the whole solution in one minute. The stability of the DNA gel is found to be strongly pH-dependent. A pH titration experiment reveals that the non-gel to gel state transition happens at pH just below 6.0, which agrees well with the earlier report that i-motif has a sharp transition around a *pKa* of 6.3. These suggest that the formation of inter-unit i-motifs is responsible for the gelling process.

The strength of the DNA hydrogel has been found to be dependent on the temperature and Y-unit concentrations. The gel strength decreases with the increasing temperature and the gelling transition point is ~37°C at 0.60 mM Y-unit concentration, closed to the melting point of Y-shape DNA assemblies. Therefore, the thermal stability of this DNA hydrogel should be precisely adjustable by the DNA sequences used in building the Y-unit, a unique advantage of this system. In additional, the DNA gel is only formed at Y-unit concentrations ≥ 0.6 mM, and its strength also increases with the increasing Y-unit concentration, suggesting that the Y-unit assembly is responsible for the observed DNA gel formation.

In summary, we have developed a novel strategy to prepare pH responsive hydrogels entirely made of DNAs. This hydrogel is formed by cross-linking a single type DNA Y-unit building block through the formation of inter-unit i-motifs and can respond quickly to pH changes to controllably trap and release cargos in a pH-dependent manner. In principle, other materials, e.g. therapeutic proteins, polymers and even protein producing system could be incorporated into such DNA gel system, allowing the development of functional, responsive biomaterials that have applications in a wide range of disciplines, biosensing, tissue engineering, nano-mechanical devices, and drug delivery etc. This pH-responsive DNA gel that happens at the physiological relevant pH range of 5-8, appears to be well-suited for targeting tumours and other pathological conditions as these sites often have a relatively high extra-cellular acidity.

Publications

Cheng, E., Xing, Y., Chen, P., Yang, Y., Sun, Y., Zhou D., Xu, L., Fan, Q. and Liu, D. (2009) A pH-trigged, fast-responding DNA hydrogel. *Angew Chem Int Ed Engl*, **48**:7660-7663.

Wang, W., Yang, Y., Cheng, E., Zhao, M., Meng, H., Liu, D. and Zhou, D. (2009) A pH-driven, reconfigurable DNA nanotriangle *Chem Commun (Camb)*, **7**:824-826.

Collaborator

Prof. Dongsheng Liu, Department of Chemistry, Tsinghua University, Beijing, China

Funding

This work was supported by the Royal Society and the National Science Foundation of China.

Astbury Seminars 2009

15th January 2009
Prof Ben Schuler, Department of Biochemistry, University of Zurich
"Protein folding dynamics from single molecule FRET"

29th January 2009
Dr Laurent Bozec, Biomaterials and Tissue Engineering, UCL Eastman Dental Institute
"Nanomechanics of Collagen: Shaping the outside from the inside"

19th March 2009
Dr Ryan Mehl, Department of Chemistry, Franklin & Marshall College
"Selecting Synthetases for Unnatural Amino Acids that don't Exist: High Yield Genetic Incorporation of Unnatural Amino Acids for Probing Protein Interactions and Dynamics"

31st March 2009
Prof Michael Rossmann, Department of Biological Sciences, Purdue University
"T4 and phi29 DNA packaging motors"

2nd April 2009
Richard Henderson, MRC-Lab. of Molecular Biology, Cambridge University
"Electron cryomicroscopy achievements and potential"

20th April 2009
Dr Martin Weik, Institut de Biologie Structurale, Grenoble
"Coupling between protein and hydration-water dynamics"

23rd April 2009
Prof Garry Taylor, Centre for Biomolecular Sciences, University of St Andrews
"Structural studies on cholera pathogenicity factors"

5th May 2009
Prof Christine Ziegler, Max Planck Institute, Frankfurt
"The X-ray structure of the osmoregulated Na+/betaine symporter BetP: Molecular basis of transport and regulation"

6th May 2009
Prof Raz Jelinek, Ben Gurion University, Israel
"New angles on membrane interactions of amyloid fibrils and oligomers"

7th May 2009
Prof Paul Ortiz de Montellano, Deptartment of Pharmaceutical Chemistry, University of California San Francisco
"Tuberculosis : oxidative enzymes and therapeutic approaches"

19th May 2009
Dr Xavier Salvatella, IRB Barcelona
'Identification of structure-conserving correlated motions in proteins using NMR and molecular simulations'

1st June 2009
Prof Jacqui Matthews, University of Sydney NSW
"Cell specific transcription complexes"

9th June 2009
Prof Jean Baum, Department of Chemistry, Rutgers University
"Structural and dynamic characterization of alpha-synuclein proteins: Implication for initiation of protein aggregation"

10th June 2009
Prof Lynn Zechiedrich, Baylor College of Medicine, Houston
"The Devil in the Details: How DNA Structure, Sequence, and Counterions Drive Biology"

23rd July 2009
Prof Rein Ulijn, Department of Pure and Applied Chemistry, University of Strathclyde
"Design and Assembly of Peptide Biomaterials: Enzymes Lend a Helping Hand"

1st October 2009
Prof Kurt Drickamer, Division of Molecular Biosciences, Imperial College London
"Recognising sugars: receptors for cell surface glycans in innate and adaptive immunity"

17th November 2009
Prof Richard Neutze, Department of Chemistry, Biochemistry & Biophysics, University of Gothenburg, Sweden
"Time-resolved structural studies of membrane proteins"

25th November 2009
Dr Ali Tavassoli, School of Chemistry, University of Southampton
"Genetic Selection as a Tool for Drug Discovery"

PUBLICATIONS by ASTBURY CENTRE MEMBERS 2009

Abou-Saleh, R., Connell, S., Harrand, R., Ajjan, R., Mosesson, M., Smith, D., Grant, P. and Ariens, R. (2009) Nanoscale probing reveals that reduced stiffness of clots from fibrinogen lacking 42 N-terminal Bβ -chain residues is due to the formation of abnormal oligomers. *Biophys J* **96**:2415-2427.

Adair, R., Patel, A., Corless, L., Griffin, S., Rowlands, D. and McCormick, C. (2009) Expression of hepatitis C virus (HCV) structural proteins in *trans* facilitates encapsidation and transmission of HCV subgenomic RNA. *J Gen Virol*, **90**:833-842.

Agarwal, A., Johnson, P. and Fishwick, C. (2009) Synthesis of *de novo* designed small-molecule inhibitors of bacterial RNA polymerase. *Tetrahedron*, **65**:1077.

Allen, L., Krivov, S. and Paci, E. (2009) Analysis of the free-energy surface of proteins from reversible folding simulations. *PLoS Comput Biol*, **5**:e1000428.

Allen, L. and Paci, E. (2009) Orientational averaging of dye molecules attached to proteins in Forster resonance energy transfer measurements: Insights from a simulation study. *J Chem Phys*, **131**:065101/1-065101/6.

Ansell, R., Tunon, P., Wang, Y., Myers, P., Ivory, C., Keen, J. and Findlay, J. (2009) Electrophoretic field gradient focusing with on-column detection by fluorescence quenching. *Analyst*, **134**:226-229.

Ansell, R., Meegan, J., Barrett, S. and Warrinner, S. (2009) On the interactions of alkyl 2-hydroxycarboxylic acids with alkoxysilanes 2. Complexation and esterification of di- and tricarboxylic acids. *Dalton Trans*, **8**:1460-1470.

Auer, S., Trovato, A. And Vendruscolo, M. (2009) A condensation-ordering mechanism in nanoparticle-catalyzed peptide aggregation. *PLoS Comput Biol*, **5**:e1000458.

Baboolal, T., Sakamoto, T., Forgacs, E., White, H., Jackson, S., Takagi, Y., Farrow, R., Molloy, J., Knight, P., Sellers, J. and Peckham, M. (2009) The SAH domain extends the functional length of the myosin lever. *Proc Natl Acad Sci USA*, **106**:22193-22198.

Bao, L., Redondo, C., Findlay, J., Walker, J. and Ponnambalam, S. (2009) Deciphering soluble and membrane protein function using yeast systems (Review). *Mol Membr Biol*, **26**:127-135.

Bartlett, A. and Radford, S. (2009) An expanding arsenal of experimental methods yields an explosion of insights into protein folding mechanisms. *Nat Struct Molec Biol*, **16**:582-588.

Barton, J., Bunka, D., Knowling, S., Lefevre, P., Warren, A., Bonifer, C., Stockley, P. (2009) Characterization of RNA aptamers that disrupt the RUNX1-CBFβ/DNA complex. *Nucleic Acids Res*, **37**:6818-6830.

Beddard, G. and Brockwell, D. (2009) A statistical approach to the estimation of mechanical unfolding parameters from the unfolding patterns of protein heteropolymers. *Phys Biol*, **7**:14001-14001.

Bernlind, C., Homans, S. and Field, R. (2009) Synthesis of prospective disaccharide ligands for *Escherichia coli* O157 verotoxin. *Tetrahedron Lett*, **50**:3397-3399.

Berryman, J., Radford, S. and Harris, S. (2009) Thermodynamic description of polymorphism in Q- and N-rich peptide aggregates revealed by atomistic simulation. *Biophys J*, **97**:1-11.

Blake, K., O'Neill, A., Mengin-Lecreuix, D., Henderson, P., Bostock, J., Dunsmore, C., Simmons, K., Fishwick, C., Leeds, J. and Chopra, I. (2009) The nature of *Staphylococcus aureus* MurA and MurZ and approaches for detection of peptidoglycan biosynthesis inhibitors. *Mol Microbiol*, **72**:335-343.

Boyne, J. and Whitehouse, A. (2009) Nucleolar disruption impairs Kaposi's sarcoma-associated herpesvirus ORF57-mediated nuclear export of intronless viral mRNAs. *FEBS Lett*, **583**:3549-3556.

Brooks B., Brooks C., Mackerell A., Nilsson L., Petrella R., Roux B., Won Y., Archontis G., Bartels C., Boresch S., Caflisch A., Caves L., Cui Q., Dinner A., Feig M., Fischer S., Gao J., Hodoscek M., Im W., Kuczera K., Lazaridis T., Ma J., Ovchinnikov V., Paci E., Pastor R., Post C., Pu J., Schaefer M.,Tidor B., Venable R., Woodcock H., Wu X., Yang W., York D. and Karplus M. (2009) CHARMM: The biomolecular simulation program. *J Comput Chem***, 30**:1545-1614.

Bruns, A., Bao, L., Walker, J. and Ponnambalam S. (2009) VEGF-A-stimulated signalling in endothelial cells via a dual receptor tyrosine kinase system is dependent on co-ordinated trafficking and proteolysis. *Biochem Soc Trans* **37**:1193-1197.

Camm, K., El-Sokkary, A., Gott, A., Stockley, P., Belyaeva, T. and McGowan, P. (2009) Synthesis, molecular structure and evaluation of new organometallic ruthenium anticancer agents. *Dalton Trans*, **48**:10914-10925.

Campbell, F. and Wilson, A. (2009) An ‘impossible' macrocyclisation using conformation directing protecting groups. *Tetrahedron Lett*, **50**:2236-2238.

Campeotto, I., Carr, S., Trinh, C., Nelson, A., Berry, A., Phillips, S. and Pearson, A. (2009) Structure of an *Escherichia coli* N-acetyl-D-neuraminic acid lyase mutant, E192N, in complex with pyruvate at 1.45 angstrom resolution. *Acta Crystallogr Sect F Struct Biol Cryst Commun* **65**:1088-1090.

Care, M., Bradford, J., Needham, C., Bulpitt A., Westhead D. (2009) Combining the interactome and deleterious SNP predictions to improve disease gene identification. *Hum Mutat*, **30**:485-92.

Carpousis, A., Luisi, B. and McDowall, K. (2009) Endonucleolytic initiation of mRNA decay in *Escherichia coli*. *Prog Mol Biol Transl Sci*, **85**:91-135.

Caryl, J. and O'Neill, A. (2009) Complete nucleotide sequence of pGO1, the prototype conjugative plasmid from the staphylococci. *Plasmid*, **62**:35-38.

Chen, R., Khormaee S., Eccleston, M., Slater, N. (2009). The role of hydrophobic amino acid grafts in the enhancement of membrane-disruptive activity of pH-responsive pseudo-peptides. *Biomaterials* **30**:1954-1961.

Chen, R., Eccleston, M., Yue, Z. and Slater, N. (2009). Synthesis and pH-responsive properties of pseudo-peptides containing hydrophobic amino acid grafts. *J Mater Chem* **19**:4217-4224.

Chen, R., Khormaee, S., Eccleston, M. and Slater, Nigel (2009). Effect of L-leucine graft content on aqueous solution behaviour and membrane-lytic activity of a pH-responsive pseudo-peptide. *Biomacromolecules* **10**:2601-2608.

Cheng, E., Xing, Y., Chen, P., Yang, Y., Sun, Y., Zhou D., Xu, L., Fan, Q. and Liu, D. (2009) A pH-trigged, fast-responding DNA hydrogel. *Angew Chem Int Ed Engl***, 48**:7660-7663.

Colgan, K., Boyne, J. and Whitehouse, A. (2009) Uncoupling of hTREX demonstrates that UAP56 and hTHO-complex recruitment onto herpesvirus saimiri intronless transcripts is required for replication. *J Gen Virol* **90**:1455-1460.

Colgan, K., Boyne, J. and Whitehouse, A. (2009) Identification of a response element in a herpesvirus saimiri mRNA recognized by the ORF57 protein. *J Gen Virol*, **90**:596-601.

Das, C., Noro, M. and Olmsted, P. (2009) Simulation studies of stratum corneum lipid mixtures. *Biophys J*, **97**:1941-1951.

Das, C., Olmsted, P. and Noro, M. (2009) Water permeation through stratum corneum lipid bilayers from atomistic simulations. *Soft Matter*, **5**:4549-4555.

Davies, M., Heikkilä, T., McConkey, G., Fishwick, C., Parsons, M. and Johnson, P. (2009) Structure-based design, synthesis, and characterization of inhibitors of human and *Plasmodium falciparum* dihydroorotate dehydrogenases. *J Med Chem* **52**:2683-2693.

Davis J., Tkac J., Humphreys R., Buxton A., Lee T. Ko Ferrigno P. (2009) Peptide aptamers in label-free protein detection II: Chemical optimisation and detection of distinct protein isoforms. *Anal Chem*, **81**:3314-20.

De Marcos Lousa, C., Dietrich, D., Johnson, B., Baldwin, S., Holdsworth, M., Theodoulou, F. and Baker, A. (2009) The NBDs that wouldn't die: a cautionary tale of the use of isolated nucleotide binding domains of ABC transporters. *Commun Integr Biol*, **2**:97-99.

Dietrich, D., Schmuths, H., De Marcos, L., Baldwin, J., Baldwin, S., Baker, A., Theodoulou, F. and Holdsworth, M. (2009) Mutations in the *Arabidopsis* peroxisomal ABC transporter COMATOSE allow differentiation between multiple functions in planta: insights from an allelic series. *Mol Biol Cell* **20:**530-543.

Dougan, L., Li, J., Badilla, C., Berne, B., and Fernandez, J. (2009) Single homopolypeptide chains collapse into mechanically rigid conformations, *Proc Natl Acad Sci USA*, **106**:12605-12610.

Duff, C., Scott, M., Kirby, I., Hutchinson, S., Martin, S. and Hooper, N. (2009) Antibody-mediated disruption of the interaction between PCSK9 and the low-density lipoprotein receptor. *Biochem J* **419**:577-584.

Dugan, G. and Hewitt, E. (2009) Dependence of the localization and function of the human

cytomegalovirus protein US6 on the transporter associated with antigen processing. *J Gen Virol* **90**:2234-2238.

Eichner, T. and Radford, S. (2009) A Generic Mechanism of beta2-Microglobulin amyloid assembly at neutral pH involving a specific proline switch. *J Mol Biol*, **386**:1312-1326.

Elwi, A., Damaraju, V., Kuzma, M., Baldwin, S., Young, J., Sawyer, M. and Cass, C. (2009) Human concentrative nucleoside transporter 3 is a determinant of fludarabine transportability and cytotoxicity in human renal proximal tubule cell cultures. *Cancer Chemother Pharmacol* **63**:289-301.

Elwi, A., Damaraju, V., Kuzma, M., Mowles, D., Baldwin, S., Young, J., Sawyer, M. and Cass, C. (2009) Transepithelial fluxes of adenosine and 2'-deoxyadenosine across human renal proximal tubule cells: the roles of nucleoside transporters hENT1, hENT2, and hCNT3. *Am J Physiol Renal Physiol* **296**:F1439- F1451.

Emmott, E. and Hiscox, J. (2009) Nucleolar targeting: the hub of the matter. *EMBO Rep*, **10**:231-238.

Fadouloglou, V., Bastaki, M., Ashcroft, A., Phillips, S., Panopoulos, N., Glykos, N. and Kokkinidis, M. (2009) On the quaternary association of the type III secretion system HrcQB-C protein: experimental evidence differentiates among the various oligomerization models, V. E. *J Struct Biol* **166**:14-25.

Fascione, M., Adshead, S., Stalford, S., Kilner, C., Leach, A. and Turnbull, B. (2009) Stereoselective glycosylation using oxathiane glycosyl donors. *Chem Commun*, **39**:5841-5843.

Foit, L., Morgan, G., Kern, M., Steimer. L., von Hacht, A.-K. , Titchmarsh, T., Warriner, S., Radford, S. and Bardwell, J. (2009) Optimizing protein stability *in vivo*. *Mol Cell,* **36**: 861-871.

Forman J., Yew Z., Quamar S., Sanford R., Paci E. and Clarke J. (2009) Non-native interactions are critical for mechanical strength in PKD domains**.** *Structure*, **17**:1582-1590.

Friel, C., Smith, D., Vendruscolo, M., Gsponer, J. and Radford, S. (2009) The mechanism of folding of Im7 reveals competition between functional and kinetic evolutionary constraints. *Nat Struct Molec Biol* **16**:318-324.

Fuller, J., Burgoyne, N. and Jackson, R. (2009) Predicting druggable binding sites at the protein-protein interface. *Drug Discov Today*, **14**:155-161.

Gage, M., Keen, J., Buxton, A., Bedi, M. and Findlay, J. (2009) Proteomic analysis of IgE-mediated secretion by LAD2 mast cells. *J Proteome Res*, **8**:4116-4125.

Gao, Z. Li, Y., Cooksey, J., Snaddon, T., Schunk, S., Viseux, E., McAteer, S. and Kocienski, P. (2009) A Synthesis of an ionomycin calcium complex**.** *Angew Chem Int Ed Engl*, **48**:5022-5025.

Gao, J., Coulson, J., Whitehouse, A. and Blake, N. (2009). Reduction in RNA levels rather than retardation of translation is responsible for the inhibition of MHC Class I antigen

presentation by the glutamic acid rich repeat of Herpesvirus saimiri ORF73. *J Virol,* **83**:273-282.

Garcia-Manyes, S., Dougan, L. and Fernandez, J. (2009) Osmolyte-induced separation of the mechanical folding phases of ubiquitin, *Proc Natl Acad Sci USA*, **106**: 10540-10545.

Garcia-Manyes, S., Dougan, L., Badilla, C., Brujic, J., and Fernandez, J. (2009) Direct observation of an ensemble of stable collapsed states in the mechanical folding of ubiquitin, *Proc Natl Acad Sci USA*, **106**: 10534-10539.

Gaskell E., Smith J., Pinney J., Westhead D. and McConkey, G. (2009) A unique dual activity amino acid hydroxylase in *Toxoplasma gondii*. *PloS ONE*, **4**:1932-6203.

Gibson, D., Homans, S. and Field, R. (2009) A sugar aminoacid for the development of multivalent ligands for *Escherichia coli* 0157 verotoxin. *Tetrahedron Asymmetry,* **20**:730-732.

Glowacki, D., Shalashilin, D. and Paci, E. (2009) Boxed molecular dynamics: a simple and general technique for accelerating rare event kinetics and mapping free energy in large molecular systems *J Phys Chem B* **113**:16603-16611.

Gooch, A., McGhee, A., Renton, L., Plante, J., Lindsay, C. and Wilson, A. (2009) Design, synthesis and binding properties of conformer-independent linear ADA hydrogen-bonding arrays. *Supramol Chem*, **21**:12-17.

Goodwin, S.,Tuthill, T., Arias, A., Killington, R. and Rowlands, D. (2009) Foot-and-mouth disease virus assembly: processing of recombinant capsid precursor by exogenous protease induces self-assembly of pentamers in vitro in a myristoylation-dependent manner. *J Virol*, **83**:11275-11282.

Gould, F., Harrison, S., Hewitt, E. and Whitehouse, A. (2009) Kaposi's sarcoma-associated herpesvirus RTA promotes degradation of the Hey1 repressor protein through the ubiquitin proteasome pathway. *J Virol*, **83**:6727-6738.

Grant C., Brockwell D., Radford S. and Thomson N. (2009) Tuning the elastic modulus of hydrated collagen fibrils. *Biophys J* **97**:2985-92.

Griffin, S. (2009) Plugging the holes in hepatitis C virus antiviral therapy. *Proc Natl Acad Sci USA*, **106**:12567-12568.

Gupta, Y., Lee, T., Edwards, T., Escalante, C., Kadyrova, L., Wharton, R. and Aggarwal, A. (2009) Co-occupancy of two Pumilio molecules on a single hunchback NRE. *RNA*, **15**:1029-1035,

Han, X., Cheetham, M., Sheikh, K., Olmsted, P., Bushby, R. and Evans, S. (2009) Manipulation and charge determination of proteins in photopatterned solid supported bilayers. *Integr Biol(Camb)*, **1**:205-211.

Hein, Z., Hooper, N., Naim, H. (2009) Association of a GPI-anchored protein with detergent-resistant membranes facilitates its trafficking through the early secretory pathway. *Exp Cell Res*, **315**:348-356.

Herbert, S., Odell, A., Ponnambalam, S. and Walker, J. (2009) Activation of cytosolic phospholipase A2-α as a novel mechanism regulating endothelial cell cycle progression and angiogenesis. *J Biol Chem* **284**:5784-5796.

Ho, V., Barcza, A., Chen, R., Müller, K., Darton, N. and Slater, N. (2009). The precise control of cell labelling with streptavidin paramagnetic particles. *Biomaterials* **30**:6548–6555.

Hodkinson, J., Jahn, T., Radford, S. and Ashcroft, A. (2009) HDX-ESI-MS reveals enhanced conformational dynamics of the amyloidogenic protein beta2-microglobulin upon release from the MHC-1. *J Am Soc Mass Spectrom,* **20**:278-286.

Horn, J., Li, H.-Y, Marsden, S., Nelson, A., Shearer, R., Campbell, A., House, D. and Weingarten, G. (2009) Convergent synthesis of dihydroquinolones from o-aminoarylboronates. *Tetrahedron*, **65**:9002-9007.

Hughes, M., Gretton, S., Shelton, H., Brown, D., McCormick, C., Angus, A., Patel, A., Griffin, S. and Harris, M. (2009) A conserved proline between domains II and III of hepatitis C virus NS5A influences both RNA replication and virus assembly. *J Virol*, **83**:10788-10796.

Hughes, M., Griffin, S. and Harris, M. (2009) Domain III of NS5A contributes to both RNA replication and assembly of hepatitis C virus particles. *J Gen Virol* **90**:1329-1334.

Jenkins, H., Baker-Wilding, R. and Edwards, T. (2009) Structure and RNA binding of the mouse Pumilio-2 Puf domain. *J Struct Biol*, **167**:271-276.

Jeuken, L., Weiss, S., Henderson, P., Evans, S. and Bushby, R. (2009) Impedance spectroscopy of bacterial membranes: Co-enzyme Q diffusion in a finite diffusion layer. *Anal Chem* **80**:9084-9090.

Jeuken, L. (2009) Electrodes for integral membrane enzymes. *Nat Prod Rep*, **26**:1234-1240.

Joce, C., Caryl, J., Stockley, P., Warriner, S. and Nelson, A. (2009) Identification of stable S-adenosylmethionine (SAM) analogues derivatised with bioorthogonal tags: effect of ligands on the affinity of the *E. coli* methionine repressor, MetJ, for its operator DNA. *Org Biomol Chem*, **7**:635-638.

Jopling, H., Odell, A., Hooper, N., Zachary, I., Walker, J. and Ponnambalam, S. (2009) Rab GTPase regulation of VEGFR2 trafficking and signaling in endothelial cells. *Arterioscler Thromb Vasc Biol*, **29**:1119-1124

Kalverda, A., Thompson, G., Vogel, A., Schroder, M., Bowie, A., Khan, A. and Homans, S. (2009) Poxvirus K7 protein adopts a Bcl-2 fold: biochemical mapping of its interactions with human DEAD box RNA helicase DDX3. *J Mol Biol,* **385**:843-853.

Kellett K. and Hooper N. (2009) Prion protein and Alzheimer disease. *Prion*, **3**:190-4.

Kennaway, C. Obarska-Kosinska, A., White, J., Tuszynska, I., Cooper, L., Bujnicki, J.,Trinick, J. and Dryden, D. (2009) The structure of M.EcoKI type I DNA

methyltransferase with a DNA mimic antirestriction protein. *Nucleic Acids Res*, **37**:762-770.

Kinnings, S. and Jackson, R. (2009) Binding site similarity analysis for the functional classification of the protein kinase family. *J Chem Inf Model*, **49**:318-329.

Kinnings, S. and Jackson, R. (2009) LigMatch: a multiple structure-based ligand matching method for 3D virtual screening. *J Chem Inf Model*, **49:**2056-2066.

Knowling, S., Figueiredo, A., Whittaker, S., Moore, G. and Radford, S. (2009) Amino-acid insertion reveals a necessary three-helical intermediate in the folding pathway of the colicin E7 immunity protein Im7. *J Mol Biol*, **392**:1074-1086.

Ko Ferrigno, P. (2009) Biological and clinical applications of biosensors. In Engineering the Bioelectronic Interface (Davis, J., ed), pp225-242, Springer, London .

Kon, T., Imamula, K., Roberts, A. Ohkura, R., Knight, P., Gibbons, I., Burgess, S. and Sutoh, K. (2009) Helix sliding in the stalk coiled coil of dynein couples ATPase and microtubule binding. *Nat Struct Molec Biol*, **16**:325-333.

Kulharia, M., Bridgett, S., Goody, R. and Jackson, R. (2009) InCa-SiteFinder: A method for structure-based prediction of inositol and carbohydrate binding sites on proteins. *J Mol Graph Model,* **28**:297-303.

Kyle, S., Aggeli, A. Ingham, E. and McPherson, M. (2009) Production of self-assembling biomaterials for tissue engineering. *Trends Biotechnol*, **27**:423-433.

Liechty, W., Chen, R., Farzaneh, F., Tavassoli, M. and Slater, N. (2009). Synthetic pH-responsive polymers for protein transduction. *Adv Mater* **21**:3910-3914.

Lynch, S., Baker, H., Byker, S. Zhou, D. Sinniah, K. (2009) Single molecule force spectroscopy on G-Quadruplex DNA. *Chem Eur J,* **15**:8113-8116.

McDowall, K. (2009) RNA stability: chemistry, measurement and modulation. In Wiley Encyclopedia of Chemical Biology 4 (Begley, T., ed), pp263-275, Wiley, Hoboken.

McPherson, M. James, K., Kyle, S., Parsons, S. and Riley, J. (2009) Recombinant production of self-assembling peptides. *Adv Chem Engin*, **35**:79-117.

Macnab, S. and Whitehouse, A. (2009) Progress and prospects: human artificial chromosomes. *Gene Ther*, **16**:1180-1188.

Manfield, I. and Stockley, P. (2009) Ethylation interference footprinting of DNA-protein complexes. *Methods Mol Biol*, **543**:105-120.

Mankouri, J., Dallas, M., Hughes, M., Griffin, S., MacDonald, A., Peers, C. and Harris, M. (2009) Suppression of a pro-apoptotic K+ channel as a mechanism for hepatitis C virus persistence. *Proc Natl Acad Sci USA*, **106**:15903-15908.

Mittar, S., Ulyatt, C., Howell, G., Bruns, A., Zachary, I., Walker, J. and Ponnambalam, S. (2009) VEGFR1 receptor tyrosine kinase localization to the Golgi apparatus is calcium-dependent. *Exp Cell Res*, **315**:877-889.

Mohl, B.-P. and Barr, J. (2009) Investigating the specificity and stoichiometry of RNA binding by the nucleocapsid protein of Bunyamwera virus. *RNA*, **15**:391-399.

Mok, N, Chadwick, J. Kellett, K., Hooper, N., Johnson, P., Fishwick, C. (2009) Discovery of novel non-peptide inhibitors of BACE-1 using virtual high-throughput screening. *Bioorg Med Chem Lett*, **19**:6770-6774.

Morton, D., Leach, S., Cordier, C., Warriner, S. and Nelson, A. (2009) Synthesis of natural-product-like molecules with over eighty distinct scaffolds. *Angew Chem Int Ed Engl*, **48**:104-109.

Muench, S., Huss, M., Song, C., Phillips, C., Wieczorek, H., Trinick, J. and Harrison, M. (2009) Cryo-electron microscopy of the vacuolar ATPase motor reveals its mechanical and regulatory complexity. *J Mol Biol*, **386**:989-999.

Murrison, S., Glowacki, D., Einzinger, C., Titchmarsh, J., Bartlett, S., McKeever-Abbas, B., Warriner, S. and Nelson, A. (2009) Remarkably slow rotation about a single bond between an sp3-hybridised carbon atom and an aromatic ring without ortho substituents. *Chem Eur J*, **15**:2185-2189.

Needham C., Manfield I., Bulpitt A., Gilmartin P. and Westhead D. (2009) From gene expression to gene regulatory networks in *Arabidopsis thaliana*. *BMC Syst Biol*, **3**:article number 85.

Nicolson, T., Bellomo1, E., Wijesekara, N., Loder, M., Baldwin, J., Gyulkhandanyan, A., Koshkin, V., Tarasov, A., Carzaniga, R., Kronenberger, K., Taneja, T., da Silva Xavier, G., Libert, S., Froguel, P., Scharfmann R., Stetsyuk, V., Ravassard, P., Parker, H., Gribble, F., Reimann, F., Sladek, R., Hughes, S.J., Johnson, P., Masseboeuf, M., Burcelin, R., Baldwin, S., Liu, M., Lara-Lemus, R., Arvan, P., Schuit, F., Wheeler, M., Chimienti, F. and Rutter, G. (2009) Insulin storage and glucose homeostasis in mice null for the granule zinc transporter ZnT8 and studies of the type 2 diabetes-associated variants. *Diabetes* **58**:2070-2083.

Noronha M., Santos R., Paci E., Santos H., Macanita A. (2009) Fluorescence lifetimes of tyrosine residues in cytochrome c" as local probes to study protein unfolding. *J Phys Chem B*, **113**:4466-4474.

O'Leary-Steele, C., Cordier, C., Hayes, J., Warriner, S. and Nelson, A. (2009) A Fluorous-tagged "safety catch" linker for preparing heterocycles by ring-closing metathesis. *Org Lett*, **11**:915-918.

O'Neill, A., Lindsay, J., Gould, K., Hinds, J. and Chopra, I. (2009) Transcriptional signature following inhibition of early-stage cell wall biosynthesis in *Staphylococcus aureus*. *Antimicrob Agents Chemother*, **53**:1701-1704.

Pan, Y.-H., Sader, K., Powell, J., Bleloch, A., Gass, M., Trinick, J., Warley, A., Li, A., Brydson, R. and Brown, A. (2009) 3D morphology of the human hepatic ferritin mineral core: New evidence for a subunit structure revealed by single particle analysis of HAADF-STEM images. *J Struct Biol*, **166**:22-31.

Pearson, A. and Owen, R. (2009) Combining x-ray crystallography and single-crystal

spectroscopy to probe enzyme mechanisms. *Biochem Soc Trans*, **37**:378-381.

Peckham, M. and Knight, P. (2009) When a predicted coiled coil is really a single α -helix, in myosins and other proteins. *Soft Matter*, **5**:2493-2503.

Periole X, Allen L., Tamiola K., Mark A. and Paci E**.** (2009) Probing the free energy landscape of the FBP28 WW domain by multiple techniques. *J Comput Chem*, **30**:1059-1068.

Plante, J., Burnley, T., Malkova, B., Webb, M., Warriner, S., Edwards, T. and Wilson, A. (2009) Oligobenzamide proteomimetic inhibitors of the p53-hDM2 protein-protein interaction. *Chem Commun (Camb)*, **34**:5091-5093.

Platt, G. and Radford, S. (2009) Glimpses of the molecular mechanisms of beta2-microglobulin fibril formation *in vitro*: Aggregation on a complex energy landscape. *FEBS Lett*, **583**:2623-2629.

Platt, G., Xue, W.-F., Homans, S. and Radford, S. (2009) Probing Dynamics within amyloid fibrils using a novel capping method. *Angew Chem Int Ed Engl*, **48**:5705-5707.

Poole, E., Groves, I., Macdonald, A., Pang, Y., Alcami, A. and Sinclair, J. (2009) Identification of TRIM23 as a co-factor involved in the regulation of NFκB by the human cytomegalovirus gene product UL144. *J Virol*, **83**:3581-90**.**

Psakis, G., Saidijam, M., Shibayama, K., Polaczek, J., Bettaney, K., Baldwin, J., Baldwin, S., Hope, R., Essen, L.-O., Essenberg, R. and Henderson, P. (2009) The sodium-dependent D-glucose transport protein of *Helicobacter pylori*. *Mol Microbiol*, **71**:391-403.

Psencík, J., Collins, A., Liljeroos, L., Torkkeli, M., Laurinmäki, P., Ansink, H., Ikonen, T., Serimaa, R., Blankenship, R., Tuma, R. and Butcher, S. (2009) Structure of chlorosomes from the green filamentous bacterium *Chloroflexus aurantiacus*. *J Bacteriol*, **191**:6701-6708.

Riley, J., Aggeli, A., Koopmans, R. and McPherson, M. (2009) Bioproduction and characterization of a pH responsive self-assembling peptide. *Biotechnol Bioeng*, **103**:241-251.

Roberts, A., Numata, N., Walker, M., Kato, Y., Malkova, B., Kon, T., Ohkura, R., Arisaka, F., Knight, P., Sutoh, K. and Burgess, S. (2009) AAA+ ring and linker swing mechanism in the dynein motor. *Cell*, **136**:485-495.

Routledge, K., Tartaglia, G., Platt, G., Vendruscolo, M. and Radford, S. (2009) Competition between intramolecular and intermolecular interactions in an amyloid-forming protein. *J Mol Biol*, **389**:776-786.

Sader, K., Studer, D., Zuber, B., Gnaegi, H. and Trinick, J. (2009) Preservation of high resolution protein structure by cryo-electron microscopy of vitreous sections**.** *Ultramicroscopy* , **110**:43-47.

Sadler, D., Petrik, E., Taniguchi, Y., Pullen, J., Kawakami, M., Radford, S. and Brockwell, D. (2009) Identification of a mechanical rheostat in the hydrophobic core of protein L. *J Mol Biol*, **393**:237-248.

Short, J. and Macdonald, A. (2009). Viral evasion of interferon-stimulated genes. *Bio-Science Horizons,* **2**:212-224.

Sisu, C., Baron, A., Branderhorst, H., Connell, S., Weijers, C., de Vries, R., Hayes, E., Pukin, A., Gilbert, M., Pieters, R., Zuilhof, H., Visser, G. and Turnbull, B. (2009) The influence of ligand valency on aggregation mechanisms for inhibiting bacterial toxins. *ChemBioChem*, **10**:329-337.

Slatter, A., Thomas, C. and Webb, M. (2009) PcrA helicase tightly couples ATP hydrolysis to unwinding double-stranded DNA, modulated by the initiator protein for plasmid replication, RepD. *Biochemistry,* **48**:6326-6334.

Slugoski, M., Ng, A., Yao, S., Lin, C., Mulinta, R., Cass, C., Baldwin, S. and Young, J. (2009) Substituted cysteine accessibility method (SCAM) analysis of human concentrative nucleoside transporter hCNT3 reveals a novel discontinuous region of functional importance within the CNT family motif (G/A)XKX3NEFVA(Y/M/F). *J Biol Chem,* **284**:17281-17292.

Slugoski, M., Smith, K., Ng, A., Yao, S., Karpinski, E., Cass, C., Baldwin, S. and Young, J. (2009) Conserved glutamate residues E343 and E519 provide mechanistic insights into human concentrative nucleoside transporter 3 (hCNT3) structure and function. *J Biol Chem,* **284**:17266-17280.

Smith, D., Knapman, T., Campuzano, I., Malham, R., Berryman, J., Radford, S. and Ashcroft, A. (2009) Deciphering drift time measurements from travelling wave ion mobility spectrometry-mass spectrometry studies. *Eur J Mass Spectrom (Chichester, Eng)*, **15**: 113-130.

Staniland, S. (2009) Magnetosomes: bacterial biosynthesis of magnetic nanoparticles and potential biomedical applications. In Magnetic nanomaterials: Nanomaterials for the life sciences series Vol. 4 (Kumar, C., ed), pp 399, Wiley-VCH, Weinheim

Staniland S., Ward F. and Harrison, A. (2009) Biomineralisation of magnetite nanoparticles by microbes. In Neutron applications in earth, energy, and environmental sciences (Liang, L., Rinaldi, R. and Schober, H., eds), pp 595-619, Springer, London.

Stalford, S., Fascione, M., Sasindran, S., Chatterjee, D., Dhandayuthapani, S. and Turnbull, B. (2009) A natural carbohydrate substrate for *Mycobacterium tuberculosis* methionine sulfoxide reductase A. *Chem Commun (Camb)*, **1**:110-112.

Stalford, S., Kilner, C., Leach, A. and Turnbull, B. (2009) Neighbouring group participation vs. addition to oxacarbenium ions: studies on the synthesis of mycobacterial oligosaccharides. *Org Biomol Chem*, **7**:4842-4852.

StGelais, C., Foster, T., Verow, M., Atkins, E., Fishwick, C., Rowlands, D., Harris, M. and Griffin, S. (2009) Determinants of hepatitis C virus p7 ion channel function and drug sensitivity identified *in vitro*. *J Virol*, **83**:7970-7981.

Stockley, P. and Persson, B. (2009) Surface plasmon resonance assays of DNA-protein interactions. *Methods Mol Biol*, **543**:653-669.

Stockley, P. (2009) Filter-binding assays. (2009) *Methods Mol Biol*, **543**:1-14.

Sutay Kocabas, D., Pearson, A., Phillips, S., Bakir, U., Ogel, Z., McPherson, M. and Trinh, C. (2009) Crystallization and preliminary x-ray analysis of a bifunctional catalase-phenol oxidase from *Scytalidium thermophilum*. *Acta Crystallogr Sect F Struct Biol Cryst Commun*, **F65**:486-488.

Tanabe, M., Szakonyi, G., Brown, K., Henderson, P., Nield, J. and Byrne, B. (2009). The multidrug resistance efflux complex, EmrAB from *Escherichia coli* forms a dimer *in vitro*. *Biochem Biophys Res Commun* **380**:338-342.

Taylor, D., Parkin, E., Cocklin, S., Ault, J., Ashcroft, A. Turner, A. and Hooper, N. (2009) Role of ADAMs in the ectodomain shedding and conformational conversion of the prion protein. *J Biol Chem*, **284**:22590-22600.

Taylor D., Whitehouse I. and Hooper N. (2009) Glypican-1 mediates both prion protein lipid raft association and disease isoform formation. *PLoS Pathog*, **5**:e1000666

Taylor, D. and Hooper, N. (2009) The enigmatic membrane microdomain: lipid rafts. *Biochemist*, **31**:16-19.

Tedder, P., Zubko, E., Westhead, D., Meyer, P. (2009) Small RNA analysis in *Petunia hybrida* identifies unusual tissue-specific expression patterns of conserved miRNAs and of a 24mer RNA. *RNA*, **15**:1012-1020.

Thomas J., Vohra R., Beer S., Bhatti K., Ponnambalam S. and Homer-Vanniasinkam S. (2009) Biomarkers in peripheral arterial disease. *Trends Cardiovasc Med* **19**:**5**147-151.

Topham, N. and Hewitt, E. (2009) Natural killer cell cytotoxicity: how do they pull the trigger? *Immunology,* **128**:7-15.

Trinh, C., Asipu, A., Bonthron, D. and Phillips, S. (2009) Structures of alternatively spliced isoforms of human ketohexokinase. *Acta Crystallogr D Biol Crystallogr*, **D65**:201-211, S201/1.

Turner, R., Kirkham, J., Devine, D. and Thomson, N. (2009) Second harmonic atomic force microscopy of living *Staphylococcus aureus* bacteria. *Appl Phys Lett*, **94:** article no:043901.

Tuthill, T., Harlos, K., Walter, T., Knowles, N., Groppelli, E., Rowlands, D.; Stuart, D. and Fry, E. (2009) Equine rhinitis A virus and its low pH empty particle: clues towards an aphthovirus entry mechanism? *PLoS Pathog*, **5**:e1000620

Vardy, E., Rice, P., Bowie, P., Holmes, J., Catto, A. and Hooper, N. (2009) Plasma angiotensin-converting enzyme in Alzheimer's disease. *J Alzheimers Dis*, **16**:609-618.

Vickers, A., Potter, N., Fishwick, C., Chopra, I. and O'Neill, A. (2009) Analysis of mutational resistance to trimethoprim in *Staphylococcus aureus* by genetic and structural modelling techniques. *J Antimicrob Chemother*, **63**:1112-1117.

Vohra, R., Walker, J., Howell, G., Homer-Vanniasinkam, S. and Ponnambalam, S. (2009) The LOX-1 scavenger receptor cytoplasmic domain contains a transplantable endocytic motif. *Biochem Biophys Res Commun*, **383**:269-274.

Walmsley, A., Watt, N., Taylor, D., Perera, W., Sumudhu S. and Hooper, N. (2009) α - cleavage of the prion protein occurs in a late compartment of the secretory pathway and is independent of lipid rafts. *Mol Cell Neurosci*, **40**:242-248.

Wang, W., Yang, Y., Cheng, E., Zhao, M., Meng, H., Liu, D. and Zhou, D. (2009) A pH-driven, reconfigurable DNA nanotriangle *Chem Commun (Camb)*, **7**:824-826.

Webb, E. and Westhead, D. (2009) The transcriptional regulation of protein complexes; a cross-species perspective. *Genomics*, **94**:369-376.

Webb, M. and Smith, A. (2009) Chlorophyll and folate: intimate link revealed by drug treatment. *New Phytol*, **182**:3-5.

Weiss, S. and Jeuken, L. (2009) Electrodes modified with lipid membranes to study quinone oxidoreductases. *Biochem Soc Trans*, **37**:707-712.

Weiss, S., Bushby, R., Evans, S., Henderson, P. and Jeuken, L. (2009) Characterization of cytochrome bo3 activity in a native-like surface-tethered membrane. *Biochem J* **417**:555-560.

Whitaker J., McConkey G. and Westhead D. (2009) The transferome of metabolic genes explored: analysis of the horizontal transfer of enzyme encoding genes in unicellular eukaryotes. *Genome Biol*, **10**:1465-6914.

Whitaker, J., Letunic, I., McConkey, G. and Westhead, D. (2009) metaTIGER: a metabolic evolution resource. *Nucleic Acids Res*, **37**:531-538.

Whitaker, John W.; McConkey, Glenn A.; Westhead, David R. (2009) Prediction of horizontal gene transfers in eukaryotes: approaches and challenges. *Biochem Soc Trans* **37**:792-795.

White, H., Hodgkinson, J., Jahn, T., Cohen-Krausz, S., Gosal, W., Müller, S., Orlova, E., Radford, S. and Saibil, H. (2009) Globular tetramers of beta$_2$-microglobulin assemble into elaborate amyloid fibrils. *J Mol Biol* **389**:48-57.

Wilson, Andrew J. (2009) Nanonose for sniffing out proteins. *Nat Chem*, **1:**429-430.

Wilson, Andrew J. (2009) Inhibition of protein-protein interactions using designed molecules. *Chem Soc Rev*, **38**:3289-3300.

Wittmann, M., Macdonald, A. and Renne, J. (2009) IL-18 and inflammation. *Autoimmun Rev,* **9**:45-48.

Xue, W.-F., Homans, S. and Radford, S. (2009) Amyloid fibril length distribution quantified by atomic force microscopy single-particle image analysis. *Protein Eng Des Sel* **22**:489-496.

Xue, W.-F., Hellewell, A., Gosal, W., Homans, S., Hewitt, E. and Radford, S. (2009) Fibril fragmentation enhances amyloid cytotoxicity. *J Biol Chem*, **284**:34272-34282.

Yang, Y., Baboolal, T., Siththanandan, V., Chen, M., Walker, M., Knight, P., Peckham, M. and Sellers, J. (2009) A FERM domain autoregulates Drosophila myosin 7a activity. *Proc Natl Acad Sci USA* **106**:4189-4194.

Yi M., Chadwick, J., Kellett, K., Hooper, N., Johnson, P. and Fishwick, C. (2009) Discovery of novel non-peptide inhibitors of BACE-1 using virtual high-throughput screening. *Bioorg Med Chem Lett*, **19**:6770-4.

UNIVERSITY OF LEEDS

Leeds, United Kingdom
LS2 9JT
Tel. 0113 243 1751
www.leeds.ac.uk